Ultra-wideband Radar Detection of Breathing Rate: A Comparative Evaluation

Nicole A. Buckingham

Thesis submitted to the Faculty of the
Virginia Polytechnic Institute and State University
in partial fulfillment of the requirements for the degree of

Master of Science
in
Computer Engineering

Thomas L. Martin, Chair
Denis Gračanin, Co-chair
Ali R. Butt

May 5, 2020
Blacksburg, Virginia

Keywords: Biosensors, Breathing Rate, Human Computer Interaction, Prognostics and Health Management, Remote Sensing

Ultra-wideband Radar Detection of Breathing Rate: A Comparative Evaluation

Nicole A. Buckingham

(ABSTRACT)

This work explores the use of a commodity ultra-wideband (UWB) radar based device to detect breathing rate for health monitoring applications. Health monitoring devices observe physiological signals to detect medical conditions. We focus on capturing the small mechanical movements caused by breathing. This is traditionally done via a strain gauge worn around the chest or stomach, but these systems limit user movement. Contactless systems provide a unique design that allows free user movement by eliminating all direct contact with the user. Additionally, these systems have the potential to support full health monitoring in a Smart Built Environment (SBE).

In this work, a comparative evaluation is performed on a commodity UWB radar based device, the Walabot, to determine the accuracy and possible health monitoring applications. Based on results from a systematic review, six research challenges were identified: (1) high cost, functional limitations based on the user's (2) location, (3) orientation, and (4) movement, (5) dependency on system hardware placement, and (6) vulnerabilities in signal processing methods. A comparative evaluation was designed to test the Walabot against a medical grade wearable system in the context of these research challenges. The data was processed using two breathing rate derivation techniques: Fast Fourier Transformation (FFT) and Peak Detection. Results suggest great potential for the Walabot coupled with the FFT technique. However, the system requires further testing to address all of the research

challenges. Overall, this work provides important steps toward using the Walabot in health monitoring applications.

Ultra-wideband Radar Detection of Breathing Rate: A Comparative Evaluation

Nicole A. Buckingham

(GENERAL AUDIENCE ABSTRACT)

The goal of research in the field of health monitoring is to gather medical information about a user by constantly collecting physiological signals emitted by their body. Four physiological signals are deemed the "vital signs" because they provide information about the overall health of the patient. These vital signs are heart rate, breathing rate, temperature and blood pressure. Breathing rate is an important vital sign that, when monitored closely, can indicate the oncoming of dangerous health conditions and events.

The act of breathing causes the chest to expand and contract. This movement can be captured by placing a strain gauge around a user's chest and analyzing fluctuation in strain readings. However, this is not practical for health monitoring applications because this system is uncomfortable to wear and the accuracy of the system is heavily dependent on the user's ability to wear the chest band constantly and correctly. Capturing this signal without any direct user contact would eliminate the user's discomfort and provide better reliability. This can be done by several methods, but the focus of this work is on systems that capture chest movements using ultra-wideband (UWB) radar.

In this work, a specific UWB radar based device, called the Walabot, is tested against a standard strain gauge system to determine if it has health monitoring applications. Other radar based devices that aim to detect breathing rate are limited by their high cost and inaccuracies in signal processing techniques. The functionality of the devices are also dependent on the user's location and body orientation relative to the system, any user movement

and the placement of the system itself. The study in this work was designed to determine the Walabot accuracy when the data is processed by two common breathing rate derivation methods. Results showed that the Walabot is cost effective and flexible in terms of user location and system placement. Overall, this work demonstrates the potential of the Walabot as a breathing rate monitor.

Acknowledgments

This work would not have been as successful without the help of my advisor, Dr. Denis Gračanin, and my senior mentor, Reza Tasooji. They provided assistance and encouragement that helped push me to reach all my research goals.

I would also like to extend my deep gratitude to my family for their love and support throughout my academic career. I would especially like to thank my mother Anne Buckingham, father Brent Buckingham, sister Megan Buckingham and grandmother Barbara Buckingham. Additionally, I would like to thank Kyle Saul, Zaara Dean, Carley Kelly and Flora Coleman for their compassion and encouragement.

Contents

List of Figures

List of Tables

Chapter 1

Introduction

1.1 Background

The human body continuously produces a variety of physiological signals. Four important signals are heart rate, breathing rate, temperature and blood pressure. These signals are known as the vital signs because they provide a well rounded indication of the overall state of the body [29].

The research area of health monitoring focuses on measuring various physiological signals and processing these signals to determine health status. Many health monitors are used as early detection systems that predict health conditions or oncoming health events by analyzing changes in the signal's rates or patterns of a particular user. Research in health monitoring and early detection systems encompasses a wide variety of systems and methodologies, but many systems utilize one or more of the vital signs [29]. To narrow down the scope, this work is focused on health monitoring methods for heart rate and breathing rate.

Heart rate is controlled by the rate at which the sinoatrial node creates electrical impulses [28]. A detailed discussion of the functionality of the heart is provided in Chapter 2. Resting heart rate depends on age, gender and exercise level, but an increase in resting heart rate can reveal declining heart health and increase in risk of heart attack. In fact, a 2010 study from the Women's Health Initiative (WHI) reported that women with increased

heart rates were 26% more likely to experience a heart attack than women of the same age with lower heart rates [106]. Additionally, an increase in heart rate can be used to predict health conditions such as stress, anxiety, anemia, dehydration, infection, hypokalemia, overactive thyroid and asthma [29, 118]. Decrease in heart rate is also associated with heart related conditions and risk of heart attack, as well as underactive thyroid, infection and hyperkalemia [118].

The respiratory system is responsible for the breathing mechanism. The rate at which breathing occurs is specifically controlled by the respiratory pacemaker [22], as further discussed in Chapter 2. Variation in breathing rate is commonly associated with conditions including asthma, anxiety, pneumonia, lung disease and congestive heart failure [29].

Traditionally, heart rate is used to determine risk of heart attack and failure. However, studies have shown that breathing rate is a more accurate way to detect heart conditions. One such study reported that high breathing rate was the most important way to predict cardiac arrest [31]. Additionally, variations in breathing patterns can indicate health conditions such as chronic heart failure [49].

Research surrounding both heart rate and breathing rate has shown their importance in predicting harmful health events. For this reason, these two vital signs are commonly used in health monitoring systems. As medical technology improves, so does the ability to constantly monitor these vital signs and interpret the findings to predict health events.

Heart rate and breathing rate based health monitoring devices can be categorized as wearable or contactless systems. In wearable health monitoring systems, the sensor(s) that gathers physiological data is attached to the user. Research in this field has moved toward adapting standard medical devices for portability and wearability, in the hopes of enabling accurate and comfortable constant health monitoring [124].

In contactless health monitoring systems, the sensor(s) is placed in the vicinity of the user but does not require any direct user contact. This unique technology strives to provide the same capabilities of wearable technology, but with the added benefit of increased comfort. This is significant in medical applications because the users may not always be reliable or capable of correctly using wearable devices due to their state of health.

The effectiveness of these monitoring systems is dependent on the environment in which they are utilized. Contactless devices, in particular, require a specific environment that caters to the technology. One such concept is a Smart Built Environment (SBE) [54, 129]. SBEs are physical, architectural spaces that utilize the Internet of Things (IoT) to acquire information and communicate between all the connected devices without any direct user interaction. Such environments are further discussed in Chapter 2.

There are currently many methods to capture heart rate and breathing rate using either the wearable or contactless design. Additionally, each of these methods has various suitable deployment environments. A systematic review of the current system methods and their viable deployment environments is presented in Chapter 2. The findings from this review reveals the limitations of current systems and promotes the increased research in contactless heart rate and breathing rate monitoring systems.

Specifically, the findings call for the improvement of ultra-wideband (UWB) radar based breathing rate monitors. Such systems emit a wide spectrum of low energy radio frequency signals to determine the chest displacement caused by breathing. These systems report high accuracy, but are vulnerable to noise and limited by user positioning. The development of a more robust UWB radar based system has the potential to enable complete monitoring of breathing rate. Further, such a system could be utilized to monitor a user constantly and predict health events in real time. However, such a system is not available at this time because of the limitations of current systems. These limitations and current research

challenges are summarized in Section 1.3 and are further discussed in Chapter 3.

To further study this research area, the idea is to analyze the validity of an untested UWB radar based commodity device as a breathing rate monitor. This idea is introduced in Section 1.4 and described in depth in Chapter 4.

1.2 Motivation

Health monitoring with early detection systems can be used to predict harmful health events. Early detection is an essential part of preventing loss of life and reducing injury caused by harmful medical events, such as heart attack and stroke. Additionally, early detection of medical conditions significantly increases the likelihood of successful treatment or management of conditions. For example, abnormalities in breathing patterns, such as periodic breathing, can indicate the oncoming of chronic heart failure. Early detection is vital in order to treat chronic heart failure before death occurs.

For both medical events and conditions, the patient has a better outcome likelihood if the symptoms are found sooner [49]. Further, many medical accidents can be prevented and conditions can be detected if the individual is aware of the symptoms. However, self detection of health conditions or events is uncommon because the symptoms of many health conditions are difficult to detect.

For example, increases in heart rate and breathing rate can indicate an increased risk of heart attack. Heart disease is the leading cause of death in the U.S. and many of the related deaths occur from heart attack events [44]. Early detection is vital to surviving a heart attack. However, heart attacks can be very difficult to detect.

There are currently devices that can be worn by individuals with pre-existing medical con-

ditions to warn of dangerous symptoms of heart attacks and other medical events, but they are functionally limited by the user's ability and memory to use the device correctly and constantly. Additionally, these devices are only used by a small group of individuals who are aware of pre-existing medical conditions and choose to use the device as a precaution.

As discussed, heart rate and breathing rate specifically can be utilized to indicate a variety of health conditions. A contactless heart rate or breathing rate monitoring system could be used to save lives by detecting distress events, alerting the individual and calling for emergency help faster.

SBEs provide a platform for the integration of contactless breathing rate systems. Further, enabling smart living environments with such systems would allow for constant health monitoring. Users would be able to simply set up the system in their home and carry on with their daily lives knowing that health conditions or events will be detected.

An illustrative example is shown in Figure 1.1. In this system, the users set up their contactless breathing rate system in their living room. The system then constantly collects breathing rate data about the residents and analyzes the information to determine if there are any abnormalities. If a user's breathing rate indicates a health condition, for example a heart attack, the system sends an alert to all connected user devices and calls for emergency help. Enabling such a system in living spaces has the potential to protect and save many lives.

1.3 Research Question and Challenges

A systematic review of the current wearable and contactless heart rate and breathing rate monitoring methods and the viable deployment environments for contactless methods is

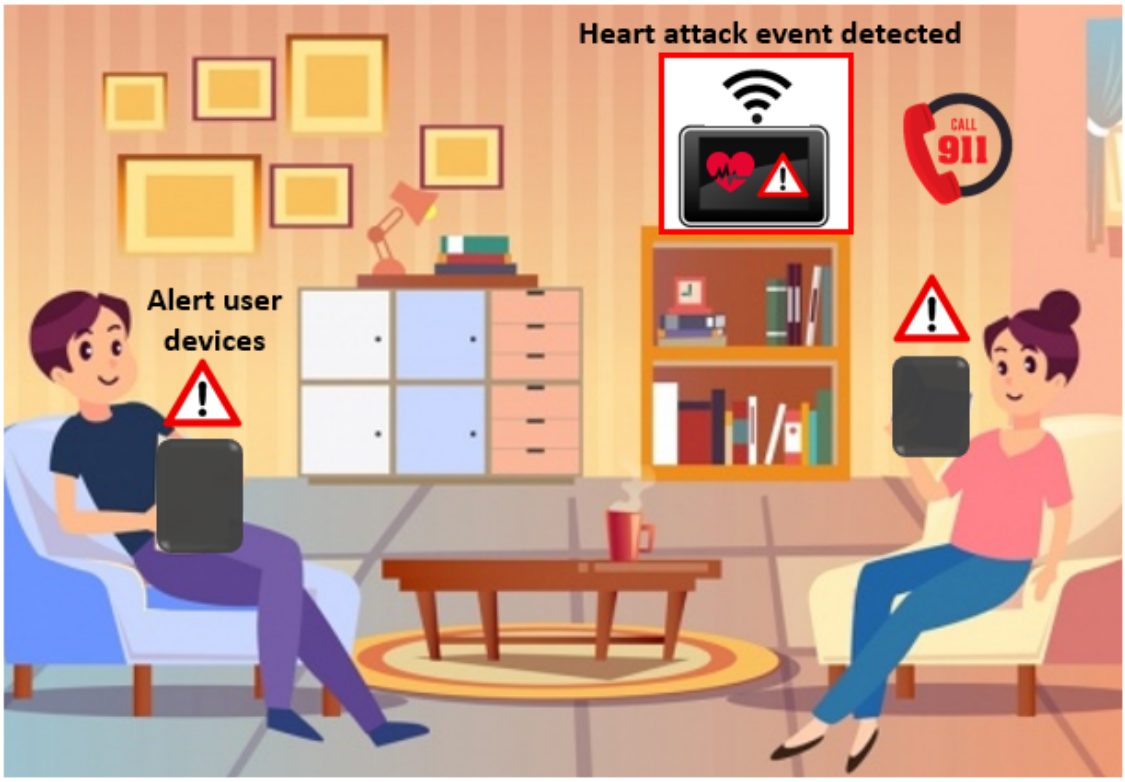

Figure 1.1: An illustrative example of using a contactless breathing rate sensor in a smart home. The background image is taken from [1].

presented in Chapter 2. The findings of this review reveal the lack of robust monitoring techniques for both wearable and contactless systems.

Specifically, wristbands that utilize Photoplethysmography (PPG) provide the most accurate and popular heart rate monitoring systems [117]. However, these systems are vulnerable to noise when the user is moving. Current research in this area is focused on reducing noise through various techniques [53, 95].

In the context of breathing rate monitoring, contactless UWB radar based systems show promising results, but current systems are vulnerable to noise and are limited by user positioning [62, 102, 141]. These systems are a topic of research currently because they have the potential to enable low cost health monitoring without any direct user interaction. The de-

velopment of a robust UWB radar based breathing rate monitor has the potential to enable complete monitoring of breathing rate. Further, such a device could be utilized to enable the theoretical system described in Section 1.2, which can monitor a user constantly and predict health events in real time.

However, the theoretical system requires a contactless breathing rate system that is fully functional, meaning it operates whenever the user is present and the results are not limited by user positioning or interaction. This leads to the following research question:

> Can UWB radar be utilized to enable a fully functional breathing rate monitoring system for an active user in a confined SBE?

Current research on UWB radar based breathing rate systems is focused on reaching fully functional status, but the systematic review reveals several important current problems being faced in research. The details of each problem is specific to the device and system design, but the generalized research challenges are as follows:

1. **Cost:** Many systems are expensive and not affordable for the common household.
2. **User Location:** Current systems are only functional when the user is in particular locations relative to the transmitter and receiver device(s).
3. **User Orientation:** Current systems are only functional when the user's body is oriented in particular angles relative to the transmitter and receiver device(s).
4. **User Movement:** Current systems are more vulnerable to noise or inaccuracy when the user is moving.
5. **System Placement:** The functionality of current systems is reliant on the placement of the transmitter and receiver device(s).

6. **Signal Processing:** Current methodology to derive breathing rate from the received signal is vulnerable to inaccuracies and noise.

These research challenges must be addressed during the development and testing of any UWB radar based breathing rate system in order to determine the functionality and limitations of the system. Unfortunately, not all available systems have been analyzed in this context. These research challenges are discussed in detail in Chapter 3.

1.4 Approach

The main objective of this work was to investigate a commodity UWB radar based device that offers a breathing rate application. Specifically, we analyzed the device's functionality in terms of the presented research question and research challenges to determine the limitations and applications of the device.

There are many UWB radar based commodity devices available. One new and inexpensive device, the Walabot, is currently being used for a variety of applications, but is popular for its ability to see wiring and pipes through walls [70, 138]. The functionality and current applications of the Walabot are discussed in depth in Chapter 5.

The Walabot is also has a breathing rate detection application [138]. However, the accuracy and limitations of this application were yet to be publicized prior to this work. Additionally, this device has not been analyzed in the context of the presented research question and research challenges.

In order to investigate the breathing rate application in the Walabot, we started by analyzing the Application Programming Interface (API) provided by the Walabot's manufacturer. Then, we used the Walabot API to understand breathing data acquisition and to collect the

necessary data from the Walabot, as explained in Chapter 5. Next, we implemented two breathing rate derivation signal processing techniques for breathing data, as described in Chapter 6.

Then, we performed a comparative evaluation to determine the accuracy of the device and the implemented signal processing techniques. The signal processing techniques were tested on the Walabot data and data from a medical grade wearable breathing rate monitor. The results are presented in Chapter 7. Finally, in Chapter 8 we used the results to discuss the Walabot in terms of the stated research challenges.

1.5 Contributions

We discuss the current state of heart rate and breathing rate monitoring devices. Additionally, we present a data acquisition script for the Walabot and a signal processing script which derives breathing rate. Finally, we analyze results from a comparative evaluation in order to understand the functionality in terms of the provided research challenges. Specifically, we provide the following contributions:

1. A systematic review of the current heart rate and breathing rate wearable and contactless system methods and the viable deployment environments for contactless methods. This review also presents a discussion of the corresponding trends and limitations.

2. A data acquisition technique for the commodity UWB radar based device.

3. Two breathing rate derivation signal processing techniques.

4. The design of and results from a comparative evaluation that analyzes the accuracy of the derived breathing rate.

1.6 Thesis Structure

In this chapter (Chapter 1), we introduced and motivated the research problem. Additionally, we outlined the research question and challenges, our chosen approach and the thesis contributions.

Chapter 2 provides a systematic review of the current heart rate and breathing rate wearable and contactless system methods and the viable deployment environments for contactless methods. The corresponding trends and limitations are also discussed.

An in-depth discussion of the research question and the corresponding research challenges is provided in Chapter 3. Then, Chapter 4 provides a thorough discussion of the proposed approach this work uses to investigate this research concept.

Chapter 5 examines the chosen commodity UWB radar based device. Specifically, this chapter includes a discussion of why the device was chosen, how the device works, and the current applications available. Additionally, the implementation of the developed data collection technique is explained.

The selected medical grade wearable breathing rate monitor is introduced in Chapter 6. Then, a detailed explanation of the signal processing techniques, including an outline of the two breathing rate computations, is provided. Preliminary testing is then discussed and analyzed.

The focus of Chapter 7 is the comparative evaluation. Specifically, the design of the study and all the results are presented. An in-depth discussion of these results are presented in Chapter 8. Finally, Chapter 9 provides the conclusion.

Chapter 2

Literature Review

2.1 Introduction

The human body continuously produces physiological signals. Among these, there are four signals that are recognized as vital signs because they measure the overall state of the body's functionality. These four vital signs are heart rate, breathing rate, temperature, and blood pressure [29]. In standard practice, doctors start any examination by measuring the vital signs in order to gather general information about the patient's health. Additionally, these vital signs can be used to predict possible diseases or conditions [29].

Health monitoring is an important research area that focuses on capturing and utilizing physiological signals to determine health status and predict harmful health events. This field continues to gain momentum because it can be used to significantly increase early disease diagnosis and prevention [150]. Commonly, the signals monitored in such applications are the vital signs [29]. As medical technology improves, so does the ability to monitor these vital signs.

The field of health monitoring is vast and continuously evolving. To narrow down the scope, this review is focused on health monitoring specific to heart rate and breathing rate. These two vital signs were chosen based on their significance and relationship. Research surrounding these two vital signs in particular has shown their importance in predicting

harmful health events. Additionally, research supports the idea that heart rate and breathing rate are intertwined. These topics are further discussed in Section 2.3.

Heart rate and breathing rate based health monitoring devices can be categorized as a wearable or contactless system. Wearable technology is not a new concept, in fact, some examples have become so normalized by society that they are difficult to recognize. Such examples include glasses and watches. These devices were among the earliest wearable devices and were revolutionary at their time of invention. In modern time, a new era of wearable devices has begun. One of the most promising applications is in the medical field. Medical devices and sensors are no longer restricted to hospitals and doctor's offices; research in the past three decades has moved toward adapting these devices for portability and constant use [124].

In recent years, research has also shifted toward designing wireless sensors. This unique technology strives to provide the same capabilities of wearable technology, but with the added benefit of being less intrusive. Within medical applications, this difference is significant as the users may not always be reliable or capable of correctly using wearable devices due to their state of health. Additionally, the wireless design is more comfortable for users.

Examination of the history and current applications of both wearable and contactless heart rate and breathing rate technology provides an important insight into the application of health monitoring. A review of the available technologies in these fields is provided in Sections 2.5 and 2.6. Additionally, a discussion about the validation process for such devices is included in Section 2.7.

The effectiveness of these technologies is dependent on the environment in which they are utilized. For wearable devices, the environment is the specialized clothing or fabric that the technology is embedded in. This topic is further discussed in Section 2.5.

Contactless devices, similarly, require a specific environment that caters to the technology. One such concept is a Smart Built Environment (SBE). SBEs are physical, architectural spaces that utilizes the Internet of Things (IoT) to acquire information and communicate between all the connected devices without any direct user interaction. This allows the environment to perform tasks and retain essential knowledge at all times. There are several applications of SBEs such as smart houses and cars. A review of these environments provides important insight to the feasible applications of contactless health monitors. This review is provided in Section 2.8.

With all the information from the review in mind, predictions about the future of this field and the unanswered questions are discussed in Section 2.9. Finally, the review is concluded in Section 2.10.

2.2 Methods

2.2.1 Research Questions

The goal of this review is to understand the functionality, limitations and applicable environments for both wearable and contactless heart rate and breathing rate monitors. In order to do so, the methodology of the review was created to answer the following questions:

1. How are heart rate and breathing rate measured?
2. What heart rate and breathing rate wearable devices are available and what are the associated limitations?
3. What heart rate and breathing rate contactless devices are available and what are the associated limitations?

4. What are the real world scenarios/environments for contactless health monitoring systems?

2.2.2 Inclusion Criteria

The following inclusion criteria was derived based on the main goals and questions:

1. Published papers
2. Reputable online articles (i.e., information published on websites of established medical facilities)
3. Academic research
4. Engineering, Computer Science and Biology subject areas
5. Written in English
6. Papers presenting new devices must provide test results

No explicit exclusion criteria was used.

2.2.3 Search Methodology

This study was conducted using Google Scholar, Scopus, and Google search engines in the following manner:

1. The Google Scholar search engine was used during the preliminary investigation stages to narrow down the topic. Google Scholar is a very powerful publication search engine

that has a wide range of articles in Engineering, Computer Science, and Biology subject areas. The main search keywords used are provided in Section 2.2.3.

2. Upon reviewing a high quality source, relevant citations included in that paper were also reviewed. Additionally, the papers that cited the original paper were investigated if relevant.

3. Scopus was used during the final stages of review. The keywords and commands in Section 2.2.3 were used to query this database. There are many published papers on this topics, so naturally additional sources were found during this search. Many more sources were reviewed and papers that presented new techniques were added. However, papers with redundant information were not included. The purpose of cross referencing with this database was to validate the conclusions and to verify this review can be replicated.

4. The use of the Google search engine was limited to established medical facilities or organizations and official device websites. The former websites were used to gather physiological perspective information and device validation procedures. The latter websites were used primarily for images of devices, but also for further understanding of device functionality.

2.2.4 Keywords

The following list contains the keywords that were used to find sources for each section. See Section 2.2.2 for details on additional search criteria. The resulting papers were sorted by relevance. Thousands of papers were available, but only up to the first 50 returned from the initial search in Google Scholar and 30 from the search in Scopus were reviewed for each

section. The total number of reviewed papers is approximately 240. See Section 2.2.3 for details about the review process.

1. **Wearable Devices:** wearable AND (ECG OR heart rate OR breathing rate)
2. **Contactless Devices:** contactless AND (wireless OR heart rate OR breathing rate)
3. **Smart Deployment Environments:** health monitoring AND (smart living OR smart home OR smart mobility)

2.3 Physiological Perspective

Before reviewing heart rate and breathing rate monitors, the corresponding vital signals must first be understood. Heart rate and breathing rate occur and are measured differently, but both provide important insight on overall health. Heart rate and breathing rate were chosen as the focus of this review because they can be used to predict various conditions and they are connected, as discussed below.

2.3.1 Heart Rate

The heart is one of the most critical muscles in the human body, as it is responsible for pumping blood throughout the body. First, the sinoatrial node creates electrical impulses that cause the atria to contract, which causes blood to flow into the ventricles. The His-Purkinje Network then sends impulses to the ventricles, which causes them to contract and release blood into the body. This cycle happens continuously, based on the speed of the impulses from the sinoatrial node. Normal heart rate occurs when the sinoatrial node fires on a consistent basis [28]. A diagram of the heart can be seen in Figure 2.1C.

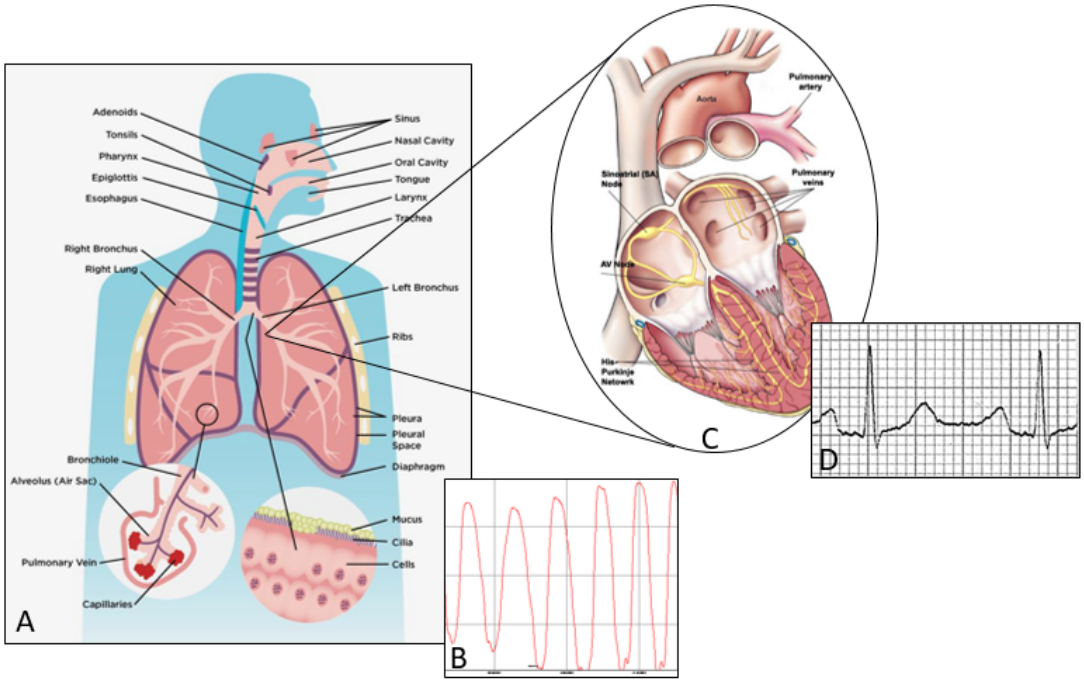

Figure 2.1: **A)** A diagram of the human respiratory system, responsible for breathing mechanism [28]. **B)** An example of signal waveform from breathing detection system [19]. **C)** A diagram of the heart [28]. **D)** An example of ECG waveform [37].

Heart rate can be measured in a variety of ways. One can easily calculate heart rate using pulse, which is the number of heart beats per minute. This is most commonly measured by placing two fingers on the inner wrist or upper neck and counting the beats felt in one minute. When the heart is in critical condition in a hospital setting, heart beat is constantly monitored using an Electrocardiogram (ECG). A typical ECG pulse waveform appears in Figure 2.1D. This device will be further discussed in Section 2.3.3.

The typical resting heart rate for a healthy adult is between 60 and 80 beats per minute [29]. Resting heart rate varies with age, gender and exercise level. Changes in resting heart rate can reveal declining heart health and increase in risk of heart attack. For example, women with increased heart rates are 26% more likely to experience a heart attack than women of the same age with lower heart rates [106]. An increase in heart rate can be used to predict health conditions such as stress, anxiety, anemia, dehydration, infection, hypokalemia, overactive

thyroid and asthma [29, 118]. Similarly, a decrease in heart rate is associated with heart related conditions and risk of heart attack, as well as underactive thyroid, infection and hyperkalemia [118].

Heart beats should be consistent, without any missed beats. However, beats are not always consistent; Heart Rate Variability (HRV) measures the changes in beat rhythm. This measurement can be used to detect heart conditions such as congestive and chronic heart failure, as well as other health conditions such as sleep apnea [83].

2.3.2 Breathing Rate

Breathing, or respiration, is a vital mechanism that all humans perform subconsciously in which air circulates in and out of the lungs, in order to provide oxygen to the body. The rate and volume of air moved is controlled by the respiratory pacemaker, which is located in the medulla of the brainstem. The respiratory muscles relax and expand relative to the commands sent by the pacemaker via the spinal cord [22]. A diagram of the respiratory system can be seen in Figure 2.1A. During inspiration, air pressure within the alveolar spaces drops and air enters the lungs through the larynx. The oxygen is removed and passed into the bloodstream. The remaining air and carbon dioxide from the bloodstream then exits the lungs when the air pressure rises, called expiration. The rate at which the air flows is determined by the pressure difference in the lungs [11, 61].

Respiration devices typically measure breathing rate and tidal volume. Breathing rate, or respiration rate, is number of breaths taken per minute. A general breathing rate waveform is shown in Figure 2.1B. Typical resting breathing rate varies per person but a rate between 12 and 20 breaths per minute for an adult is considered normal, whereas a resting rate over 25 or under 12 is considered unhealthy. Various health conditions affect resting breathing

rate, such as asthma, anxiety, pneumonia, congestive heart failure and lung disease [29]. Additionally, changes in breathing rate in hospital patients is correlated with an increase in mortality rate. Consequently, the breathing rate of critical patients is monitored every four to six hours [27].

Tidal volume is the volume of air intake during inspiration. Typical tidal volume is dependent on the individual but a volume of 400 to 500 mL is considered healthy [58]. In healthy adults, tidal volume is quite consistent between breaths, but infrequent changes in air intake caused by yawns or sighs are considered normal. Tidal volume may also change in situations where breathing rate changes, such as exercise [22].

One limitation of breathing rate is that the measurement can be affected by the time over which is it measured. Some studies extract breathing rate from a shorter time, such as 15 seconds. However, this measurement is subject to inaccuracy because breathing rate can change between measurement periods due to changes in air intake, as described in the previous paragraph. Studies have shown that the time period with the least variability is 1 minute [39].

2.3.3 Relation between Heart Rate and Breathing Rate

It is intuitive that breathing rate is directly connected to heart rate. Further investigation to this phenomenon shows that heart rate naturally increases while breathing in and decreases during exhaling. This occurrence is called Respiratory Sinus Arrhythmia (RSA). The amplitude of RSA is dependent on depth and frequency of breathing [63].

The relationship between heart rate and breathing rate has been known for decades, and this relationship continues to be investigated as an application for health monitoring. Many devices found in this review utilized breathing rate to determine heart rate or vice versa.

As described previously, changes in heart rate or breathing rate can indicate various health conditions. One important similarity between heart rate and breathing rate is they both can be used to predict heart related conditions such as congestive heart failure and cardiac arrest. In the past, heart rate has been more commonly used to detect such heart events, but current research suggests that breathing rate may be a better indicator [40, 123].

One common medical device to measure heart functionality overall is the ECG. This device gathers detailed information of the heart by recording the electrical activity [27]. To do so, electrodes are placed on predetermined locations on the body. Placement is typically on the chest but can also include the back, arms or legs [64]. These electrodes provide different viewpoints of the heart, which provide information about heart rate and breathing rate [4]. Combined data from electrodes is used to evaluate the comprehensive activity of the heart [64].

2.4 Signal Processing

In general, medical devices interact with a biological system by collecting changes in physiological function, or biosignals. The medical devices discussed in Section 2.5 and Section 2.6 aim to monitor the heart or respiratory systems by collecting the biosignals discussed in Section 2.3: ECG, heart rate or breathing rate [115].

These biosignals are captured using a biotransducer which converts the external energy carried by the signal to an analog signal. This signal is then converted to a digital signal using an analog-to-digital converter [116]. Additionally, the signal may require conversion between the time and frequency domains. This is performed using a Fast Fourier Transformation (FFT) [32].

All biosignals captured will contain unwanted variance, or noise. The signal-to-noise ratio (SNR) reveals the quality of the received signal [115]. A common limitation of the device methods reviewed in Section 2.5 and Section 2.6 is signal vulnerabilities to low SNR. Current research aims to develop software that performs signal processing that can overcome this challenge for each data acquisition method described. A partial list of the current signal processing methods is as follows: amplification, filtering, and machine learning pattern detection [32].

Amplification is used on signals with a low amplitude [32]. Filtering is useful to eliminate noise and spurious frequency components. Among the filters available, band-pass filters are most commonly used for respiratory based devices whereas low-pass filters are typically used to extract breathing rate from ECG devices [13, 32]. This a very limited list, however, as there are over 100 methods for extracting breathing rate from ECG and PPG data alone [26]. A popular topic in current research is developing breathing rate extraction methods from radar methods [80, 127].

Machine learning offers a way to recognize respiratory patterns. This approach commonly requires feature extraction and classification selection first. Then, a machine learning algorithm such as support vector machines, naive Bayes or artificial neural networks can be used to learn and recognize various breathing patterns [32].

2.5 Wearable Devices

The functionality of current wearable medical devices, also called Body Sensor Networks (BSNs), provides important insight on possible methods for detecting health related events [105]. There are a variety of wearable medical devices on the market and even more are being developed and tested. These devices appear as normal clothing or accessory articles, but they

consist of small sensors that can read a variety of biometric data.

This type of health monitor has the potential to protect countless individuals by enabling home or on the go health monitoring. Within these devices, sensors are commonly embedded into clothing, chest bands or wristbands so they can be comfortable for daily use. The integrated sensors commonly gather data such as heart rate, temperature, blood pressure, breathing rate, ECG, and electomyogram (EMG). Additionally, activity can be monitored using integrated accelerometers, gyroscopes, and magnetic field sensors [84].

Some wearable devices require a wired connection to their computing system, whereas others utilize Bluetooth or WiFi to transmit information wirelessly. Although the computing system may be separate and not require user interaction, these devices are still considered wearable because the sensors must be attached to the user.

An important aspect of these devices is the material used. The devices must be comfortable and well fitting for all body shapes. Materials such as plastic and elastomeric substrates provide a lightweight platform for integration. Some sensors are already created using flexible materials. If this is not the case, the sensors can be transferred onto flexible materials. In general, silicon-based sensors are the most efficient and accurate. A hybrid approach that uses flexible materials as the platform for silicon sensors provides the best performance and adaption ability [69].

This review of wearable health monitors is specifically focused on devices that measure breathing or heart rate. Such devices can be classified into the following categories based on methodology: ECGs, heart rate monitors and breathing rate monitors. A summary of these wearable health monitors appears in Table 2.1.

Table 2.1: A summary of wearable ECG, heart rate and breathing rate devices.

Category	Method	Description
ECG	No gel required	Use electrodes that do not require gel, such as dry foam electrodes and capacitive electrodes [76, 131]
	Embedded electrodes	Embed the electrodes into wearable materials (can use conductive yarn to increase conductivity) [7, 96]
	Replace DRL	Replace the DRL electrode with different system, such as two capacitive sensors and two anti-parallel biasing diodes [72]
	Electrical Impedance Tomography (EIT)	Use electrodes to capture functionality information by introducing AC currents [143]
Heart Rate	Photoplethysmography (PPG)	Use a pulse oximeter to detect the changes in blood volume inside in pulsating vessels [117]
	Piezoelectric pressure sensors	Detect the arterial pulse wave created by the heart's pulsing rhythm using electrospun PTFE material [128]
Breathing Rate	Audio	Collect breathing sounds by placing a microphone near the nose, mouth or neck [30]
	Airflow	Record temperature changes, nasal pressure or CO_2 changes by placing sensors near nose, mouth or neck [4]
	Chest displacement	Measure mechanical signal of chest movement using strain gauges or impedance methods [4]
	ECG-derived respiration	Derive breathing rate from ECG signal, using the fluctuations in the mean cardiac electrical axis [92]
	CO_2	Measure the changes in CO_2 by monitoring the diffusion of gas to the skin [4]
	O_2 by PPG	Measure blood oxygen saturation using PPG method [4]

2.5.1 Wearable ECG

As stated above, typical ECG devices require electrodes placed on predetermined locations on the body such as the chest. To make an ECG device wearable outside of a hospital

setting, the system must be altered slightly. Typically, the electrodes are contained within a wearable unit and the data captured is sent wirelessly over Bluetooth. Additionally, the ECG device must be adapted for easy use. Historically, the electrodes are attached to the body using a conductive gel. In order to integrate these sensors into an easily wearable system, researchers have investigated novel ways to establish a connection without using wet electrodes.

One approach is to use an electrode that does not require gel. Such types include dry foam electrodes and capacitive electrodes [76, 131]. These electrodes can be embedded into wearable materials such as chest bands to increase comfort levels, but they require skin contact which can be intrusive. Additionally, dry electrodes are subject to electrode-skin impedance, which commonly increases interference with environmental noise [144].

To eliminate the need for skin contact, electrodes can be embedded into wearable materials such as shirts or wristbands. In this case, the electrodes do not directly touch the skin and the material acts as the conductive gel [85, 96]. Additionally, a dry conductive material, such as a conductive yarn, can be used to increase conductivity. Such materials commonly rely on body moisture to increase conductivity [7]. This method can appear less intrusive, but the testing of such devices and systems still received complaints from test subjects for being obstructive [96].

These systems use a driven right-leg (DRL) electrode to function as a common electrode and stabilize the signal. DRL electrodes are commonly positioned far away from the wearable device and require wired connection, decreasing the wearability of the systems. One method which avoids the use of a DRL electrode utilizes two capacitive sensors and two anti-parallel biasing diodes. Results show that this method is functional but is at risk for high signal disruptions [72].

A novel approach utilizes Electrical Impedance Tomography (EIT). This method uses electrodes to capture functionality information by introducing Alternating Currents (AC). For the purpose of this review, this method is categorized as ECG because it uses electrodes to gather information about heart rate and breathing rate simultaneously. One application of this method is to mount electrodes on a wearable belt [143].

These systems provide evidence to prove the feasibility of wearable ECG devices. However, the discussed systems require advanced signal processing techniques. Many methods available are dependent on gathering clear data so they are not always reliable. Research in this field is continuously improving such processing techniques [113]. Additionally, these systems are designed for experimental procedures instead of for commercial use. An accurate and user friendly system is required in order for these systems to be used for continuous heart health monitoring.

Such systems do exist but their effectiveness is limited. One example of such a system utilizes a small wearable ECG sensor and mobile phone application to help individuals self diagnose a heart attack. When an individual feels symptoms occurring, they can use the system to run ECG recordings and see their results. This application proved effective but required accuracy improvements. Additionally, the device is limited to helping individuals who have the sensor nearby and have already detected symptoms [78].

ECG devices provide detailed information about heart activity. However, the current wearable ECG systems are either intrusive or have limited effectiveness. This type of wearable heart monitoring device requires improvements.

2.5.2 Wearable Heart Rate Trackers

Another approach to monitor the heart is to directly record heart rate data. This provides fewer details than ECG data, but heart rate alone can be used for health monitoring.

Two widely known examples of wearable devices that detect heart rate are fitness trackers and smart watches. Fitness trackers are typically worn as a wristband and track real-time data including steps taken, calorie intake, heart rate and sleep patterns [67]. Smart watches appear as normal watches with a digital screen and are capable of tracking similar biometric information. Today, most fitness trackers and smart watches can be synced to computers or smart phones and have the power to provide very specific movement and biometric data for a user's daily life [67, 120].

Wristband devices that detect heart rate commonly use PPG. This technique can be traced back to the 1930s, when the PPG waveform was first uncovered. The applications of this waveform weren't discovered until 50 years later, when the pulse oximeter was introduced. This device detects changes in blood volume inside a pulsating vessel using a light source, such as an LED, and a light detector, such as a photo diode [117]. The accuracy of the PPG method has been tested against the Holter ECG. Results confirmed the used of PPG in wearable devices as a heart rate detector [126].

There is a lot of positive marketing about these fitness trackers and sales have continued to increase each year. Based on marketing alone, it appears that these devices are very accurate and have potential to be expanded to medical health monitoring. Several studies investigated the accuracy of such devices. One review from 2015 tested the Apple Watch, Motorola Moto 360, Samsung Gear Fit, Samsung Gear 2 and Samsung Gear S against a clinically validated finger pulse oximeter, the Onyx Vantage 9590, during walking. The respective reported accuracies were 99.9%, 92.8%, 97.4%, 97.7%, and 95.0%. The corresponding box plot can

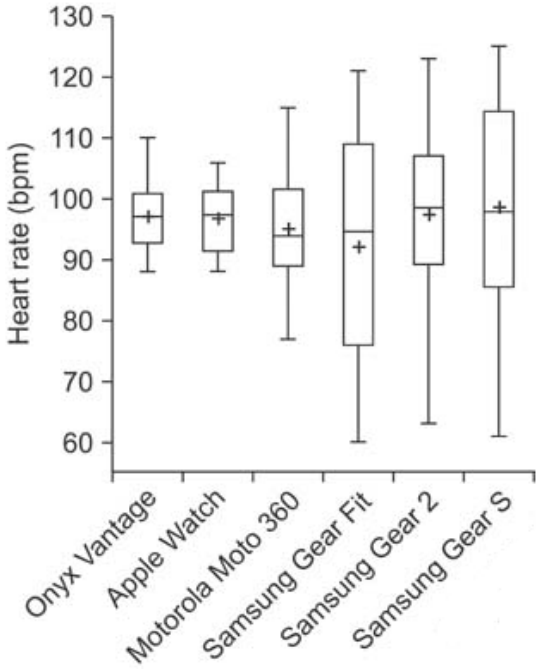

Figure 2.2: Box plot of heart rate measurements against the Onyx Vantage 9590 [38].

be seen in Figure 2.2 [38].

A review from 2016 evaluated the Scosche Rhythm, Mio Alpha, Fitbit Charge HR, Basis Peak, Microsoft Band and TomTom Runner Cardio against the validated Polar RS400 watch and chest transmitter pair. The corresponding statistics can be seen in Table 2.2 [122]. This study also tested these trackers during running and concluded that the heart rate measurement accuracy decreases during exercise [122].

There are other types of wristband devices with heart rate trackers as well. For example, the Empatica wristband appears similar to common fitness trackers, but it is used specifically to monitor vital biometric signals. This device contains four biometric sensors: PPG, electrodermal activity (EDA), 3-axis accelerometer and temperature sensor. It can capture a recording of data or use Bluetooth to process data in real-time [47]. Due to the easy use and accurate results, the Empatica has been used in many research studies that require discrete

Table 2.2: Heart rate statistics against the Polar RS400 [122].

	N	Mean ± SD (BPM)	Minimum	Maximum
Polar RS400	1794	109.06 ± 29.3	55	194
Scosche Rhythm	1779	108.22 ± 29.9	33	194
Mio Alpha	1794	110.54 ± 30.3	45	194
TomTom	1110	111.13 ± 30.9	55	204
Microsoft Band	1758	109.38 ± 28.8	52	199
Basis Peak	1714	109.27 ± 28.7	53	192
Fitbit Charge HR	1781	105.00 ± 30.6	53	193

health monitoring [34]. Figure 2.3 shows four of the aforementioned watches and fitness trackers.

One limitation of the PPG method is signal noise caused by user motion. As found in the study by Stahl et al., many wrist band devices have a lower accuracy when the user is running [122]. Recent research has explored methods to reduce this noise. A review from 2019 discussed all the current research methods to extract heart rate with minimal noise [21]. One example uses particle filters to filter out motion artifacts [95]. Another method is to apply the FFT on sections of incoming data to remove motion noise [53].

Another way to detect heart rate is using piezoelectric pressure sensors to detect the arterial pulse wave created by the heart's pulsing rhythm. Such sensors were integrated into a wristband using electro-spun polytetrafluoroethylene (PTFE) material. Testing deemed the wristband accuracy similar to the ECG signal found. Additionally, this system proved to be less vulnerable to signal discrepancies [128].

Wearable heart rate trackers are highly beneficial and preferred by users because they have high accuracy and low intrusiveness. Such wristband devices are easy to use, but still require direct contact with a user. In the case of user error or incompetency, these devices become ineffective. Additionally, further research is needed to reduce noise caused by motion.

Figure 2.3: Wristband heart rate monitors: **A)** Apple Watch Series 5 [9]. **B)** Samsung Gear Fit [112]. **C)** Fitbit Charge HR 101 [41]. **D)** Empatica E4 [65].

2.5.3 Wearable Breathing Rate Monitor

From a physiological perspective, breathing rate offers a unique opportunity for wearable devices. In contrast to heart rate, which is measured using internal signals, physical signals caused by breathing rate can be recorded using audio, airflow or the low frequency mechanical signal caused by small chest inflections [4, 46]. These physical effects have made breathing rate a popular subject of wearable device research.

Auditory breathing sounds can be recorded by placing a microphone near the nose, mouth or neck [30]. Airflow can be recorded using temperature changes, nasal pressure or CO_2 sensors. However, both audio and airflow methods are limited as sensor placement is intrusive and uncomfortable for users [4].

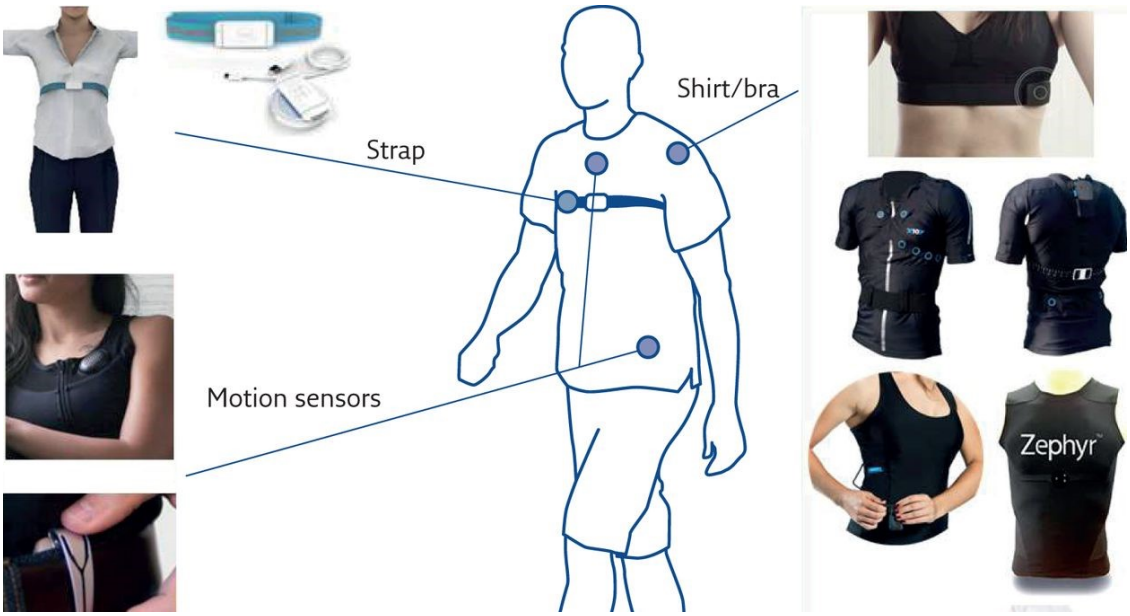

Figure 2.4: Sensor placement of wearable breathing rate devices that use mechanical signal from chest [5].

Common ways to capture the mechanical signal of chest movement use strain gauges, impedance methods or accelerometers. These methods typically require sensors placed around the ribs or abdomen, or motion sensors placed near the hips [4, 5]. A diagram illustrating the sensor placement options is shown in Figure 2.4 [5].

Commercial breathing monitor devices commonly use the mechanical method. Two such devices that are commonly used for research purposes is the BIOPAC respiration transducer chest band and the MindWare respiration belt [82, 88]. To make this method more comfortable, strain sensors, such as piezoelectric sensors, can be incorporated into fabrics, such as piezoresistive yarns [46, 101]. An example of a commercial device that embeds the sensors into fabric for more comfortable use is the VITALI Smart Bra. There are also a few devices that use motion sensors, such as the Spire Health Tag. These devices can be seen in Figure 2.5.

Breathing rate can also be found using non-physical signals. As mentioned previously,

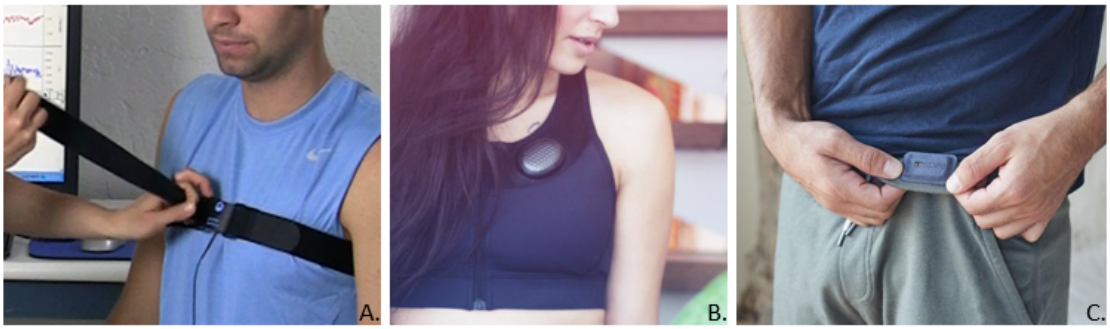

Figure 2.5: Mechanical based wearable breathing rate devices: **A)** BIOPAC respiration transducer chest band [17]. **B)** VITALI Smart Bra [133]. **C)** Spire Health Tag [60].

breathing rate can be derived using ECG. This method was coined the ECG-derived respiration (EDR) technique, and the general concept is to utilize the fluctuations in the mean cardiac electrical axis [92]. There are a variety of specific signal processing techniques that aim to provide the most accurate data [27]. The methods to contain ECG devices in wearable units was discussed previously.

Some researchers argue that the above methods do not capture full respiratory information because they focus on breathing rate and tidal volume, opposed to measuring changes in CO_2 and O_2 [42]. One method is to measure the changes in CO_2 by monitoring the diffusion of gas to the skin. This is typically done by placing a heated electrode and conductivity gel on an arm. This method requires constant medical attention to detect any skin burning or discomfort. Another method is to measure blood oxygen saturation using a pulse oximeter [4]. As described above, this technique can simultaneously provide heart rate data.

Overall, these devices have roughly the same effectiveness as the wearable heart rate devices described above. However, these devices also have the same important limitation, they still require direct contact with a user. Wearable breathing rate monitors are also more intrusive to users which can affect their functionality.

Table 2.3: A summary of contactless heart rate and breathing rate devices.

Category	Method	Description
Heart Rate	Video/imaging	Observe PPG or small head motions caused by the flow of blood during each heart beat [5, 12, 91, 104]
	Thermal imaging	Observe the changes in vein temperature due to pulsating blood pressure [48]
Breathing Rate	Video	Monitor chest movement, skin vibrations or thorax movement [8, 94]
	Thermal imaging	Capture changes in facial skin temperature [4]
	Acoustic	Use speaker and microphone to capture the Doppler effect on air caused by breathing [142]
	Lasers	Detect changes in chest movement using laser sensors [73]
	Ultrasonic Sensors	Detect changes in chest movement using ultrasonic sensors [86]
	Radar	Detect changes in chest movement using microwaves [81, 99] or radio frequency [102, 110, 132, 141]

2.6 Contactless Devices

The devices in the previous section provide opportunities to monitor heart rate and breathing rate outside the doctor's office. However, these devices have many limitations. The primarily limitation is these devices must be worn in order to function. Further, the user must actively participate by putting on the device correctly. User fault could render these devices useless. Additionally, these devices can be irritating to users which decreases the usability.

Contactless health monitors, or Wireless Body Area Networks (WBANs), provide a way to support contactless sensing. These devices can gather equivalent data, without any physical contact between the user and the sensors [79]. Development of such devices is on the rise because they have the potential to improve health monitoring dramatically. However, there are a very limited number of commercial products available currently. A summary of the contactless heart rate and breathing rate monitors appears in Table 2.3.

2.6.1 Contactless Heart Rate Detection

As discussed previously, there has been extensive research into detecting heart rate using wearable devices such as wristbands. Such devices are accurate and common. In contrast, there has been limited research into detecting heart rate without skin contact. The majority of related research revolves around detecting breathing rate and uses the information to derive heart rate. Such devices will be discussed in the next section.

Among the methods to directly gather heart rate data contactlessly, the most common utilizes one of many proposed computer vision algorithms to analyze video streaming or photography [119]. One interesting method uses cameras to perform the PPG method without contact. This technique is currently limited to a stationary user [5]. Another technique measures heart rate by observing small head motions caused by the flow of blood during each heart beat. Specifically, Principal Component Analysis (PCA) is used on the recorded head movements to determine which movement is directly related to heart beat [12, 91, 104].

A similar method utilizes video streaming of thermal imaging. This method observes the changes in vein temperature due to pulsating blood pressure [48]. Results from several studies prove these concepts are comparable to a conventional ECG system, but are sensitive to movement [12, 48, 91, 104].

2.6.2 Contactless Breathing Rate Detection

Monitoring breathing rate without wires or skin connection is a novel topic of research. Typical contactless methods utilize visual information, thermal sensors, acoustic changes, lasers or radar.

There are many techniques that utilize visual information. One method is to monitor the

chest movement caused by breathing. In one study, a fiber grating vision sensor projected invisible infrared light onto the subject and a Charge-Coupled Device camera recorded the movement of the spots that occurred with chest inflections [8]. Another study captured breathing rate by detecting chest fluctuations and skin vibrations concurrently [3].

Another visual method is to monitor the movement of the thorax. A camera can be used to capture the surface of the thorax. Light is then projected onto the recording and the light intensities change according to breathing pattern [94]. Visual methods are promising, but limited testing has been done and the effectiveness of this method is greatly affected by user movement.

Thermal sensors and imaging has been utilized in a variety of breathing device studies. Commonly, thermal imaging captures changes in facial skin temperature. This concept has potential, but has not been proven as effective as medical grade devices [4].

One novel technique is based on acoustic changes caused by airflow. One such system uses a speaker, which emits inaudible sound waves, and a microphone, which captures the Doppler effect on the surrounding air caused by breathing. This method proved accurate but testing was limited to sleeping subjects [142].

As discussed in Section 2.5, wearable breathing rate monitors commonly utilize the low frequency mechanical signal caused by small chest inflections. In contactless devices, this chest movement can be detected using lasers [73], ultrasonic sensors [86] or radar methods.

Radar methods encompass techniques that utilize microwave or radio frequency (RF). Such methods rely on the idea that a stationary person's breathing rate matches the phase shifts of signals reflected off the person [81, 99]. These methods are typically categorized as continuous-wave (CW), frequency-modulated continuous-wave (FMCW), impulse radar and ultra-wideband (UWB) radar [24]. CW and FMCW often utilize Doppler radar [56].

Radar devices typically use the following basic technique: the transmitter sends a signal, the phase and amplitude of the signal is modified by the chest inflection of the user, the signal is reflected back to the receiver. Changes in the received signal are used to extract respiratory rate [62]. Such devices often have high accuracy, but can be expensive. Recent research has shifted to developing devices that utilize the same concept in less expensive ways.

One inexpensive way to utilize the radar method is to use commodity WiFi devices. This can be done using Received Signal Strength (RSS) or Channel State Information (CSI). The former method, RSS, utilizes a network of transceivers and advanced signal processing to extract breathing rate from the RSS data stream [141]. RSS measurements have been utilized in the field of person detection as a way to estimate a person's location by identifying signs of breathing. In many experiments of using this method, measurement errors are caused by the person's motion. Recent research methods have been proposed to reduce this error [102].

The CSI method exploits fine-grain channel information to extract breathing rate. This method has shown accurate measurements. However, the results can be unreliable depending on the user's position and movement. Wang et al. investigated the use of the Fresnel Zone theory to explain the user's effect on the data. Results conclude that user's location and orientation relative to Fresnel zones effects the quality of respiratory signals [141].

After the Federal Communications Commission (FCC) legalized the use of UWB in 2002, this has been investigated as a new way to determine breathing rate. This method presents an improved alternative to the Doppler radar method because UWB signals are able to record accurate, real-time measurements through walls [110, 132].

One new and inexpensive device, the Walabot, as seen in Figure 2.6, has the potential to remotely monitor breathing patterns using UWB radar. This device is currently being used for a variety of applications, but is popular for its ability to see wiring and pipes through

Figure 2.6: Walabot Do It Yourself Version [138].

walls [70, 138]. Inside this Walabot there is a Vayyar sensor chip, which uses non-ionizing UWB microwave radio waves with a frequency range of 3.3 to 10.3 GHz [66]. The device uses several transmit-receive antennas to gather signals and construct an image of the surrounding environment. This device also has a breathing pattern monitor application, but it has not been thoroughly tested [138]. One research team in Japan is currently testing the breathing application in an infant monitoring system to prevent infant death syndrome [111].

In a comparison study of RSS, CSI and UWB radar breathing rate devices, each method was effected by the transmitter and receiver type, the relationship of transmitter and receiver antennas and the number of antennas. Additional results showed that each device has the ability to monitor respiratory function, but they also are limited by user movement and require improvement [62].

Contactless respiratory devices have great potential, but all current devices are limited by the orientation and position of the user. These devices rely on specific and sometimes fixed positioning in order to collect usable data. When investigating contactless respiratory

devices, it is important to determine their limitations and the use cases in which these devices are effective.

2.7 Device Validation

When new devices are developed, researchers perform extensive testing to determine efficiency, viable applications and limitations. Upon completion of development, the intention of the new devices determines how it must be validated.

New technology that is intended for use in medical facilities must undergo official testing in order to be validated as a medical grade device. The validation process is typically specified by a government agency of that country or geographical area. In the United States, medical devices must be cleared or approved by the Food and Drug Administration (FDA) before it can be sold as a medical grade device for use in medical facilities. A heart rate or breathing rate monitor with the intention of hospital use is classified as a medical device according to the FDA because it is "intended for use in the diagnosis of disease or other conditions" [43].

The medical device FDA validation process is dependent on the device's classification, which is based on the corresponding risk. Regulatory requirements, including specifications for safety and effectiveness, becomes more strict as the device classification increases. Additionally, the process is dependent on the existence of an equivalent approved device. A new device need only be cleared if it is deemed equivalent to an approved device. The clearing process involves a Premarket Notification submission that proves the device is equivalent. Otherwise, the device must be approved. The approval process requires a Premarket Approval (PMA) application, which demonstrates the effectiveness and safety of the device, or a Humanitarian Device Exemption (HDE), which is applicable to devices intended for treatment or diagnosis of a health condition that affects less than 8,000 people in the United

States per year [43].

However, heart rate and breathing rate monitors that are not intended for use in medical facilities do not necessarily require FDA approval. For example, devices intended for use only in research purposes do not generally required FDA approval.

In the case where approval is not required, companies may choose to get certification from a trusted source such as the International Organization for Standardization (ISO). The ISO is a non-governmental, international organization that publishes safety, quality and efficiency standards for services, systems and products [45]. ISO certification is not required by law, but receiving certification is a way to show customers the product has been approved for safe use. For example, BIOPAC Systems Inc, is a widely used and trusted manufacturer of medical devices such as respirator transducers. Their products are intended for research purposes only, so they do not require FDA approval. However, the company chooses to meet ISO standards [18]. Companies may choose to apply for certification under other organizations as well.

Late stages of verification testing for any new device typically involves performing a clinical trial or user study that compares the new device against a currently trusted device that performs the same functionality. In this realm of research, new health monitor devices must be compared to FDA approved or otherwise certified devices. For example, Droitcour et al. validated a Doppler radar based respiratory rate sensor by benchmarking the data against a Welch Allyn Propaq Encore model 242, an FDA approved device, in a user study with 24 subjects. The results demonstrated their device agreed with the approved device within the 95% limits of agreement, or within 5 breaths per minute [36]. User studies are an important aspect of testing as they reveal the limitations of the device.

2.8 Smart Deployment Environments

As discussed in Section 2.5, developing wearable sensors requires the integration of the device into a viable material. Similarly, developing contactless sensors requires the integration of the device into a viable environment. Further, in order to provide an extensive review of contactless sensors, the applicable environments must also be reviewed.

SBEs utilize IoT to become completely connected and enable communication. IoT is a commonly used term for the widespread expansion of Internet capabilities into ordinary electronic physical devices. With the added use of the Internet, these devices can communicate autonomously and be remotely managed. With the development of cloud computing, IoT is becoming more cloud-centric. This capability allows data and information to be offloaded onto the cloud, giving the physical devices more computing power. In the past year, the IoT cloud platforms have been used to improve wearable medical devices and smart homes [90, 120].

There are many applications of SBEs, including smart living and smart mobility. Each offers different specific benefits for its particular use. We provide a review of SBEs to determine what environments are viable for contactless health sensor integration.

2.8.1 Smart Living

Smart living based environments are SBEs that are created for living purposes (i.e., smart homes). The term smart living encompasses the various aspects of home automation, including security and energy management. The most developed applications of smart living today are home system controls, such as lighting, heating, and security controls, using Bluetooth technology [74, 145].

The idea of the Health Smart Home (HSH) was established in the early 2000s as a way to integrate health services into smart living. One of the first applications of such homes was to provide health care to people with special needs [109].

One important application of HSHs is health monitoring and fall detection of the elderly population. In Canada, the Technology Assisted Friendly Environment for the Third Age (TAFETA) was created to develop technology to meet the needs of the elderly who live independently. In 2007, TAFETA proposed the use of the following sensors in homes to meet these needs: magnetic switches, thermistors, accelerometers, RF identification, infrared motion sensors, microphone arrays, smart grab bars, pressure sensitive mats and electronic noses [10].

In a 2008 literature review of the available smart living technologies, the following categories were identified: physiological monitoring, functional monitoring/emergency detection and response, safety monitoring and assistance, security monitoring and assistance, social interaction monitoring and assistance, and cognitive and sensory assistance. This research showed that current technologies are focused on physiological and functional monitoring, whereas social interaction monitoring technology is lacking. Additionally, results did not find any technologies that provide early illness detection and intervention [35].

The placement of contactless biometric sensors in SBEs could be utilized for behavior change detection (BCD), health event identification and to send alerts when needed. One research team, led by Washington State University, theorized that an algorithm, such as BCD, implemented in a SBE can be utilized to understand the behavioral impacts of health events, and potentially be used for early detection of these events. To investigate this idea, the team equipped smart homes with combination door/temperature and motion/light sensors on cabinets, doors and ceilings. Overall, this study provides evidence that detecting behavior change and health events can be done with contactless sensors in SBEs [121].

These concepts can be incorporated together to combine the capabilities of smart living, such as appliance control, with the medical services desired in HSHs, to create a SBE with complete health monitoring [71]. Such a SBE provides the necessary technology for the integration of contactless heart rate and breathing rate monitors.

2.8.2 Smart Mobility

The other focus of this application is smart mobility. The ability to get around a city is vital. As the population density in cities increases, the problems surrounding mobility such as traffic, pollution and safety, become rapidly more important to solve. Benevolo et al. classified the current initiatives to support smart mobility into the following categories: public organizations, private companies, public bodies, and the combination of these three categories. Each category has different priorities and uses different technologies to meet their goals. Some of the initiatives shared by these categories are electric vehicles, autonomous vehicles, ride sharing services and traffic control systems [16].

Just as the concept of IoT is vital to smart living, the idea of Internet of Vehicles (IoV) is important to smart mobility. The automotive industry is changing rapidly as the focus turns to autonomous vehicles. These vehicles must gather information and communicate with each other without user interaction. To tackle this communication hurdle, the IoV is being constructed and the idea of a Vehicular Cloud was proposed in 2014 to provide services to these vehicles [51]. The idea of the vehicular cloud was further expanded to the Vehicular Social Network (VSN). This concept integrates the IoV and social networks to increase user information and interaction. Current applications of the VSN are Apple's Carplay and Google's Android Auto [98].

One benefit of transitioning to smart mobility is the potential to greatly reduce accident

rates. Currently, there are low level autonomous features being implemented in cars to help drivers react to other cars quicker and operate the vehicle safer. One application is collision warning systems. There are a variety of systems available that generate warnings to the driver when potential collisions may occur including forward, back-up, blind-spot, lane-departure, intersection and pedestrian collisions [20].

One specific type of collision warning system monitors the driver's awareness and generates warnings when the driver is drowsy or distracted. If the driver does not respond, some systems can take control of the vehicle [20]. Driver monitoring can be done is several ways. Commonly, vision-based systems use a camera mounted on the dashboard to interpret facial features such as eye direction and head orientation. Accuracy of such systems are around 85% and 90% and show great promise, but still require improvement [77, 134].

Although most driver monitoring systems are focused on collision detection and driver drowsiness, they have potential to be used for medical applications. A system that involved both driver awareness and health detection was implemented in 2012. This system detected eye features, but also utilized sensors that collected biometric data including ECG, PPG and temperature [75].

A handful of systems have been developed in the past decade that focus on driver health monitoring. Many of these systems utilized cameras to measure heart rate [107, 149]. Visual systems, however, are less reliable than physiological measurements. In a review of the available systems, Kang suggested that the following sensors are more reliable: ECG, electroencephalogram (EEG), electromyogram (EMG), electro-oculogram (EoG) and PPG. Several systems have utilized these sensors, but such systems typically used wearable devices, as discussed earlier [68].

A recent study by Sinnapolu et al. used the heart rate data collected by an Apple watch

and an in-vehicle microcontroller to monitor health and provide pull over assist is needed. Additionally, this system utilized cloud-centric IoT for communication mechanisms [120]. This system uses a less intrusive device which aids in the performance of the system. These systems could all be improved by gathering biometric data with the contactless sensor techniques discussed in Section 2.6.

As vehicles become more autonomous, they are consequently transitioning to a SBE platform. Further, smart built vehicles (SBV) can provide similar capabilities as SBEs. Additionally, the frameworks highlighted here support the feasibility of health monitoring in these SBVs. This application provides an additional viable environment for contactless heart rate and breathing rate monitors.

2.9 Discussion

In this review, we illustrated the importance of health monitoring using heart rate and breathing rate and discussed the available wearable and contactless devices. Overall, research in this area has made great strides toward enabling constant health monitoring. However, these devices are still limited at this point.

Specifically, wearable devices are often limited by the usability of the device. Wearable ECG and breathing rate devices in particular are often intrusive or uncomfortable for the user, which will prevent the devices from being used constantly and correctly. Wearable heart rate devices, on the other hand, show great promise. As discussed, heart rate trackers that use PPG are commonly found in fitness trackers and other wristband devices. Although the signal can be effected by motion, methods to decrease this noise are under study currently. If the current trend continues, these devices will continue to increase in popularity and accuracy, and will become more prevalent in health monitoring applications.

Contactless devices, in contrast, are nonintrusive, but they are typically affected by the position and orientation of the user. In this category of devices, breathing rate systems show more potential than heart rate systems. Among the available contactless breathing rate devices, current trends are focused on radar based systems. These systems show great potential, but are expensive. To reduce the cost, research has shifted toward using commodity WiFi devices. Results indicate that the accuracy of WiFi devices is similar to that of radar based systems. However, accuracy depends on the user's location and orientation. This may be overcome with mathematical modeling advances, device addition or device location manipulation. This area of research continues to increase in popularity and advance at a rapid pace. We expect the development of improved contactless breathing rate devices in near future.

We also outlined the potential applications for contactless health monitors. Research in smart homes, and HSHs in particular, continues to develop better platforms for constant at-home health monitoring using contactless breathing rate devices. Further, we believe HSHs provide the most practical and viable test bench for contactless breathing rate monitors because they can be easily incorporated into the WiFi devices already available in these IoT enabled homes. We expect the use of HSHs for testing and deploying health monitoring systems will continue to increase.

SBVs also provide a platform for enabling health monitoring in mobility. Such developments would allow individuals at risk of health events to be monitored at home and during transportation, to enable more freedom while still benefiting from complete health monitoring. SBVs have been used for limited health monitoring applications, but they are not currently a widely popular test or deployment environment for contactless breathing rate devices. Instead, SBVs offer a potential future application of such health monitors. However, we do not believe SBVs will become a main deployment environment in the near future.

Another possible research application of contactless breathing rate monitors and other health monitoring systems is in Smart Growth of Smart Cities. The goal of Smart Growth is to integrate information and communication systems into the basics of urban infrastructure such as transportation and energy distribution [59]. One necessary component of Smart Growth is the development of urban IoT. In this scenario, IoT aims to immerse the Internet into the entirety of daily life by interweaving communication into personal items such as home appliances and vehicles, and into city wide services and security systems. Establishing interactions between all these devices has the power to provide people with new information that can improve daily life in a widespread of domains. This new influx of data can also drive the development of Smart Cities [148].

There are many elements of Smart Cities. In 2010, Giffinger et al. defined the following key aspects of Smart Growth: smart economy, mobility, environment, people, living and governance [52]. In the context of implementing contactless breathing rate monitors into Smart Cities, this review has shown the current upward trend of implementing such devices in smart living applications and the possibility of smart mobility applications in the distant future.

Some may argue that these health monitoring systems can be expanded to the other aspects of Smart Cities. One concept is to create city-wide health monitoring systems by embedding a network of such devices into public buildings. This may be physically possible as city buildings continue to integrate WiFi devices.

However, integrating medical devices into any aspect of Smart Cities raises security and privacy questions. Specifically, the following questions need to addressed:

1. Who will own the data?

2. Who will have permission to access the data?

3. How will the data be used?

4. What security measures will be taken to protect the data?

5. Will citizens have the ability to opt out of data collection?

In most countries or geographical areas, health data is protected by a law or governing agency. For example, the United States passed the Health Insurance Portability and Accountability Act (HIPAA) in 1996. The Privacy Rule of this Act created standards for the use and disclosure of personal health information by certain covered entities (i.e., health care facilities, providers or insurers). Additionally, this rule established the individual's right to control how their health information is used. The Office for Civil Rights (OCR) is responsible for enforcing this act [100].

As with most of the similar laws or standards, the Privacy Rule covers the electronic transmission of any health information by the covered entities. That is especially important for health-related applications [55]. However, not all health monitor manufacturers are covered by HIPAA and many manufacturers create their own privacy agreements [5]. For example, Continuous Glucose Monitors (CGMs) can be obtained with a prescription and used to collect glucose readings. CGM manufacturers are not covered by HIPAA and can choose how to control the data collected [23].

Currently, the heart rate and breathing rate devices discussed in this paper are not covered by HIPAA. The manufacturer of each device controls how the health data collected is stored and shared. Prior to using one of these devices, the user is required to agree to the privacy policy. Commonly, fitness trackers and smart watches share or sell all de-identified health data. Additionally, some manufacturers share personal information as well. In the majority of the policies, the receivers of the shared data is unspecified [25].

This insight leads us to more specific security questions:

1. Should contactless heart rate and breathing rate monitor manufacturers be covered by a governing agency or law such as HIPAA?
2. Should the health data be transmitted to a doctor or medical professional?
3. Should the health data be used for research purposes?
4. How much control should be given to the user?
5. Should the answers to security questions be affected by the environment (e.g., smart living, smart mobility or other aspects of smart cities) in which the device is used?

These security and privacy questions must be addressed for all health monitoring systems. In the context of contactless heart rate and breathing rate monitors, these security and privacy topics remain unanswered and we believe these problems will hinder the implementation of such devices in all environments. Further, we foresee privacy to be the prominent hurdle in the implementation in any public aspects of Smart Cities.

2.10 Conclusion

Heart rate and breathing rate are important vital signs that can indicate a variety of health conditions. These rates are measured differently, but they are related and can both provide information regarding health status. Constant monitoring of these vital signs provides a way to predict harmful health events.

The review of wearable devices that monitor heart rate and breathing rate revealed the accuracy of such devices. However, this review also found these devices are significantly limited by their reliance on the direct contact with users. Contactless devices, in contrast, provide a comparable level of accuracy and are less intrusive. These devices, however, are

affected by orientation and movement of the user. This review suggests the need for further research to develop a contactless system that is less restrained.

Additionally, the environments in which contactless health monitors are applicable were discussed. Results suggest the primary application for these monitors is smart living, such as HSHs. This discussion also uncovered the unanswered security and privacy questions that will hinder the implementation of such health monitors. This review is limited by the concentration only on systems that detect heart rate and breathing rate. A review of systems that utilize the two other vital signs (blood pressure and temperature) is required to understand the full context of the health monitoring field. Additionally, this work is focused on methods rather than specific systems. Further work could provide details of the various systems available.

Chapter 3

Problem Definition

Chapter 2 provided a systematic review of the current methodology for heart rate and breathing rate monitors for both wearable and contactless systems and the viable deployment environments for contactless systems. The findings from the review reveal the limitations of the current systems and promotes the increased research in contactless breathing rate monitoring systems. Specifically, the findings call for the improvement of UWB radar based breathing rate monitors. This information was used to formulate a main research topic and research question, as well as to identify the corresponding research challenges.

3.1 Research Question

Radar methods encompass techniques that utilize microwave or RF. Commonly, such techniques derive breathing rate by capturing the low frequency mechanical signal caused by small chest inflections during the breathing cycle. The concept behind such methods is such: a stationary person's breathing rate matches the phase shifts of signals reflected off the person [81, 99]. One specific type, called UWB radar, emits a wide spectrum of low energy RF. UWB radar based systems show promising results, but this research is still in infancy. Further research is required to answer the following research question:

Can UWB radar be utilized to enable a fully functional breathing rate monitoring

system for an active user in a confined SBE?

The concept of fully functional is up for interpretation. For this work, we define a fully functional system as one that derives accurate breathing rate data within 10% of the true breathing rate. Further, such a system should maintain accuracy at all times in which the user is present in the confined space and should not be limited by user location, orientation or movement. The specific area covered by the system is dependent on the particular system but the minimum area should cover an average bedroom or living room. For the scope of this work, the system will be restricted to one user within range at a time.

As discussed in Chapter 1, the ideal system would collect breathing rate for each user, detect distress events, alert the user's connected devices and even call for emergency help when necessary. However, the scope of this research is focused on the breathing rate detection system. Further, a system will be considered fully functional based on the accuracy of the data collected and not on its ability to determine distress event occurrences. Additionally, system communication is not required either. These characteristics should be evaluated in future work on devices that are deemed fully functional.

The systematic review in Chapter 2 reveals that there are very few, if any, findings that address the research question. The UWB radar systems found show promising results but are not considered fully functional because they do not meet the requirements described above. Specifically, these systems are vulnerable to noise or limited by user positioning [62, 102, 141]. Current research is attempting to develop and test a system that answers yes to the presented question.

3.2 Research Challenges

In order to develop a system that answers the presented research question, there are several important challenges that must be overcome. The details and severity of each challenge is specific to the device and system design, but the generalized research challenges are as follows:

1. **Cost:** Many developed systems are expensive, causing them to be unaffordable for the common household.

2. **User Location:** Current systems are only functional when the user is in particular locations relative to the transmitter and receiver device(s).

3. **User Orientation:** Current systems are only functional when the user's body is oriented in particular angles relative to the transmitter and receiver device(s).

4. **User Movement:** Current systems are more vulnerable to noise or inaccuracy when the user is moving.

5. **System Placement:** The functionality of current systems depends on the placement of the transmitter and receiver device(s).

6. **Signal Processing:** Current methodology to derive breathing rate from the received signal is vulnerable to inaccuracies and noise.

Each research challenge will be discussed at length in the following subsections.

3.2.1 Cost

The cost of the system is important because it affects the population of users that are able to buy and benefit from the system. Traditional radar methods are expensive to develop and buy, causing them to be unaffordable for the common household. A breathing rate monitor is considered an amenity, not a necessity, for the common household. Even users with the highest risk of medical conditions and events will not prioritize this amenity if it is not affordable.

Recent research has shifted toward developing devices that utilize the same concept in less expensive ways. As discussed in Chapter 2, a current trend is to utilize commodity WiFi devices to extract breathing rate using the Radio Signal Strength (RSS) or Channel State Information (CSI) [102, 141]. Additionally, UWB is currently being investigated [110, 132]. These new methods provide affordable options, but they are still in the development phase and face the remaining presented challenges.

3.2.2 User Location, Orientation and Movement

One important advantage of contactless systems is the reduced intrusiveness. However, UWB radar based breathing rate monitors are still affected by the user's location, orientation and movement. In this context, location refers to the positioning of the user relative to the transmitter and receiver. Commonly, the accuracy of current systems is reduced or completely halted when the user is positioned too far away or in particular areas.

Orientation here refers to the angle in which the user's body is oriented relative to the transmitter and receiver device(s). UWB radar based systems rely on changes in chest inflection to derive breathing rate. These changes are undetected from the back of a user, so breathing rate can be incorrectly determined when the user is oriented away from the

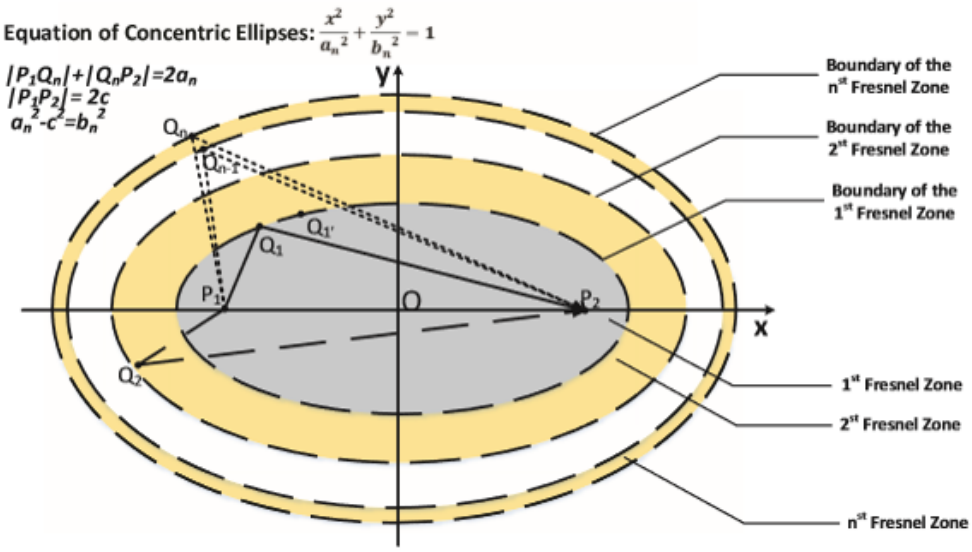

Figure 3.1: Fresnel Zones [141].

transmitter and receiver device(s). Further, the accuracy can be affected by even small changes in user orientation.

Wang et al. used the Fresnel Zone theory to explain the relationship between body location and orientation and breathing rate data when using the CSI method. The Fresnel Zone is the set of concentric ellipses formed around two transceivers. In Figure 3.1, the transceivers are P_1 and P_2 and the first Fresnel zone is the gray ellipse. More than 70% of the energy is transferred in this first zone. A total of n ellipses are then formed, including the first ellipse, with the width between ellipses decreasing [141].

When P_1 transmits a signal to P_2, the amplitude and phase shift of the received signal are determined by the distance between P_1 and P_2. When an object is placed on the boundary of a Fresnel zone, an additional signal path is formed and the received signal at P_2 is now a linear combination of the two signals. When an object is located at an odd numbered zone, such as Q_1, the phase shift is constructive which causes the received signal to be stronger than before. When an object is placed at a even numbered zone, such as Q_2, the phase shift

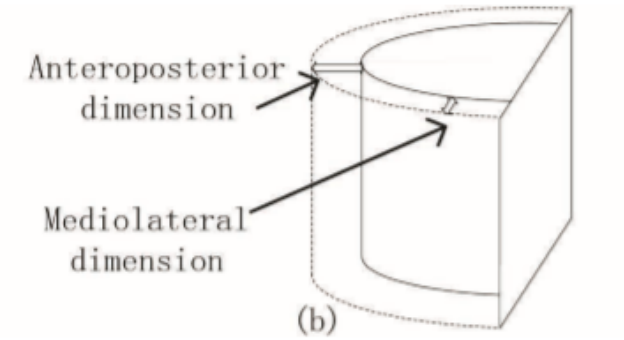

Figure 3.2: Model of human respiration system as a varying-size semi-cylinder [141].

is destructive which causes the received signal to be weaker than before [141].

When the object moves along an ellipse, such as $Q_{1'}$, the linear combination of the signal is constant, so the received signal is not affected. If the object instead moved outward from Q_1 to Q_n, the phase shift changes back and forth from constructive to destructive and the length continuously changes. The result is a signal with peaks and valleys [141].

To verify the existence of WiFi Fresnel zones, Wang et al. created an experiment using two WiFi devices, placed 70 cm apart and a metal cup. Then, they outlined the expected Fresnel ellipses and moved the cup along various axes. Results showed peaks and valleys in the received signal, as expected [141].

To relate this theory to breathing rate, the authors model a human as a varying-size semi-cylinder, as seen in Figure 3.2. Essentially, the chest moves in and out during respiration. The outer position occurs during inhale and the inner position occurs during exhale. This chest displacement is converted to the change of the reflected path length, which is further converted to the phase change. The authors estimate the phase change during the respiration cycle is between 60 and 150 degrees [141].

The respiration cycle includes inhale, pause, exhale, pause. The received signal is also four parts: a waveform generated by inhalation, a straight line caused by the pause, a waveform

generated by exhalation and another straight line. The depth of the breath affects the phase change and therefore, the generated inhalation and exhalation wave forms [141].

However, it's not that simple. This phase change is also affected by the location of the user. The authors show that the location with the worst accuracy is on the boundary of a zone and the best accuracy occurs in the middle of a zone. Additionally, the closer zones are more accurate than the outer zones [141].

To complicate this even further, the phase change is also affected by the orientation of the user. This method is not effective when the signal is reflected off of the subjects back because the body displacement on the back during respiration is almost zero. It is most accurate when the user is facing toward the line tangent to the ellipse [141].

To validate their theory, Wang et al. implemented a real-time respiration detection system using off-the-shelf WiFi devices. In the system, WiFi CSI data is collected and handled by their Signal Preprocessing module to reduce noise. Then, the data is analyzed by the Breathing Rate Estimation module. The authors used this setup to run two experiments [141].

In one experiment, the pair of WiFi device locations were fixed and one user was moved to various locations and orientations. To vary the location, the user was asked to sit in various chairs with 0 degree orientation. Results showed this method is effective when the user is located near the middle of the zone. However, the system fails when the user is located at a zone boundary. The location heat map shown in Figure 3.3 illustrates this claim [141].

To test orientation, the user sat in the middle of a zone and moved to various orientations. The system was most effective when the user was at 0 degree orientation, meaning they were facing the line tangent to the ellipse, and effectiveness was reduced as the orientation degree increases. At 90 degrees, the system became ineffective because the body was blocking the signal. The orientation heat map shown in Figure 3.4 illustrates this claim [141].

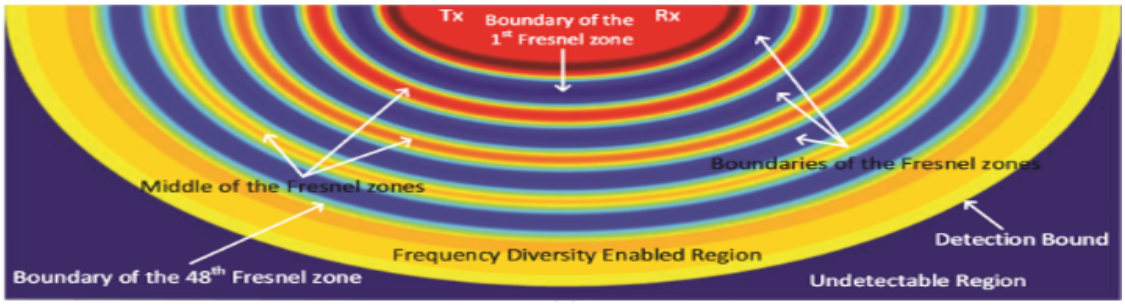

Figure 3.3: Location Heat Map [141].

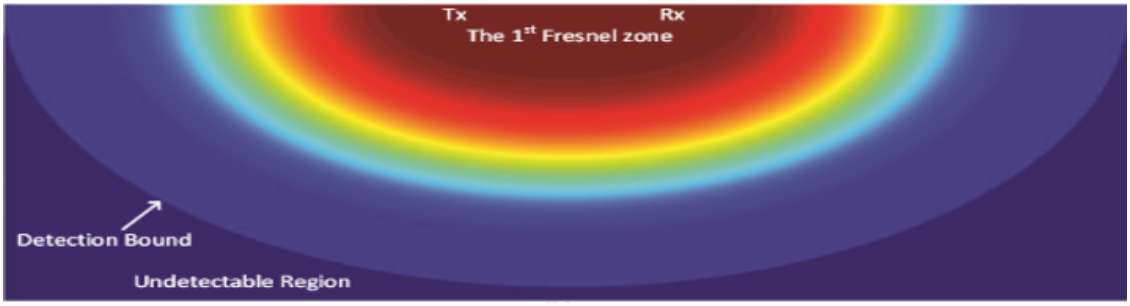

Figure 3.4: Orientation Heat Map [141].

These experiments revealed useful information about the effects of user location and orientation. However, these studies, and many others, only offer data for a still user. Further, the users are never asked to perform any movements during the data collected. This begs the question: are the results the same when the user is moving or are these devices not functional during user movement? There are a lack of user studies that address this question currently.

In order to be considered a fully functional device, it is important that accurate measurements are taken whenever the user is present. This should not be limited by user location, orientation or movement throughout the space.

3.2.3 System Placement

Another challenge of UWB radar based breathing rate monitors is the dependency on the placement of the transmitting and receiving devices. The specifics of this challenge is dependent on the system design. Some systems, such as the one used by Wang et al., use separate transmitters and receivers. In this case, the accuracy and area covered are dependent on the placement of each device. Wang et al. extended the previously described experiment to test this challenge. Results showed that placing the devices more than 3 meters away from each other decreased the accuracy because the system became vulnerable to noise [141].

Other systems use a single device to transmit and receive the signal. In this case, the placement of the single device will simply effect the area that is covered. Device placement must be taken into consideration when designing and installing such systems.

The area covered is also affected by the specific system design. As stated in Section 3.1, the minimum area covered should fit an average bedroom or living room in order to be considered fully functional. Many of the current systems are only functional in very small and specific areas. This dramatically decreases the usefulness of the system. Systems must overcome this challenge to be effective.

3.2.4 Signal Processing

Another challenge for breathing rate monitors is specific to the processing of the received signal. This topic is discussed in Chapter 2. To reiterate, a primary limitation of current device methodologies is signal vulnerabilities to noise. Current research aims to develop software that includes signal processing that can reduce noise for each data acquisition method described. These techniques are helping reduce this challenge, but more work is needed to ensure the data collected is accurate.

In summary, the following research challenges have been identified: cost, user location, user orientation, user movement, system placement and signal processing. The details and severity of each of these challenges are dependent on the specific system design. However, each of the discussed research challenges are vital aspects to consider when designing or evaluating a system in the context of the research question. Further, each challenge must be overcome in order to design a fully functional UWB radar based system.

Chapter 4

Proposed Approach

In Chapter 3, the main research question and the corresponding research challenges were identified. In order to investigate the research question, the aim for this work was to evaluate a newly developed commodity UWB radar based breathing rate monitor. Specifically, the breathing rate application in the Walabot was tested and analyzed in the context of the identified research challenges. In the rest of this chapter, the approach is explained and the main objectives of this work are broken down.

4.1 Approach

The proposed approach is based on our previous work on monitoring and analyzing psychological signals. Specifically, heart rate was monitored through a PPG enabled wearable wristband in several studies [34, 130]. Research surrounding these projects led to the discovery of a new and inexpensive commodity UWB radar device, the Walabot, that may have breathing rate monitoring capabilities. To gain a better understanding of this field, the current radar based breathing monitors were investigated during the systemic review. As discussed in Chapter 3, the findings from the systematic review helped formulate the research questions and corresponding research challenges.

The Walabot stood out as an interesting system because the breathing rate application is affordable and already available to consumers. However, the application's accuracy and

limitations have not been fully tested. Could the Walabot provide a solution to the proposed research question or does it face the same research challenges identified? The goal of this work was to thoroughly test the Walabot in order to uncover the accuracy and limitations of this breathing rate application in the context of the research question and challenges. The specific objectives for this work are broken down in Section 4.2.

The first step in evaluating this device was to provide an in-depth discussion of the device functionality and the breathing application provided. This started with a review of the available versions of the Walabot and the corresponding uses. Then, the breathing application was investigated, including a discussion of the software contained in the API. Next, we used the API to implement a breathing data acquisition technique for the Walabot (Chapter 5).

We then chose a medical grade wearable breathing rate monitor that could be used to draw comparisons. Such available monitors were reviewed in Chapter 2. For this work, we selected the MindWare Mobile Impedance Cardiograph device coupled with the Respiration Belt. This device was chosen because it uses a non-intrusive chest band that has been tested and is highly regarded as a reliable breathing rate monitor (Chapter 6).

After data is acquired from the Walabot and the Mobile, the data sets must be post processed to compute breathing rate. The signal processing techniques were implemented in a Matlab script. The script contained raw data comparison, two breathing rate computation techniques and breathing rate accuracy calculation capabilities. Chapter 6 describes and discusses preliminary script testing.

Next, we performed a comparative evaluation to determine the accuracy of the breathing acquisition and breathing rate derivation techniques for both devices. The study was designed in a such a way that provides insight to the research question. As discussed in Chapter 3, the research question is the following: can UWB radar be utilized to enable a fully functional

breathing rate monitoring system for an active user in a confined SBE? This concept of a fully functional breathing rate monitoring system was defined as one that derives accurate breathing rate data within 10% of the true breathing rate continuously while a single user is present within a confined space. Additionally, it was important that the study design reflected how the device would be theoretically used in a daily living space in order to make the data useful for real world applications. The following research challenges were also identified: cost, user location, user orientation, user movement, system placement and signal processing.

The definition of the research question and challenges and the emphasis on real world applications led to six design choices. These choices will be discussed in detail in Chapter 7 and are listed below:

1. Only one user can be present in the designated space.
2. The user must use different breathing rates to test the full range of possible breathing rates.
3. There must be at least one trial where the user must remain still and there must be at least one trial where the user must move.
4. The confined space should be approximately the size of an average living room or bedroom.
5. The Walabot must be placed in a variety of orientations with respect to the user's chest.
6. There must be at least one trial where the user sits, stands and walks in place.

With this study design in mind, four data acquisition procedures were designed. These procedures included breathing rate variation, horizontal placement variation, vertical placement

variation and user movement variation. Within each procedure, data sets of one minute each were acquired and the user was asked to count their breaths taken during each set. Multiple sets were acquired within the same data file, or trial. The breathing rates computed and the associated accuracies for each set are documented in Chapter 7. Finally, the results from the comparative evaluation is discussed in the context of the research question and challenges in Chapter 8.

4.2 Objectives

The main goal of this work was to analyze the effectiveness and limitations of a commodity UWB radar based device as a breathing rate monitoring system against a medical grade wearable breathing rate monitor. The commodity UWB radar based device chosen for analysis is the Walabot and the wearable system is the Mobile.

The second goal was to discuss the Walabot in the context of the posed research challenges to determine if this field can benefit from this system. The two main goals of this work can be broken down into the following objectives:

1. Analyze and discuss the methodology used to gather breathing rate provided by the Walabot breathing rate API.

2. Develop a breathing data acquisition script for the Walabot.

3. Develop and implement a signal post processing technique to compute the breathing rate of data collected by the Walabot and the Mobile.

4. Design a comparative evaluation to test the accuracy and limitations of the Walabot data acquisition and breathing rate derivation techniques.

5. Provide results from the comparative evaluation and discuss the accuracy and limitations of the Walabot data acquisition and breathing rate derivation techniques.

6. Discuss the Walabot in the context of the posed research question and challenges.

Chapter 5

Walabot Overview

There are many devices in research or production that use radar to remotely detect breathing rate. For this work, we focused on a new and inexpensive commodity device that uses UWB radar, called the Walabot. In this chapter, we discuss why the Walabot was chosen, how the Walabot works and the applications available. Then, the Walabot set up is explained and the given breathing rate application is analyzed. Finally, the developed data acquisition script is presented.

5.1 Motivation

As introduced in Chapter 4, the Walabot stood out as an interesting system because this device is available for consumers today and it is advertised as having breathing monitor capabilities. However, the application's accuracy and limitations were not fully tested prior to this work.

In the context of the presented research question, the Walabot is a UWB radar based device that may or may not be able to act as a fully functional breathing rate monitoring system for an active user in a confined SBE. There was potential for this device to provide a solution to the research question, but testing was required to reveal the effectiveness.

Prior to testing, it was evident that the Walabot does overcome the first research challenge:

cost. The version of the device that was tested in this work is available online for $599.95, which is too expensive for a common household. However, there are other versions of the Walabot available for $99.95 and $74.95 [139]. These versions provide the same breathing monitor capabilities at an affordable price. Further, an average household that is in need of a health monitor would be able to buy this device for a reasonable price.

Additionally, the Walabot provided an advantage for the user location and system placement research challenges because the system is contained in one piece of hardware, rather than having a separate transmitter and receiver. This allowed for simplification of the both challenges. Further, the manufacturer claimed the Walabot is functional within an area that is specified in the data acquisition software. Therefore, the user's location should not effect the functionality as long as the user is within the chosen area. Finally, the device could easily be placed on one side of the room with the front of the device facing the chosen area and the back facing the wall.

The Walabot's vulnerability to the remaining research challenges was unknown prior to this testing. Consequently, this device will be tested in the context of these challenges during this work to determine if it can provide the service of a fully functional breathing monitor.

5.2 Overview

The Walabot is a 3D imaging sensor that uses UWB radar to gather signals and construct an image of the surrounding environment [66, 140]. Inside the Walabot, there is a Vayyar YYR2401 A3 system-on-chip Integrated Circuit (IC) and an array of linearly polarized broadband antennas. The Walabot and the corresponding antenna array can be seen in Figure 5.1. The IC is responsible for producing and recording the radio frequency signals [140]. The information gathered is transmitted to the host environment via a USB cable. A block

Figure 5.1: **Left:** Walabot black shell case. **Right:** Antenna array [14].

diagram of this set up is shown in Figure 5.2.

This device uses non-ionizing UWB radio waves with a frequency range between 3.3 and 10 GHz. This frequency range is special because it allows the signals to transmit through dielectric materials, such as drywall and concrete, but the signals still reflect off most other materials such as wood and metal. Additionally, multiple pairs of transmit-receive antennas are used in order to develop a 3D image and sense movement or changes [66, 140]. This technology allows for a range of capabilities such as in-room imaging, in-wall imaging, object detection, location and tracking, change detection, speed measurement and motion sensing [140].

It is important to note that the exact frequency range is dependent on the model and the country. Specifically, the frequency of radio waves emitted is regulated by the Federal Communications Commission (FCC) in US models and received the CE Mark in European models. These chosen frequency ranges have been approved for safe human exposure [140].

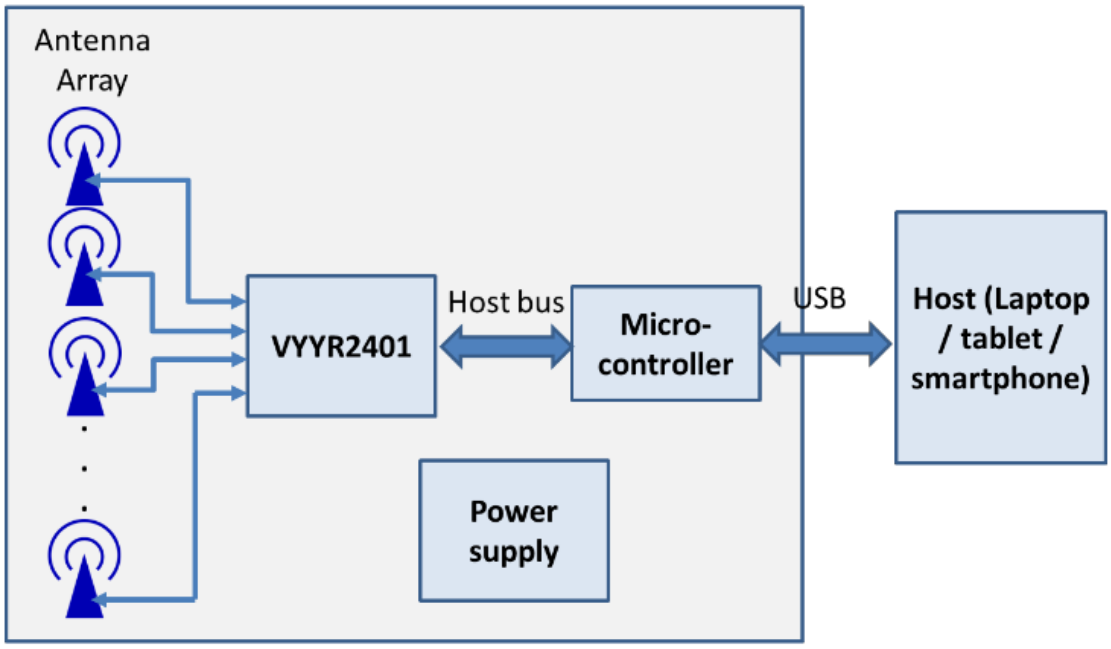

Figure 5.2: Block diagram of Walabot [140].

In fact, Vayyar is testing this technology for the use of a UWB mammography scanner in hopes of developing a contactless cancer screening device [103]. Additionally, a research team in Japan is currently testing the Walabot breathing application in an infant monitoring system to prevent infant death syndrome [111]. Many UWB radar based devices are also currently being developed and tested for human detection systems [6, 147, 151].

5.2.1 Versions

Currently, there are three versions available. The original device, called Walabot DIY (Do It Yourself), is advertised as a wall scanner that can be used for home renovation and construction. The device connects to the corresponding smart phone application, and allows users to see a real time video of the wood, pipes, wiring, metal or animals behind their walls [138]. An illustration of this functionality is shown in Figure 5.3

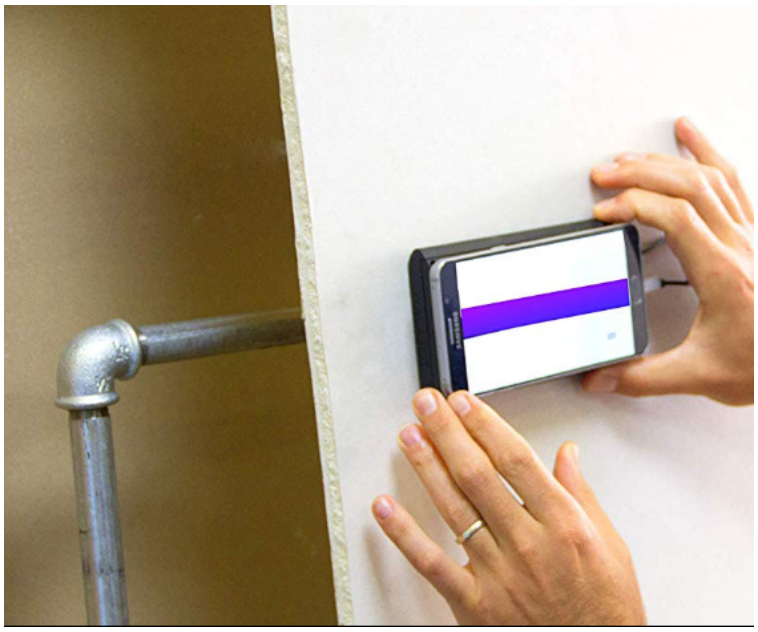

Figure 5.3: Walabot DIY model [125].

In 2018, Walabot released a new version called the Walabot Home, which provides contactless fall detection inside a home. In addition to the Vayyar sensing chip, the Walabot Home has a touchscreen, a machine learning tracking system and a two-way speakerphone. These elements can be seen in Figure 5.4. The device needs to be set up in the home once, where it learns the environment. The device then continuously monitors the movement of each individual in the home. In the event of a fall, the unit sends a text message and calls the inputted emergency contact [137].

The last version available is called the Walabot Maker. With this version, the user can develop custom applications using C++ or Python. Instead of connecting to a pre-made app, the Walabot Maker connects to a Raspberry Pi, Windows or Linux machine. There are three options for this version: the Developer, Creator and Starter. These options come with 18, 15 and 3 antenna arrays respectively, which have differing capabilities. An important difference is the Developer version includes the raw signal data. It is also important to note that all three versions include the breathing rate API, API documentation and code

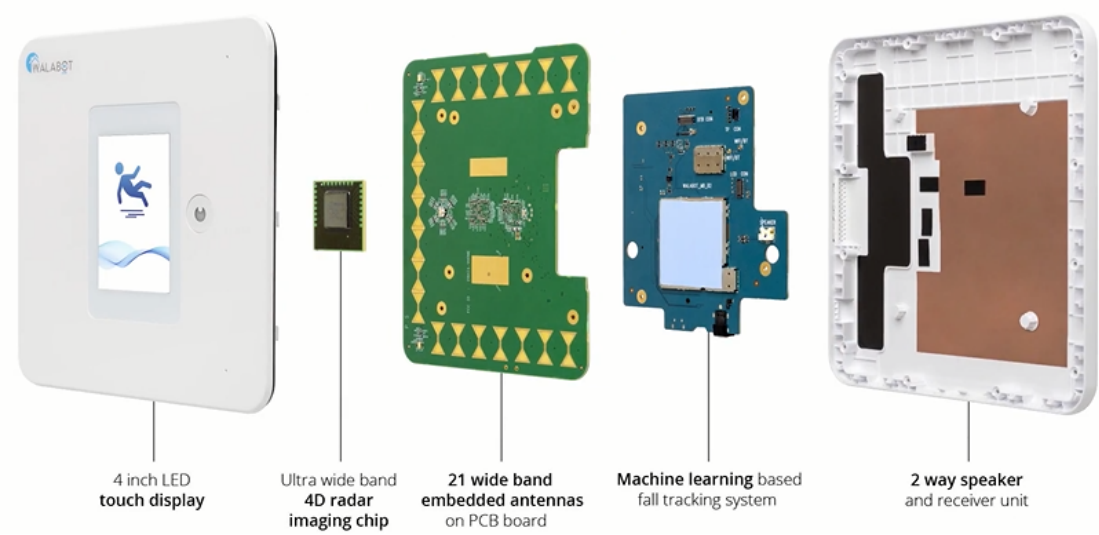

Figure 5.4: Walabot Home model system [137].

examples [139].

For this work, we choose the Maker version with the Developer Pack. The Maker version was intentionally picked for the flexibility and ability to develop and modify the software. The Developer Pack was chosen for the raw signal feature.

5.3 Walabot Developer Pack

The Walabot Developer version comes with the following specs: 18 antennas, Radar API, Breathing API, Range measurement, Motion detection, High 3D resolution, Imaging API, Raw signal data and Walabot black shell case [139]. Information about the API can be found at https://api.walabot.com/.

After receiving the Developer Pack, the first step was to download the SDK on the host machine. SDK version 1.2.2 was downloaded to a Windows machine for this work.

The installer includes a tutorial application called “walabot api tutorial“ and sample code [139].

In the tutorial application, there are five tabs to select from at the top: *HOW-TO*, *Sensor - Target Detection*, *Sensor - Breathing*, *Imaging - Short Range* and *Raw Signals*. The first tab, *HOW-TO*, provides a four step set up guide for the device. The two sensor tabs are the main topics of this chapter and are discussed below.

An important tab to note is *Raw Signals*. This feature shows the raw signals received in the form of amplitude over time. The signal strength of each antenna pair is affected by the positioning of the object in relation to the location of both the transmit and receive antenna.

Within this feature, the user can specify up to four antenna pairs to be shown on the live image. The corresponding antenna graphs (1–4) are displayed in red, green, blue and yellow respectively, as shown in Figure 5.5.

5.4 Set Up and Calibration

Before this device can be used, the device must be set up and calibrated. In this section, the physical set up and the parameters are discussed. Then, the Target Detection feature is used to perform preliminary testing on the device accuracy.

5.4.1 Physical Set Up

It is important to understand how to physically set up the Walabot. The device has semi-rectangular black shell case with the Walabot symbol on one side. The side with the symbol is considered the back of the device. The opposite side is plain black and is considered the front. The antenna array is located below the case in this position and the antennas are configured as shown in Figure 5.6. This side should always face the person or target object.

On the bottom of the device there are three connection ports. One of the micro-USB

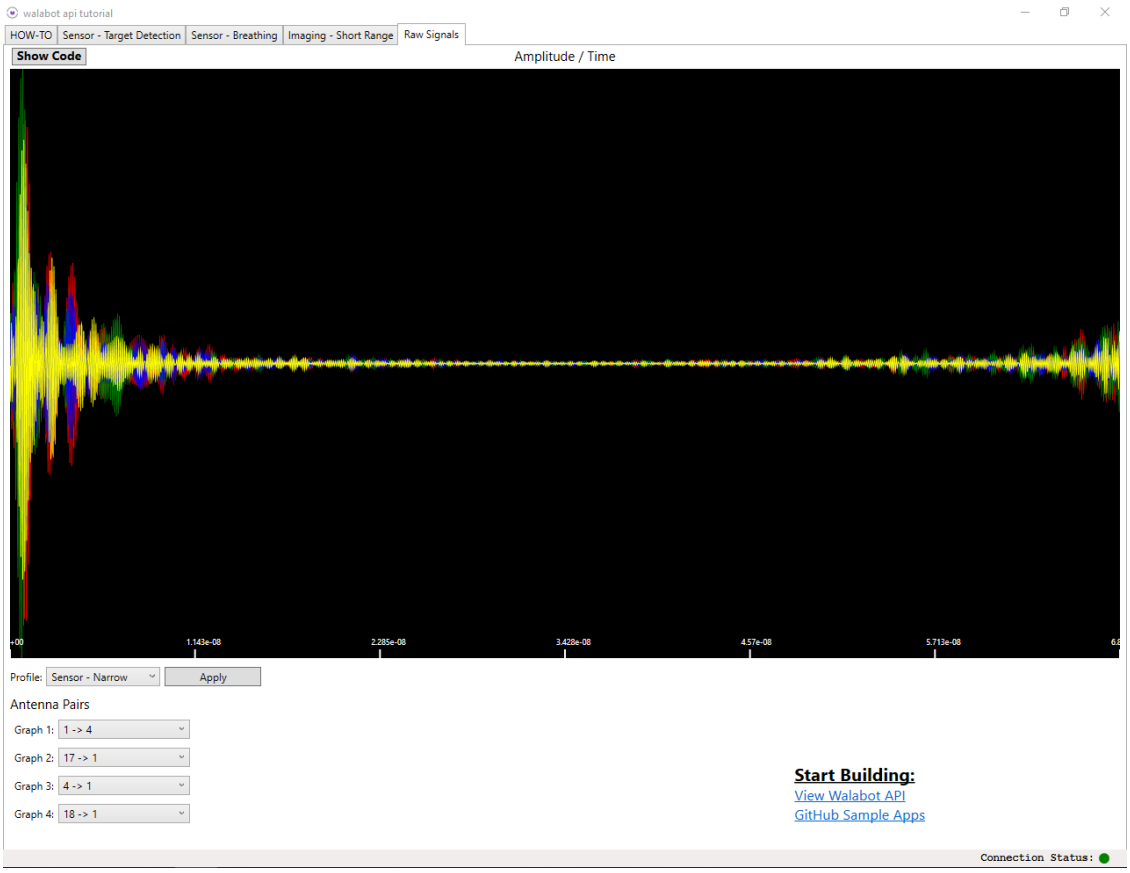

Figure 5.5: Screenshot of *Raw Signals* tab.

connection ports is used to connect the device to the machine using a micro-USB to USB cable. The other ports were not used in this work.

With this orientation in mind, the origin is the center of the front side and the Cartesian and spherical coordinate systems are as shown in Figure 5.7. How these coordinate systems are used is discussed in Section 5.4.2.

5.4.2 Parameters

In the Developer pack, there are 18 antennas available. However, not all 18 antennas are used for every application. A parameter called the profile is used to set what antenna pairs

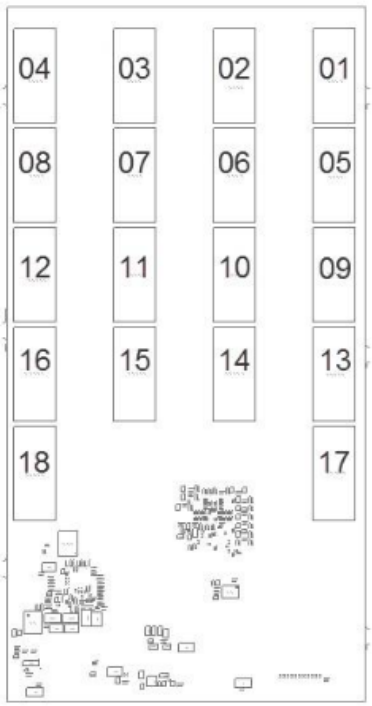

Figure 5.6: Walabot Developer antenna arrangement [140].

can be used. There are four profile selections available in the code: short range imaging, tracker, sensor and sensor narrow.

The first profile, short range imaging, is primarily used for in wall detection [136]. The tracker and sensor profiles are used for distance scanning with high-resolution, but slow capture. The target detection feature is an example of an application that uses the sensor profile [136]. The sensor narrow profile is also used for distance scanning, but it has a lower resolution and a faster capture rate. This profile is used for movement detection applications, such as breathing rate monitoring [136].

The area in which the sensor scans is known as the Arena. Note that the device should be oriented as explained above and shown in Figure 5.7 to ensure correct understanding of the Arena and the coordinate systems. For short range imaging, the Arena is approximately the size of the device and can be specified using the X, Y and Z parameters, known as the

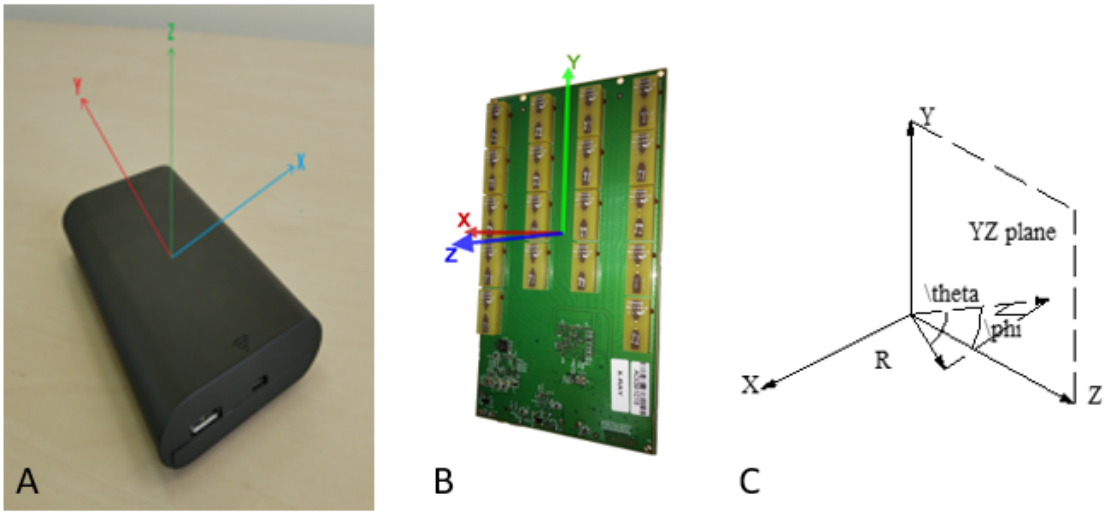

Figure 5.7: Walabot coordinate systems: **A)** Cartesian coordinates shown in black shell case, **B)** Outside of black shell case, **C)** Cartesian and spherical coordinates [136].

Cartesian coordinates [136]. X and Y can be up between -10 and 10 cm, while Z can be set from 1 to 20 cm.

For all other profile types, the Arena is specified by the following spherical coordinate parameters: R, *theta* (θ) and *phi* (ϕ) [136]. R is used to set the Z range from 1 to 1000 cm, while *theta* and *phi* give the Arena a cone shape by setting the horizontal and vertical range (Y and X axis) respectively, from 0 to 90 degrees.

When developing a new application, a user can choose to set the Arena using Cartesian or spherical coordinates. When necessary, the application automatically converts spherical coordinates to Cartesian coordinates (Equations 5.1–5.3) [136].

$$X = R * \sin\theta \tag{5.1}$$

$$Y = R * \cos\theta * \sin\phi \tag{5.2}$$

$$Z = R * \cos\theta * \cos\phi \tag{5.3}$$

Regardless of the coordinate system used, each parameter has a corresponding resolution parameter that can be set between 0.1 and 10. These resolution parameters dictate the power of their corresponding parameters [15]. It is important to note that the ranges for all the parameters are dependent on the feature being used.

There is an additional important parameter, called the threshold. This parameter is used to specify the intensity of signal filtering. Specifically, signals with a strength below the threshold are eliminated [136]. This can be set between 0 and 100. When the threshold is a lower number, the device is more sensitive and the image is more detailed. However, this may result in the detection of shadows or other reflections of background objects.

The Walabot API provides two options for dynamic-imaging filters: moving target identification filter and derivative filter. These filters are typically only used for applications that require movement tracking. The moving target identification filter eliminates static signals so only the moving signals are reported. This filter is used in the fall detection application [136]. The derivative filter is used to report the rate of change in data. This is used to see the small changes in chest movements during breathing in the breathing application [136].

Each time any parameter is altered in the tutorial application, the device must be calibrated using the *Apply&Calibrate* button. This calibration process allows the device to ignore the background environment such as walls and reflections. It is best to calibrate in a still environment because moving objects can disrupt the calibration process [15].

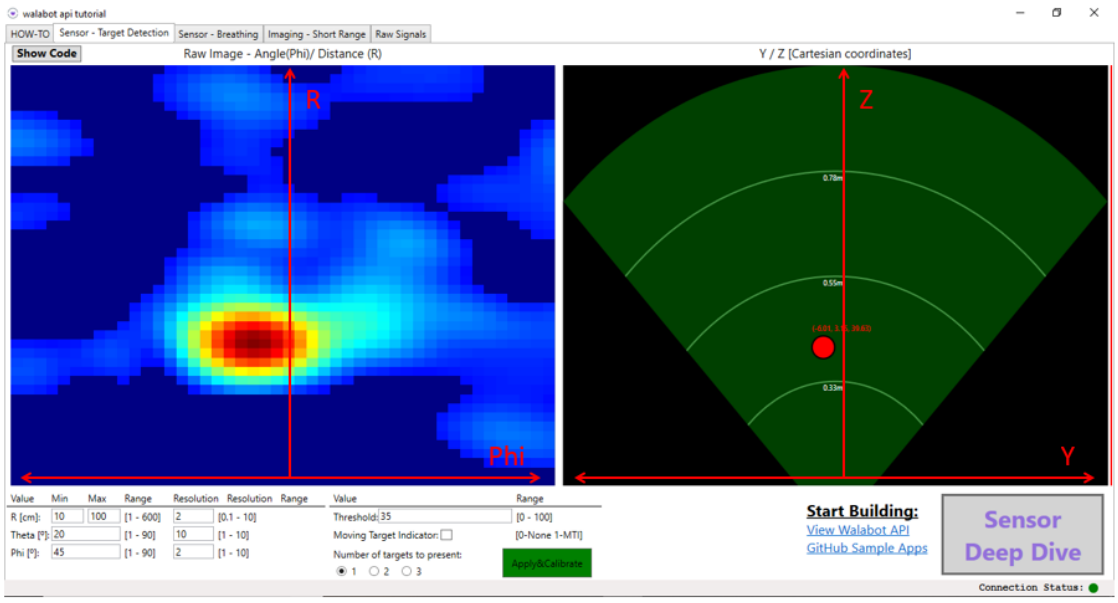

Figure 5.8: A screenshot of *Sensor - Target Detection* tab with corresponding axes.

5.4.3 Accuracy Testing using Target Detection

The first tab in the tutorial application, *Sensor - Target Detection*, is a great starting point because it allows a new user to become familiar with the device. This tab, as shown in Figure 5.8, contains two live images which are visual representations of what the antennas are receiving within this Arena. In simple terms, these screens indicate what the device is "seeing" in the *Z*-*Y* plane, as specified by *R* and *phi*. On the left is the raw image, which illustrates the intensity of the reflected signals [15]. Red represents the highest intensity, or the most reflected signals, while light blue is the lowest intensity, or a very small amount of reflected signals. Additionally, the location of these colors corresponds to the position in the Arena in which the signals are reflected from, in the *R*-*phi* plane.

The information received from the antennas are processed and used to detect object(s). The number of objects detected is set between 1 and 3 by the number of targets present parameter. The screen on the right illustrates where the detected object(s) is located in

the Y-Z plane with a red circle. See Figure 5.8 for an illustration of the Y and Z axes. Additionally, the circle includes exact X, Y and Z coordinates.

Note that the cone in the right hand image is dependent on the size of the Arena. The *phi* parameter changes the shape of the cone and the R parameter changes the measurements labeled on the cone. The *theta* parameter does control the size of the Arena, but it is not illustrated in this feature.

There is another parameter available in this screen, the moving target indicator. This parameter can be checked or unchecked. In Figure 5.8, this indicator is unchecked, meaning the images will show both still and moving objects. When this indicator is checked, the software will filter out still objects and only show moving objects [15].

The *Sensor - Target Detection* tab was used for preliminary accuracy testing and selection of parameters. First, the Walabot was set up with the front facing an open room and connected to a laptop placed on a table below the device. A tape measure was placed on the floor from the point of the device until 350 cm in the Z direction. To ensure the 70 cm wide table was not identified during testing, the R range was set between 70 and 350 cm. The remaining parameters were left at their default values, as seen in Figure 5.9.

After calibration, a user moved to various positions on the measuring tape aligned on the Z axis to check the accuracy of the reported Z value. The set up and an example of user positioning at roughly 125 cm is shown in Figure 5.10. Figure 5.9 illustrates the corresponding feedback from the device, reporting the object was 126.76 cm away. The results from preliminary testing can be seen in Table 5.1.

Using only the data points reported in Table 5.1, the Walabot identified the user within 6 cm of their true Z position. However, there are important issues with the data collection process used that may have led to the slight inaccuracy of the data. First, the user was

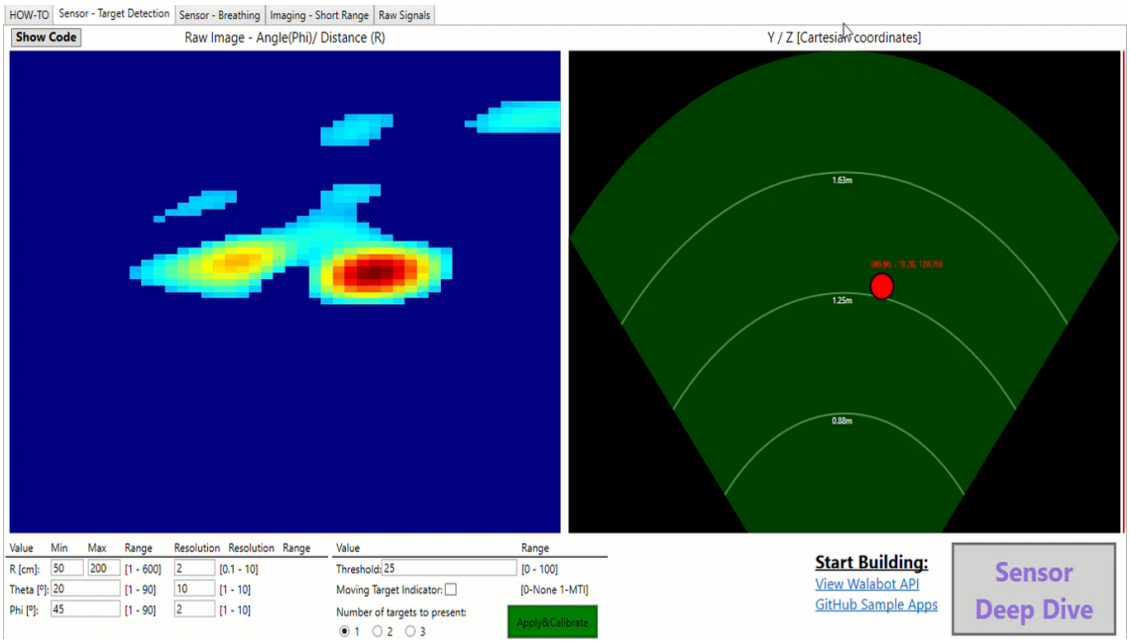

Figure 5.9: A screenshot of preliminary testing of *Sensor - Target Detection* tab.

Table 5.1: Target detection preliminary testing results.

User Z Position (cm)	Walabot Target Z Position (cm)
100	105.75
150	154.66
200	202.50
250	246.43
300	301.21
350	Target identified but numbers not shown

instructed to stand with one foot on each side of the measuring tape at a designated spot, such that the indicated position was at the middle of their feet. To the human eye, the user appeared to be lined up correctly during each collection point. However, the exact position of the user's feet and rest of their body has a great affect on the reported location. If the user was not lined up exactly the same each time, the points will be slightly inaccurate.

Additionally, the device continuously receives signals bouncing off the entire user's body. Since human bodies are not flat objects, the received signals will be from various reflection points [97]. This caused the reported value to constantly change during testing, even when the user was standing still. The estimated variance in the detected location during one data

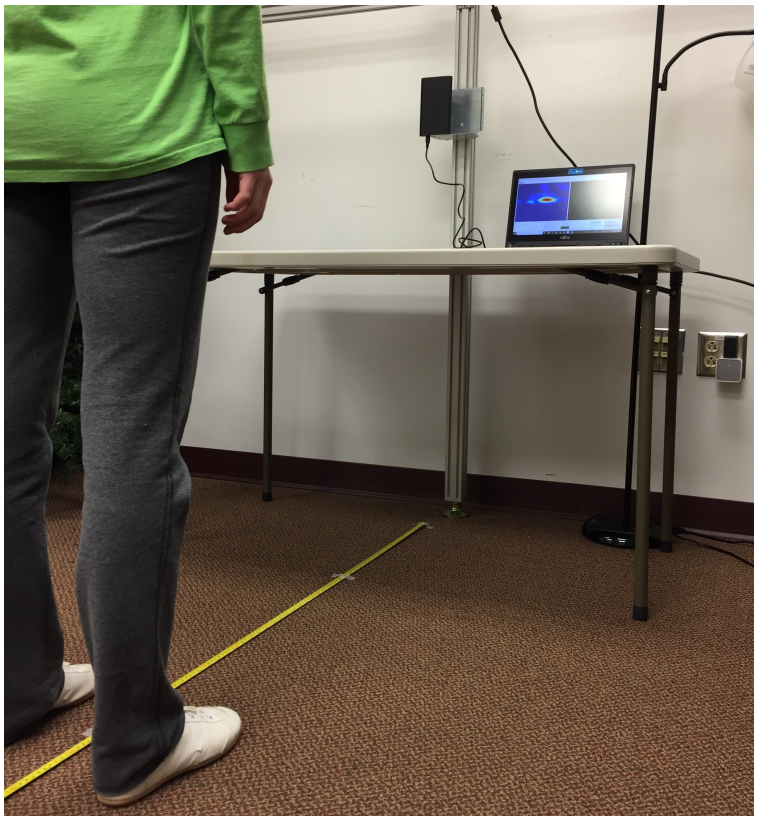

Figure 5.10: Set up and example position during preliminary testing of *Sensor - Target Detection* tab.

collection sample was roughly 5 cm.

It should be noted that when the user was located at 350 cm, the target was detected and shown on the screen with a red circle. However, the circle was at the very edge of the range so the exact detection location could not be seen on the screen.

Additional testing was performed by varying the parameters to see their effect on the accuracy of the data. For this room and the desired effect, the default values yielded the best results.

Finally, the moving target indicator was tested. The indicator was turned on and the device was calibrated with no extra objects in the Arena. Then, a chair was placed in the Arena and a user moved around. When the user and the chair were right next to each other, the

device registered this as one moving entity. However, when the user moved away from the chair, the device identified the moving user and filtered out the chair as desired. This testing revealed the same results when the number of targets to detect was increased to two.

Overall, preliminary testing of the Target Detection feature was satisfactory. This test proved the effectiveness of the Target Detection feature, but it also revealed issues that will be taken into account in later testing. Further, the results were accurate within reason and the parameters affected the results as expected. Additionally, this testing helped the users gain understanding of the Arena and the device functionality.

5.5 Breathing Data Collection

The previous section provided a preliminary understanding of the Walabot, the corresponding parameters and the accuracy. In this section, the focus is the breathing application. First, the breathing feature in the tutorial application is tested and the corresponding code from the Walabot API is discussed. Then, we discuss an example of breathing code provided online. Finally, we outline the code we used to capture breathing data in this work.

5.5.1 Breathing API

The tutorial application provides a simple breathing activity where a user can watch a live image of their breathing. In the bottom right corner of this tab, there is an illustration of the appropriate Walabot orientation. When the user hovers over this image, it becomes larger. As illustrated in Figure 5.11, the device should be placed on a table on the long edge of the device such that the front is facing the user at the height of the user's chest and the bottom of the device is on the left hand side.

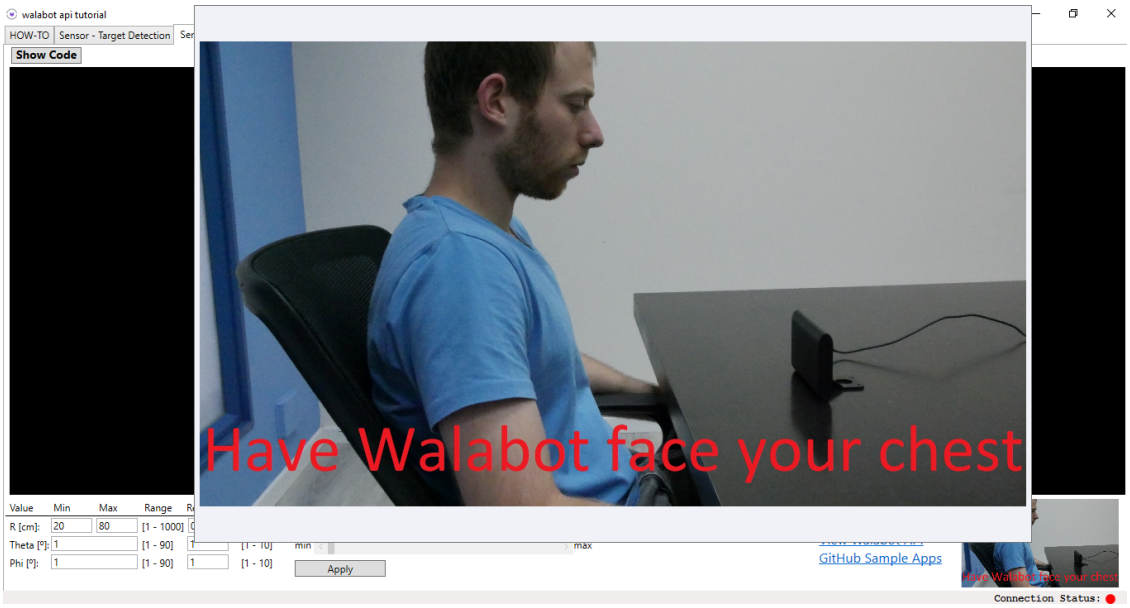

Figure 5.11: Proper orientation of Walabot during breathing data collection.

To test this application, the device was set up in front of a user as described. The distance between the device and the user was measured at approximately 40 cm, so the R parameter was set to range between 30 and 60 cm. The *theta* and *phi* parameters were set to 1 by default. These low values dictated that the Arena only protruded 1 degree in all directions. Increasing these parameters increased the Arena size, but it caused the live image to slow down significantly. To keep the image live, the parameters were kept at 1 each. The resolution of R, *theta* and *phi* were varied in attempt to determine the best combination. For this test, the values of 0.2, 5 and 5 gave the clearest results for R, *theta* and *phi* respectively.

Unfortunately, this feature appeared to have a low SNR in preliminary testing. Further, any extra movement caused the data to be effected greatly. Even when the user was completely still, the data was inconsistent and difficult to interpret. Additionally, the breathing activity was only distinguishable when the breaths were deeper than a normal subconscious breath. A screenshot of the breathing activity recorded during the best trial is shown in Figure 5.12.

In this tutorial application, the user can click on the *Show Code* button to see the pseudo

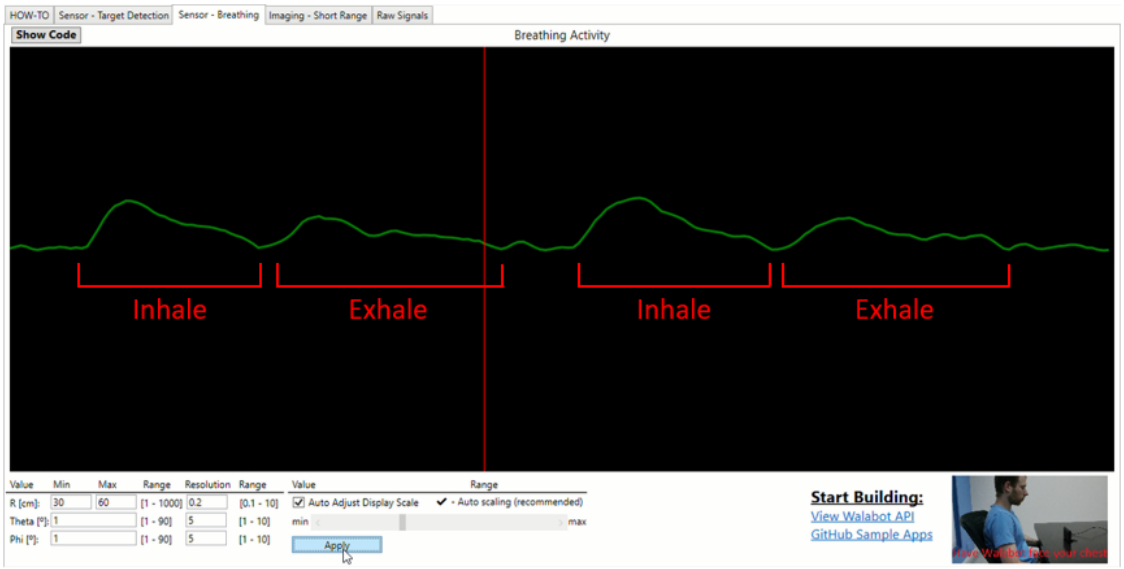

Figure 5.12: Best trial of breathing activity feature from tutorial application.

code for this breathing activity, as illustrated in Figure 5.13. This code is not complete but it does give the user a basic understanding of the data collection process used in this tutorial feature. Many of the lines are functions that are specific to the device and are included in the API. A short description of each function is provided in the right side of the pseudo code line. To see the full explanation of each function, see the API at `https://api.walabot.com/_sample.html`.

This program starts by connecting to the device. Then the profile type, Arena size and image filter type are specified. As discussed in Section 5.4.2, for any breathing application, the correct profile is sensor - narrow, and the recommended filter is the derivative filter.

The device is then started and a loop is used to continuously trigger a data reading, find the image energy and process the collected data. An important function used here is called GetImageEnergy. According to the API, this function "provides a number representing the sum of all the raw image's pixels' signal power" [135]. As described in Section 5.3, the signal strength of each antenna pair is affected by the positioning of the object in relation

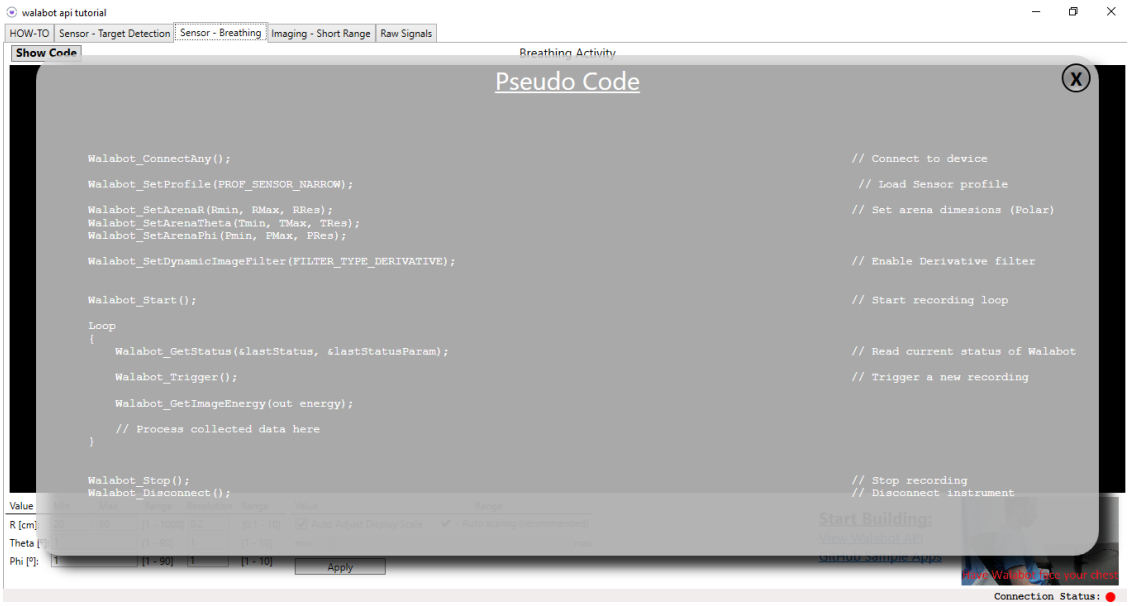

Figure 5.13: Pseudo code for breathing activity feature from tutorial application.

to the location of both the transmit and receive antenna. The recorded signal strength from each antenna pair is added together to determine the total strength, or energy, during the captured instance.

At this point, the pseudo code simply states "Process collected data here". In simple terms, the energy values are processed and then displayed on the graph in real time. The exact processing technique is not provided, but it can be assumed that the derivative filter is used to find the rate of change in energy values.

A similar but slightly different version of the code, in both C++ and Python, can be found in the API. This version provides numerical output, called energy, instead of graphical output. The energy is found using the GetImageEnergy function described above.

To fully understand how this breathing activity works, the Python code from the API was examined and run. This program follows the same structure of the pseudo code, but does not have any data processing. Instead, the energy value is simply outputted to the terminal.

It is important to note that this energy calculation does not appear to be affected by the use of the derivative filter [135]. When the Python code is run on its own, these untouched energy values are printed to the terminal. The values change constantly, but are typically between 200 to 3000 during static readings and get as high as 100,000 during movement readings.

5.5.2 Open Source Breathing Data Collection

After examining the API provided code, the internet was searched to find any other implementations of a breathing application using the Walabot Developer. Very limited information was found. As mentioned, one research team in Japan is currently testing the breathing application in an infant monitoring system to prevent infant death syndrome [111]. This team presented an overview of their system but details of their breathing application were not provided and the team is currently in the testing phase.

The only comparison of the Walabot breathing application to a trusted breathing monitor was found on the blog Hackster. The author, Kilani, is a researcher at the Research Institute for Aging in Waterloo, Canada, working on contactless breathing monitors [70].

Kilani started with the Python code for the breathing application provided in the API and made some modifications. The parameters he choose for R range and R resolution were 20 to 80 cm and 0.2. He set *theta*, *theta* resolution, *phi* and *phi* resolution all to 1. He also choose to not use the suggested derivative filter because the wearable device he was testing against did not use a derivative filter.

One significant addition to the code was file saving capabilities. Specifically, the energy and the time it was captured are saved to a comma separated values (csv) file each time a capture is triggered. This format allows the data to be easily post processed.

Figure 5.14: Walabot versus Bioradio respiratory belt data from Kilani testing [70].

Kilani also added a real time energy processing technique. During each data capture, the energy data was averaged with the last five data points before plotting. This was likely added to increase stability and reduce noise.

Finally, Kilani added an animation feature which outputs a real time graph of the averaged energy data, similar to the tutorial application. To output the data in real time, he used the matplotlib library and plotted 110 points at a time [70].

Kilani then tested the performance of his code against a Bioradio respiratory measurement belt. A graph of the Walabot and Bioradio data is shown in Figure 5.14. The two devices report data with the same shape in this output, suggesting the Walabot may be a viable breathing monitor. However, Kilani reported that the user had to sit completely still in order to maintain valid results [70]. This is only preliminary testing, but it does advocate for further testing of the Walabot's accuracy and limitations.

5.5.3 Breathing Data Acquisition Script

The code provided by Kilani was used as a starting point for this work. During preliminary testing, minor modifications were made including structural changes. One significant change at this time was the addition of the derivative filter. This was done in order to replicate the technique used in the tutorial application so the data could be visualized compared to the tutorial application.

The remaining parameters were varied for testing purposes but the majority of the param-

eters chosen by Kilani were ultimately kept as they provided the best waveform. One set of parameters that had a large impact on the waveform was *theta* and *phi*. As described earlier, these parameters set the size of the Arena. Instinctively, a larger Arena seems more useful. However, increasing the Arena size significantly reduces the sampling frequency (fs). This was first discovered when testing these parameters in the tutorial application and this held true during testing with this script. To keep the fs high, the ranges for *theta* and *phi* were both set to -1 to 1°.

One parameter that changed was the R range. This was altered such that the range was 20 to 80 cm, to reflect the position that the user was located during our testing. Specifically, the user sat in a chair such that their chest was approximately 60 cm away from the Walabot.

The results from preliminary testing of the adapted code can be seen in Figure 5.15. This waveform resembles the shape of the waveform found by the tutorial application in Figure 5.12. However, the new waveform was significantly steadier and less vulnerable to noise. This was likely caused by the processing technique added by Kilani which averaged the energy values before plotting.

Overall, the results from preliminary testing of the adapted code were promising. The waveform indicated a correct shape of breathing detection and the data collection process was easier than the tutorial application. However, the animation and average calculations restricted the fs to approximately 10 Hz or lower. The fs value is dependent on the rate in which the data was collected, which was determined by setting the interval at which data samples were taken in the animate function. To test this parameter, data sets were collected with the following intervals: 1, 100 and 200, where 1 corresponds to a fs of approximately 10 Hz. The smallest interval allowed was 1, and this interval proved to collect the data that appeared most consistent with the desired graph during testing.

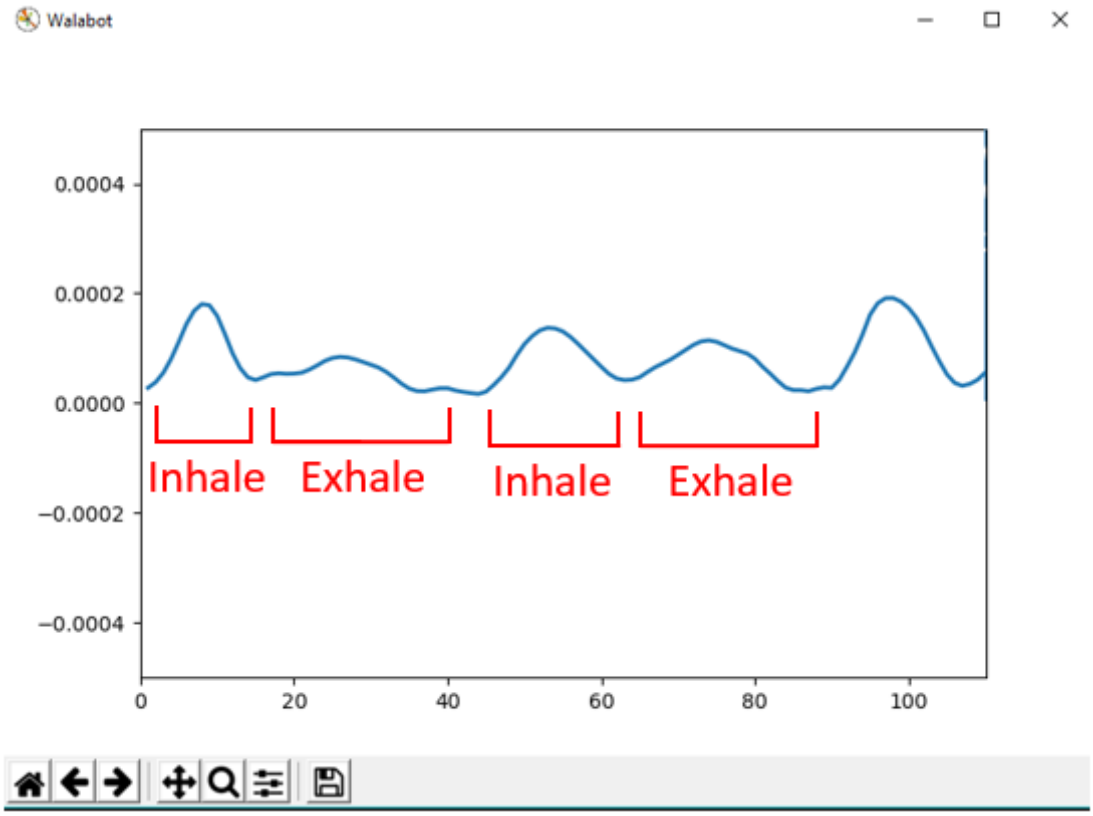

Figure 5.15: Output display of new breathing application.

Although a fs of 10 Hz appeared visually competent to collect breathing rate data, this frequency is very small in comparison to the fs of 500 Hz used in the wearable device. This wearable device fs cannot be changed, nor did we want to reduce this rate. Having a higher frequency is desired because this allows for an increase in resolution during signal processing.

With this in mind, the code was modified in order to reach the highest fs possible. As stated, the animation functionality and the average calculations restricted the fs. In order to increase the fs, these aspects were eliminated. After these changes were made, a consistent fs of approximately 40 Hz was reached.

One final change was made at this time: the use of the derivative filter was taken away. To recap, the derivative filter is used in the tutorial application and it is suggested for breathing

applications in the API, but Kilani did not use it in his work. We added the derivative filter to our modified version of Kilani's code during initial testing in order to replicate the technique used in the tutorial application. This allowed the data to be visualized compared to the tutorial application. After the animate function was eliminated and the visual was no longer the priority, the use of the derivative filter was removed.

This decision was made because Kilani proved in his work that this filter should not be used when comparing the Walabot to wearable devices. During preliminary testing of the signal processing technique described in the next chapter, this concept was validated. Specifically, the Walabot data is only comparable to the wearable data when the filter is not used because the wearable device does not use a derivative filter.

This code was used for the Walabot data collection for the rest of the work. The script has the following features:

1. Profile = sensor – narrow
2. R (radial) range = 20 – 80 cm
3. R (radial) resolution = 0.2 cm
4. *theta* (polar) range = -1 – 1°
5. *theta* (polar) resolution = 1°
6. *phi* (azimuth) range = -1 – 1°
7. *phi* (azimuth) resolution = 1°
8. Filter = none
9. fs = 40 Hz

10. User Specification = `username` specifies the folder name and `trial` specifies the file name.

11. Output = `.csv` file containing energy and time of capture columns.

Chapter 6

Data Collection and Signal Processing

In this Chapter, we first introduce the medical grade wearable breathing rate monitor chosen and discuss the device in detail in order to understand what the Walabot data is compared against. We then outline the methodology used to collect data from both devices.

As discussed in Chapter 2, the gathered data must be processed to extract breathing rate information. We outline the signal post processing script, including the methdology for aligning the data points and the techniques for deriving breathing rate.

6.1 Wearable Respiration System

The goal is to determine how the Walabot performs against a medical grade wearable breathing rate monitor. Such devices were reviewed in Chapter 2. As introduced in Chapter 4, the medical grade system chosen uses a Respiration Belt coupled with the Mobile Impedance Cardiograph, as seen in Figure 6.1 and Figure 6.2. The Mobile was chosen based on its high regards in the academic community and its non-intrusive nature. Version 1.4.1 of the firmware for this device was downloaded for free from the MindWare Support website [89].

The Mobile has the following channels: Bio, Z0, dZ/dt, GSC and Accelerometry. These various channels can be used for a variety of applications including ECG, EMG, EOG, GSR, Cardiac Impedance and Piezo Respiration Sensors, as seen in Table 6.1 [87].

Figure 6.1: MindWare Mobile Impedance Cardiograph [87].

For the majority of applications, data is collected by attaching electrodes to the subject at predefined locations. However, respiration data is collected by fitting a belt containing piezo sensors around the user's chest or stomach and connecting the belt to the Mobile via Bio channel 1 or 2. These bio channels are differential, DC-coupled voltage inputs channels. For this work, the Bio1 channel was used to attach the respiration belt.

In order to collect the best respiration data, MindWare suggests observing the user to see where the largest movement occurs on their torso during natural breathing. Then, the user should lift their arms and the belt should then be placed around the torso in that spot, such that two fingers can be fit between the torso and the belt [33].

The respiration belt contains piezo respiration sensors. As discussed in Chapter 2, piezoelectric sensors are a type of strain sensor that is commonly used to derive respiration rate in wearable systems. More specifically, piezoelectric sensors measure the piezoelectricity, or charge, created when stress occurs on a material, which is generated by the changes in chest

Figure 6.2: MindWare respiration belt for transducer module [88].

Table 6.1: MindWare Mobile input channels [87].

Signal Label	Color	Channel Name	Typical Use
BIO 1	Brown	Bio 1	EKG, EMG, Respiration, HRV
BIO 2	Orange	Bio 2	EKG, EMG, Respiration, HRV
CCS	Red	Z_0 and dZ/dt	Cardiac Impedance
SNS	White	Z_0 and dZ/dt	Cardiac Impedance
GSC	Green	GSC	GSC, GSR, EDA
GND	Black	None	Ground

movement in this application [2]. Due to the nature of breathing, the stress will be higher during inhalation and lower during exhalation. Visually, the data should resemble the sine wave shown in Figure 6.3 where the frequency is related to the breathing rate [93].

The Mobile can be configured to use WiFi mode or local mode. In WiFi mode, the Mobile can connect to the available WiFi and perform wireless data transmission to the BioLab Acquisition Software. This software can collect and record the desired data in real time. In local mode, all the gathered data is recorded on the SD card as a `.mwi` (MindWare) file. This file can then be visualized, edited and saved as an tab-delimited text file (ASCII) using the BioLab Acquisition Software [87, 114].

BioLab can be downloaded for free via the Mindware Support website [89]. For this work,

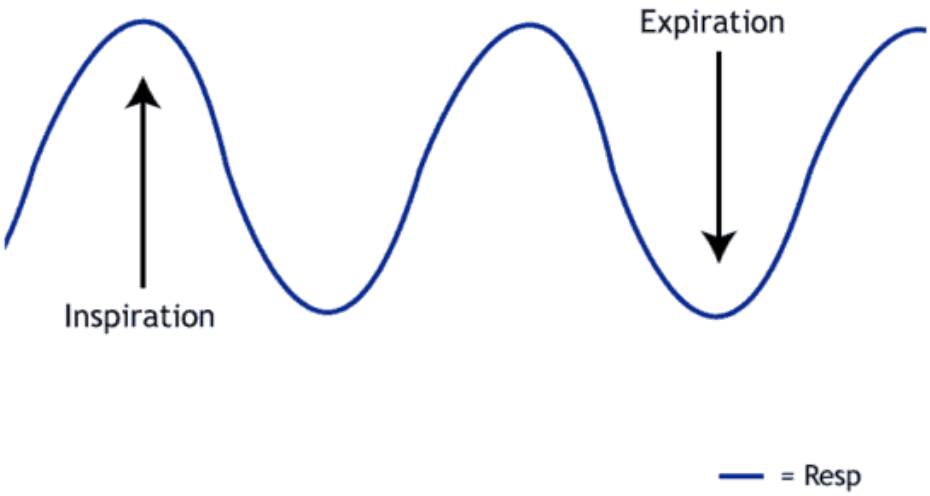

Figure 6.3: Breathing curve expected from MindWare Mobile respiration belt [93].

version 3.1.1 was downloaded onto a Windows 10 machine.

WiFi mode was chosen for this work because it offers more capabilities. Specifically, since the data is collected and transmitted to BioLab in real time, the collected data can be constantly observed to guarantee the collection process is functioning correctly. Additionally, BioLab contains 11 keyboard buttons that can be pressed during the recording time. When a button is pressed, the time of the corresponding keyboard event is recorded in a text file. These buttons were utilized to keep track of different data sets within one data capture. Specifically, keyboard button 1 was used to signify the start of a new data set and keyboard button 2 was used to represent the end of the latest data set. The process of aligning the Walabot and Mobile data using these keyboard button presses is outlined in Section 6.3.1.

Prior to recording data, BioLab must be connected to the corresponding Mobile. To do so, the Mobile and the machine running BioLab must be connected to the same Access Point (AP). Upon starting the software, BioLab automatically detects any Mobiles that are connected to that AP. The desired Mobile and the correct channels can be selected at this

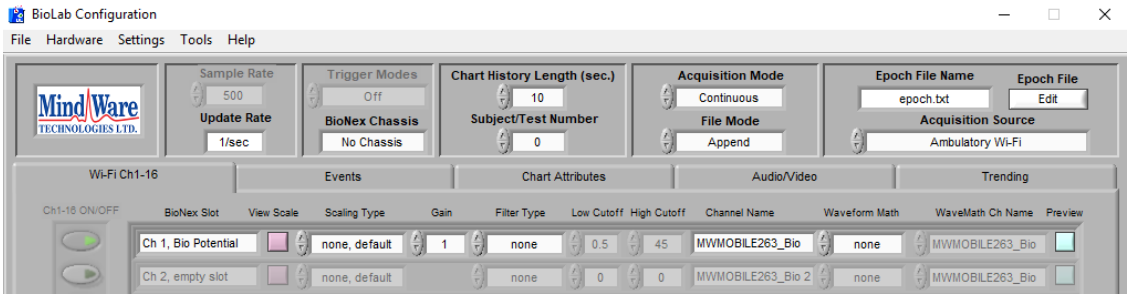

Figure 6.4: BioLab acquisition software channel settings.

time.

Next, BioLab must be configured with the correct channel settings, as seen in Figure 6.4. The Mobile's name can be seen in channel name slot. This channel has a set sampling frequency of 500 Hz. Since WiFi mode is used, the default acquisition mode is continuous and the default file mode is append, which allows the data to constantly be reported and added to a specified file.

Next, a filter type can be set. When choosing the respiration filter, the low cutoff frequency is set to 5 Hz, meaning only frequencies below 5 Hz will be recorded. This filter can be used at this point, but we chose to implement a low pass filter during post-processing instead. Data was compared with and without this respiration filter and the results were not effected significantly.

Finally, a trend can be set in order to track the breathing rate throughout data collection. To set a trend, the *Trending* window is chosen and the trend type *Resp Rate* is selected for the corresponding channel, as shown in Figure 6.5. In general, the chosen trend is a calculation that is graphed and recorded to a text file during data acquisition. When the respiration trend is set, the breathing rate, or breaths per minute (BPM), is reported. According to the MindWare Support Portal, the breathing rate is calculated over a sliding window of 5 seconds using FFT [93]. This technique will be discussed in Section 6.3.3.

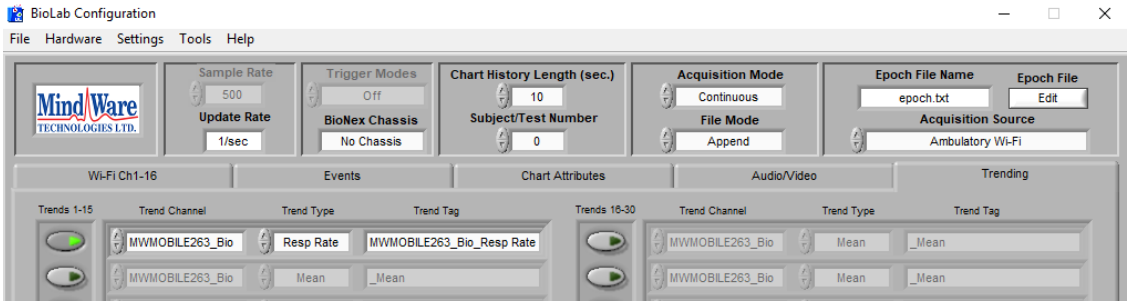

Figure 6.5: BioLab acquisition software trend settings.

6.2 Data Acquisition Methodology

In order to compare data from the Walabot and the Mobile, data must be collected from both devices at the same time. First, both devices and their corresponding data acquisition software were prepared.

When setting up the Walabot, it is important the device is physically orientated correctly, as illustrated in Figure 5.7 and Figure 5.11. For this work, the device was placed on a table on its long edge such that the front is facing the user at the height of the user's chest and the bottom of the device is on the left hand side. Due to the Walabot's rounded side edges, the device cannot stand in this way on its own so the device's box was placed directly behind it to provide support. Finally, the Walabot and laptop were connected via the micro-usb to usb cable. This setup can be seen in Figure 6.6.

As discussed in Chapter 5, a Python script was developed to perform Walabot data acquisition. Before each data collection, the script was prepared by editing the fields `username` and `trial` to reflect the correct user ID and trial number for the data collection. This step was important because the `username` field specifies the folder name and the `trial` field specifies the file name for the data file created. In this work, the Python script was edited and run in PyCharm 2019.2.1.

Figure 6.6: Walabot setup during data acquisition.

The Mobile required a more complex setup. First, the Mobile was turned on and WiFi mode was selected. The Mobile was then connected to the AP used in this work. See Section 6.1 and the MindWare Mobile Manual for detailed instructions regarding the set up of the Mobile device [87]. Then, the laptop was connected to the same AP and the BioLab Aquisition Software was started. Once the software initialized, it automatically detected the Mobile that was connected to the AP. The device was selected and Bio1 channel was initialized. Then, the BioLab channel and trend settings were configured with the settings shown in Figure 6.4 and Figure 6.5.

The respiration belt was then placed on the user. As explained in Section 6.1, MindWare suggests first observing the user to see where the largest movement occurs on their torso during natural breathing, Then, the belt was placed around the torso in that spot, such that two fingers can be fit between the torso and the belt [33]. Finally, the leads were be connected to the Mobile. Specifically, the red and black leads were attached to the Mobile via the Bio1 positive and negative connections respectively.

Then, the user was positioned as desired for the particular data collection set. At this point

Figure 6.7: Mobile respiration belt setup during data acquisition.

in the testing process, the user was asked to sit in a chair facing the Walabot. The chair was placed such that the user's chest was approximately 60 cm away at the same height as the Walabot. Additionally, the user was asked to sit up straight, place their arms by their side or behind the back of the chair and sit as still as possible. These specifications were added after preliminary testing revealed that even small movements or other arm placements greatly increased the noise picked up by the Walabot. This setup can be seen in Figure 6.7.

To finish preparing BioLab, the *Acquire* button was pressed. A prompt then appeared asking for the file name. In this work, we created a new file with the same folder name and file name as the Walabot. The software then took a few moments to configure.

The data was now ready to be collected using the following steps:

1. Initiate the Walabot data collection by starting the Python script. Upon start up, the Walabot status will be outputted to the terminal. Once the device is connected and

data acquisition is started, the terminal will read *Collecting Data*. This window can be minimized for now.

2. Initiate the Mobile data collection by pressing *Start* in BioLab.

3. Instruct the user to stay in position and breathing steadily at their normal breathing rate throughout the data acquisition.

4. Inform the user that the data set is about to begin. Ask them to count their breaths taken during the set. Start a data set by hitting *Keyboard Button 1* in BioLab. After 1 minute, end the data set by hitting *Keyboard Button 2* in BioLab. Ask the user to report the number of breaths they counted. Record this number in a text file.

5. Repeat the previous step until all desired data sets are taken.

6. Stop the Mobile data collection by pressing *Stop* in BioLab.

7. Stop the Walabot data collection by ending the Python script.

Five data files were used in post processing: the Walabot data file, the Mobile data file, the Mobile event recording, the Mobile trend recording and the user reported text file. The Walabot data file and the Mobile trend recording are saved automatically. The user reported text file should be generated during data collection.

To retrieve the other files, we opened the Mobile data file with the corresponding folder and file names specified in BioLab by pressing *File* then *Open File*. Then, the event recording was saved by pressing *File* and *Export Events*. Next, we pressed *View*. The File Playback window appeared, as shown in Figure 6.8. We then selected *Absolute Time* and dragged the time selection bar all the way to the right. Finally, we right clicked the small black wave button below the courser, then pressed *Export* and *Export Data to Excel*. The Mobile data file was then saved as an excel spreadsheet file.

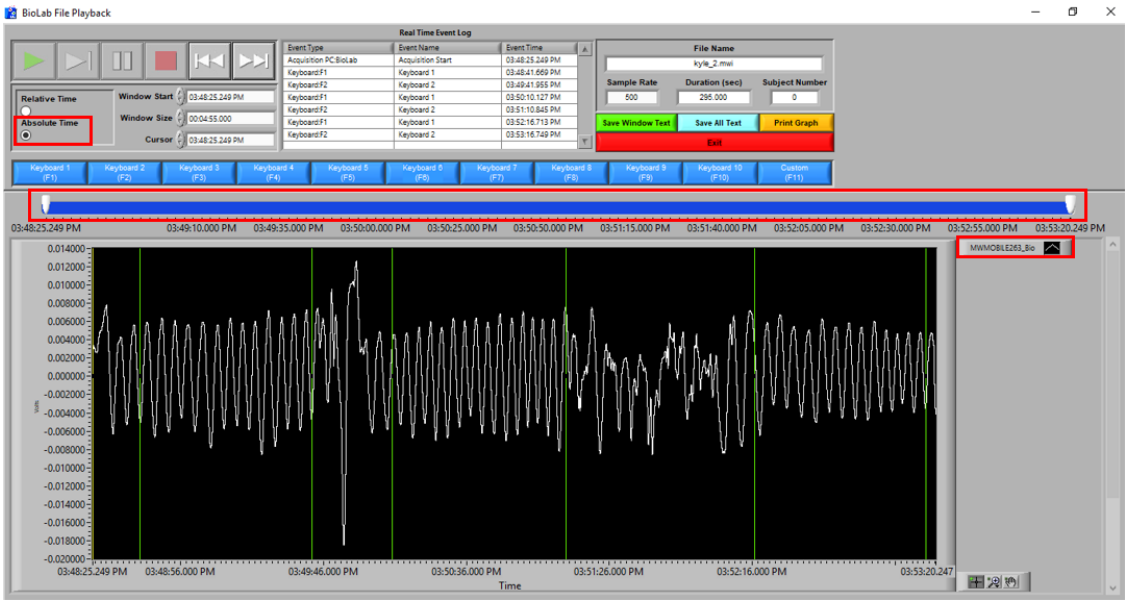

Figure 6.8: Buttons to press in BioLab *File Playback* window to save Mobile data file.

6.3 Signal Post Processing

After data from the Walabot and Mobile were collected, these signals needed to be post processed. A single Matlab script was created to perform all the post processing for this work. The first goal of the script was to align the two data sets, so that they could be compared. Next, a processing technique was needed to extract breathing rate from each signal. Two different techniques were developed: FFT and peak detection. Each technique is discussed thoroughly below.

6.3.1 Aligning Walabot and Mobile Data

Once data is collected from each device, the data needed to be aligned relative to time and fs. First, the post processing script reads in the five data files. Then, for each table, the column with the time data is extracted and the Matlab *datevec* function is used to create a separate table that contains 6 columns which correspond to the day, month, year, hour,

minute and second. This was done so that each element of the time (hour, minute and second) could be compared.

Next, the Walabot data is synchronized into the corresponding sets using the time stamps of the keyboard events. Specifically, the Walabot data from the data point with the closest time stamp to the time of the keyboard 1 event to the data point with the closest time stamp to the time of the keyboard 2 event is saved for each set.

At this point, the average fs for each Walabot set is also calculated. The fs is expected to be approximately 40 Hz, but this number is calculated each time to account for discrepancies caused by lagging in the Walabot data capture.

Then, the Mobile data points that correspond to the time stamps of each Walabot data points are saved for each set. Recall that the Mobile collects data using a fs of 500 Hz, while the fs for the Walabot is 40 Hz, as discussed in Chapter 5. This step is necessary because it aligns the fs of the two data sets while maintaining the precise time alignment.

Finally, the trend data for each set is synchronized using the event time stamps. This trend data reports the Mobile calculated breathing rate once per second during the set.

6.3.2 Raw Data Comparison

At this point, the data is aligned relative to set number, time and frequency. However, there are still important two differences in the Walabot and Mobile data: magnitude and stability. Although the devices collect the same information, they do so differently and the magnitude of the two signals shouldn't be directly compared. As illustrated in Figure 6.9, the Mobile raw signal does not have a significant DC component, whereas the Walabot has a large DC component. Once the Walabot DC component is removed, the difference in magnitude in the signals is visually noticeable.

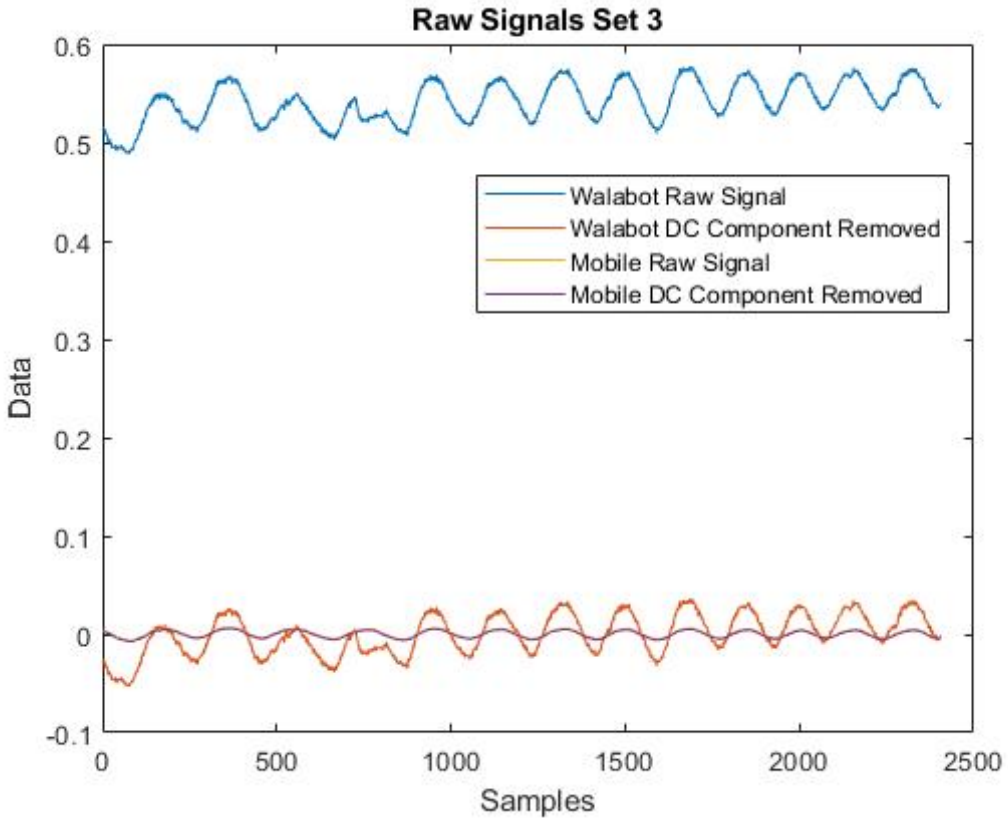

Figure 6.9: An example of raw Walabot and Mobile signals.

Instead, the shape and frequency of the wave should be compared. As explained in Section 6.1 and shown in Figure 6.3, the shape of both signals should resemble the expected respiration sine waveform with peaks and valleys corresponding to inhaling and exhaling respectively and the frequency of the wave should correspond to the breathing rate.

To disregard the magnitude element, the signals can be normalized using Matlab's *norm* function. In this work, we chose to normalize both signals between -1 and 1 for the best visual illustration of the signals.

With regard to stability, the Walabot data is noticeably less stable than the Mobile data. Kilani fixed this issue by averaging the collected energy values over a sliding window of five samples. However, we deleted this from the Walabot Python script in order to maximize

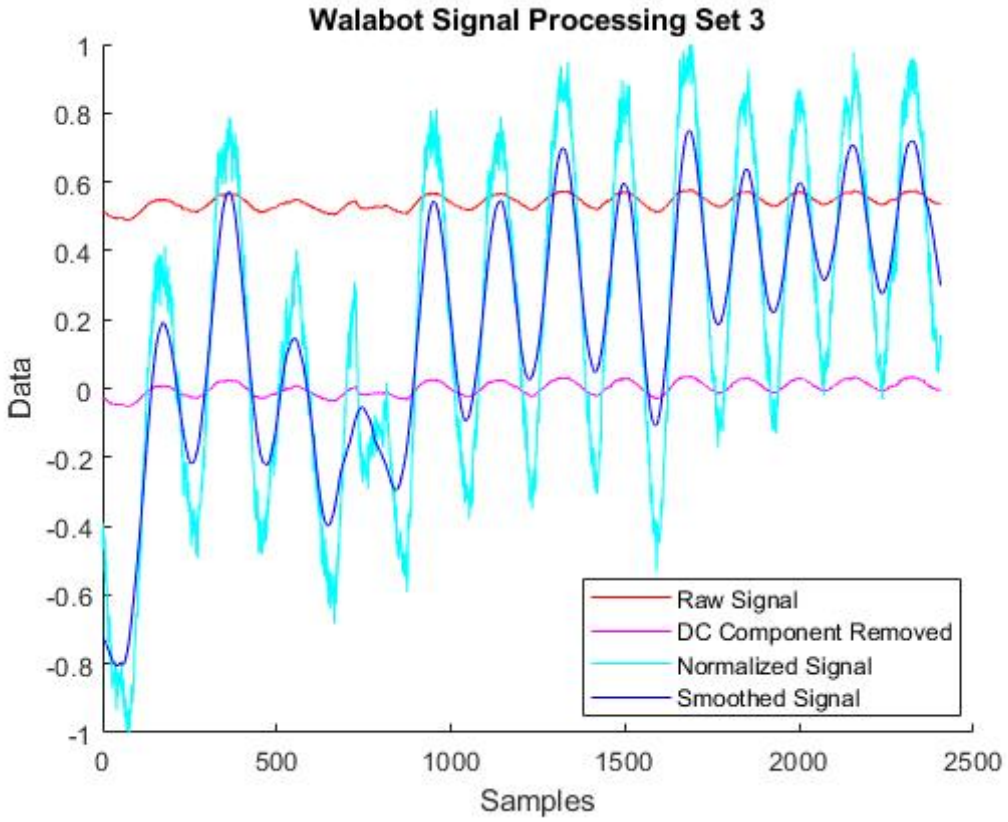

Figure 6.10: An example of the effects of normalization and smoothing on a Walabot signal.

the fs. Instead, this signal can be stabilized using the Matlab function *smoothdata*. This function is very similar to Kilani's implementation as it calculates the average using a sliding window. The effects of normalization and the smoothing can be seen in Figure 6.10.

The Walabot and Mobile data sets are now ready for comparison. The simplest way to compare the data is to graph each signal and visually compare the shape of the curves. In an effort to quantify this comparison, the Matlab *corr* function is used to find a correlation between the two signals. The outputted correlation coefficient is a number between 0 and 1, where a higher number indicates a higher correlation. However, the correlation coefficient is not a determination of signal accuracy because the concept of accuracy in this work is based on the breathing rate calculated from the signals. Further, the signals may have a

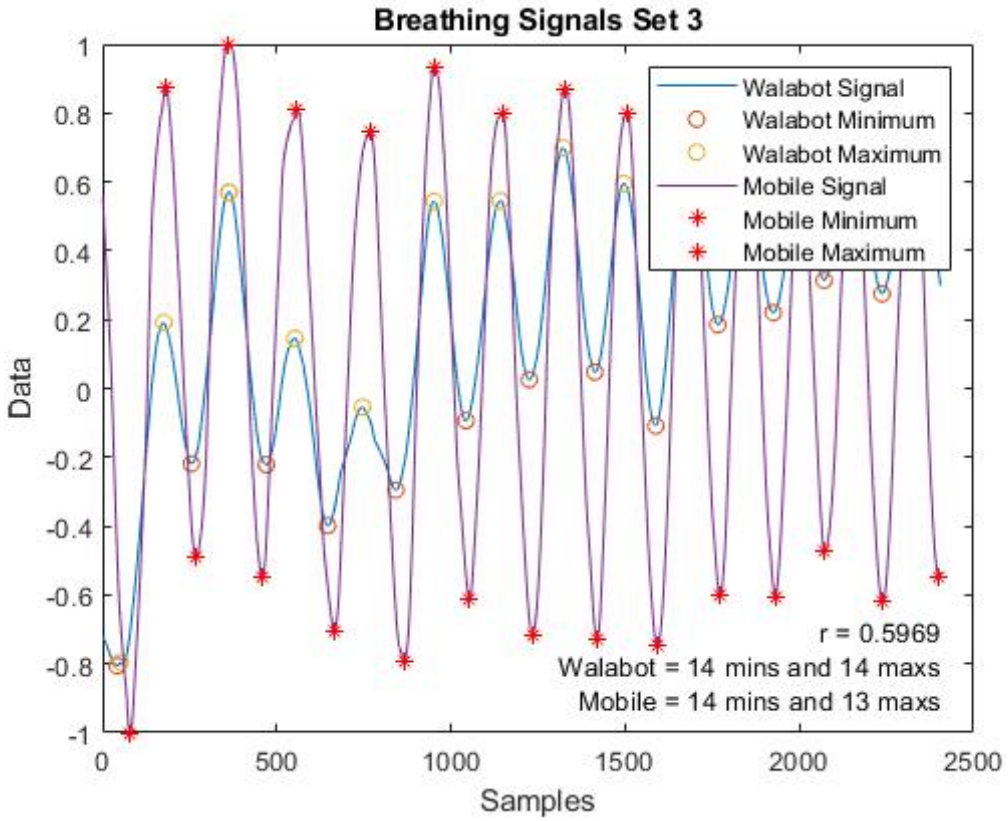

Figure 6.11: An example of processed Walabot and Mobile signals and their extrema and their correlation coefficient.

low correlation coefficient but both be highly accurate. Instead, the number of extrema within each signal is a better indication of accuracy because this number corresponds to the breathing rate. The Matlab functions *islocalmin* and *islocalmax* were used to locate and count the number of extrema in each signal.

An example of this signal comparison appears in Figure 6.11. The correlation coefficient is shown in the bottom right corner of the graph. In this example, the coefficient is 0.6755. Visually, the signals appear to have very similar frequencies and there are a very close number of minimums and maximums between the Walabot and Mobile signals. The correlation coefficient is not 1, however, because the shapes of the two signals vary.

6.3.3 FFT Signal Analysis Technique

Extracting breathing rate from raw data is a complex process that is still being researched today. In fact, there are over 100 methods for extracting breathing rate from ECG and PPG methods alone [26]. For this work, breathing rate must be extracted from the Walabot, which is categorized as a UWB radar based device. Signal processing of radar data to find breathing rate is a popular topic is research currently [80, 127]. There are many proposed extraction methods, but there is no gold standard technique for the Walabot at this point.

As a starting point, we attempted to replicate the calculation method used by the Mobile, as introduced in Section 6.1. Specifically, the Mobile uses a low pass filter, then calculates a respiration trend once per second using the FFT technique over a sliding window of 5 seconds [93].

The Matlab function *lowpass* can be used to implement a low pass filter that eliminates frequencies above 5 Hz. This frequency was chosen because the Mobile suggested this number for respiration signals.

Next, the sliding window was implemented using a while loop. In initial implementation, the window was set as five times the fs value, or 5 seconds. With a window of this size, the resolution was very low. This is a documented issue with the FFT technique and researchers suggest increasing the window size to increase the resolution in this case [146]. To test this, the window size was tested at 5, 7 and 10 seconds. The full test results are discussed in Section 6.3.5.

During each iteration of the loop, a FFT was performed on that window of the filtered data using the Matlab *fft* function. The FFT is a well-known technique used to calculate the Discrete Fourier Transform (DFT). Essentially, applying a FFT is used to convert the signal from the time to the frequency domain [32]. Commonly, this is done in a sliding window in

order to see smaller time periods and to evaluate the changes over time [57].

The DFT was used to find the fundamental breathing frequency. Specifically, the Matlab *max* function was used to find the index of the frequency with highest magnitude. At this point, the breathing rate could of been calculated by multiplying this frequency by 60. However, this data contains very few data points which causes the resolution of the DFT to be very low. With a low resolution, the calculated breathing rate is not very accurate.

To increase the resolution, spline interpolation was used [50]. Essentially, the point before, on and after the max index were cubically interpolated using the Matlab *interp1* function with the *spline* option. This option interpolates the three given samples points such that the cubic curve structure is maintained, as seen in Figure 6.12. The index of the frequency with the highest magnitude is now a more precise estimate and the breathing rate is calculated by multiplying this frequency by 60.

When the sliding window finishes, an extra filtering step is performed to clean up the breathing rate calculations. Specifically, the first and last breathing rate calculations are deleted. Then, any calculations below 6 or above 25 are deleted to disregard any values deemed unrealistic. These numbers were derived from the estimation that the average breathing rate for a healthy adult is between 12 and 20 BPM [29].

Then, the *mean* function is used to find the average breathing rate calculated throughout the set. To determine the accuracy of the average breathing rate, percent error was calculated and subtracted from 100, as shown in Equation 6.1. The mean and the accuracy were then outputted to the command window for viewing.

$$accuracy = (1 - \frac{abs(Calculated\_BPM - User\_Reported\_BPM)}{User\_Reported\_BPM}) * 100 \tag{6.1}$$

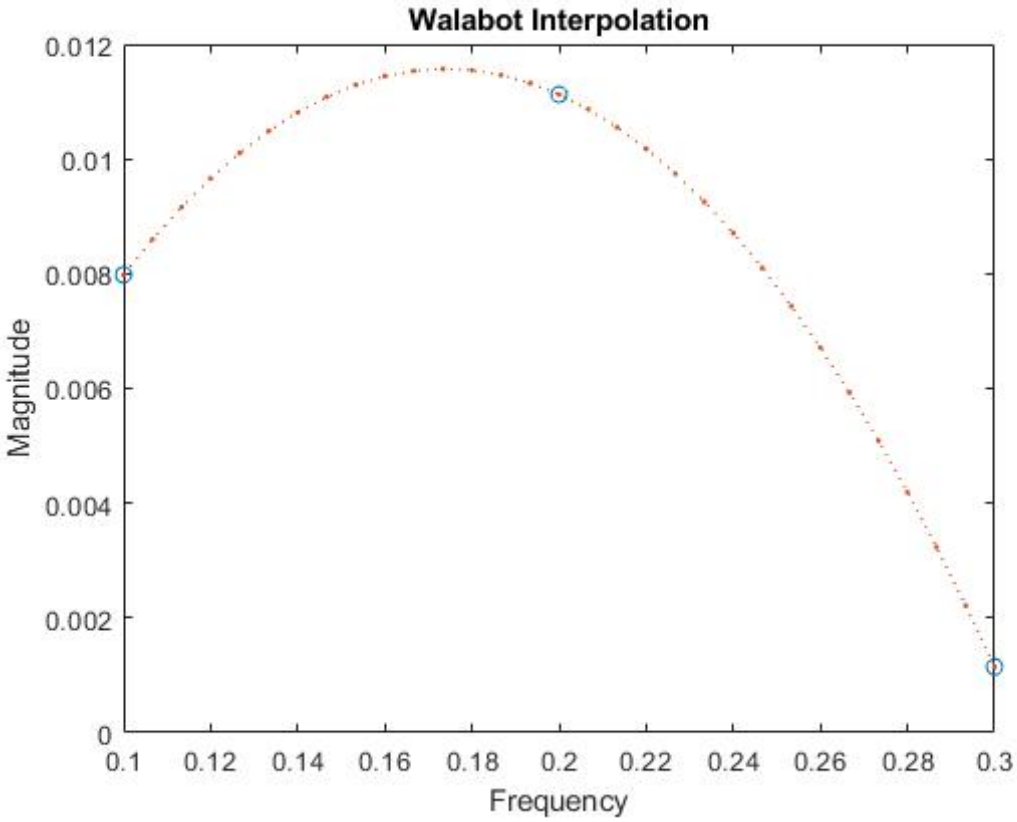

Figure 6.12: An example of spline interpolated Walabot fundamental frequency.

The entire procedure explained was used to calculate the breathing rate for both the Walabot and Mobile signals for each set. To illustrate the results, the calculated breathing rates and the averages were graphed, as shown in Figure 6.13. In this set, the average breathing rate for the Walabot was found to be 12.84 BPM and the average breathing rate for the Mobile was found to be 12.53 BPM.

Finally, the trends reported by BioLab for the breathing rate of the Mobile is graphed, as seen in Figure 6.14. In this example, the average reported breathing rate is 11.21 BPM.

The calculated average breathing rate for the Mobile data is 1.33 BPM above the reported average breathing rate. However, during this trial, the user counted roughly 13.5 BPM. Further, the reported breathing rate was not correct within 10%, while the calculated breathing

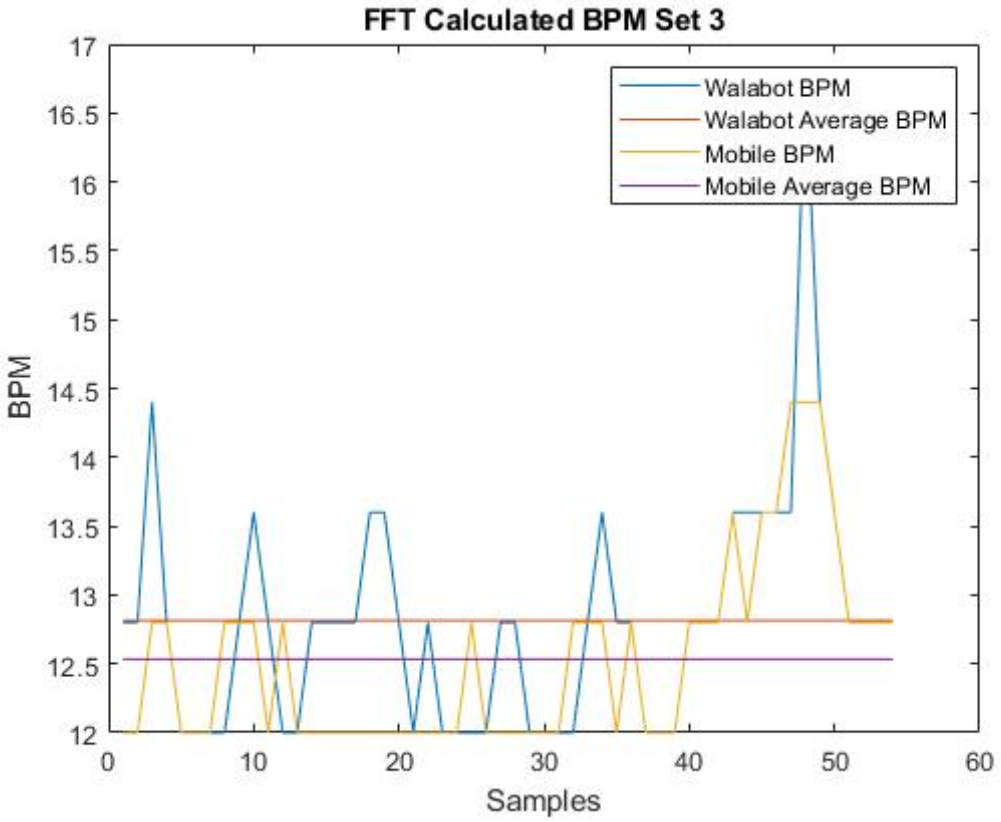

Figure 6.13: An example of BPM calculated from Walabot and Mobile data using the FFT technique.

rate for the Walabot and Mobile were both correct within 10%. This created doubt about the accuracy of the trend reported breathing rate, but it continued to be used in testing at this point.

6.3.4 Peak Detection

We implemented a second breathing rate extraction method. Yang et al. proposed the use of time-domain peak detection in order to extract breathing rate within a window of one breathing cycle, or 5 seconds. This technique was tested with Doppler radar, an ECG and a respiration band and yielded highly correlated results between the two contact sensors [146].

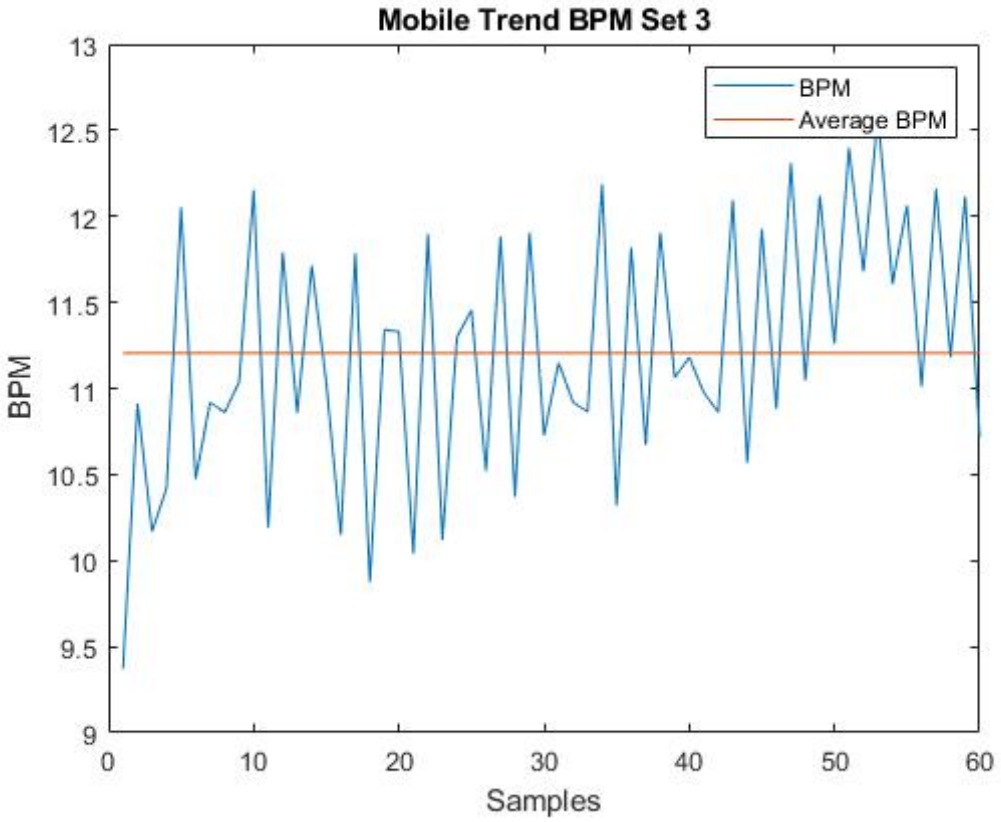

Figure 6.14: An example of BPM calculated by BioLab.

This test is quite similar to our work as it used both radar and a respiration band. Additionally, this technique was deemed a viable option based on visual observation of our collected data.

The first step was to implement the same lowpass filter used in the FFT technique. Yang et al. suggested the use of a bandpass filter, but we used a lowpass filter to maintain consistency between the post processing and the Mobile processing suggestions [146].

Next, the sliding window from the FFT technique was implemented again. As Yang et al. suggested, this technique can be done with a sliding window as small as 5 seconds. To fully test and compare our processing techniques, windows with 5, 7 and 10 seconds were tested. The full test results are discussed in Section 6.3.5.

For each window, the Matlab functions *islocalmin* and *islocalmax* were used to locate the indices with the local minimum and maximum points. The period was then calculated by doubling the time between the minimum and maximum points. Finally, the breathing rate was calculated using Equation 6.2.

$$BPM = \frac{fs}{period} * 60 \tag{6.2}$$

When the sliding window finishes, the extra filtering step that was implemented in the FFT technique is used again here to clean up the breathing rate calculations. Then, the average breathing rate and corresponding accuracies are computed.

This procedure was used to calculate the breathing rate for both the Walabot and Mobile signals for each set. To illustrate the results, the calculated breathing rates and the averages were graphed, as shown in Figure 6.15. In this set, the average breathing rate for the Walabot was found to be 13.38 BPM and the average breathing rate for the Mobile was found to be 13.68 BPM. With this extraction technique, the calculated breathing rate for the Walabot and Mobile were both correct within 10% of the user reported 13.5 breaths.

Additionally, the trends reported by BioLab for the breathing rate of the Mobile data were graphed, as seen in Figure 6.14. As explained in Section 6.3.3, the average reported breathing rate is 11.21 BPM for this data set which is not within 10% of the user counted breaths of 13.5 BPM.

6.3.5 BPM Calculation Comparison

To compare the accuracy of the Mobile reported breathing rate, FFT technique and Peak Detection technique, 3 sets of data were taken on a 23 year old male user. During each set,

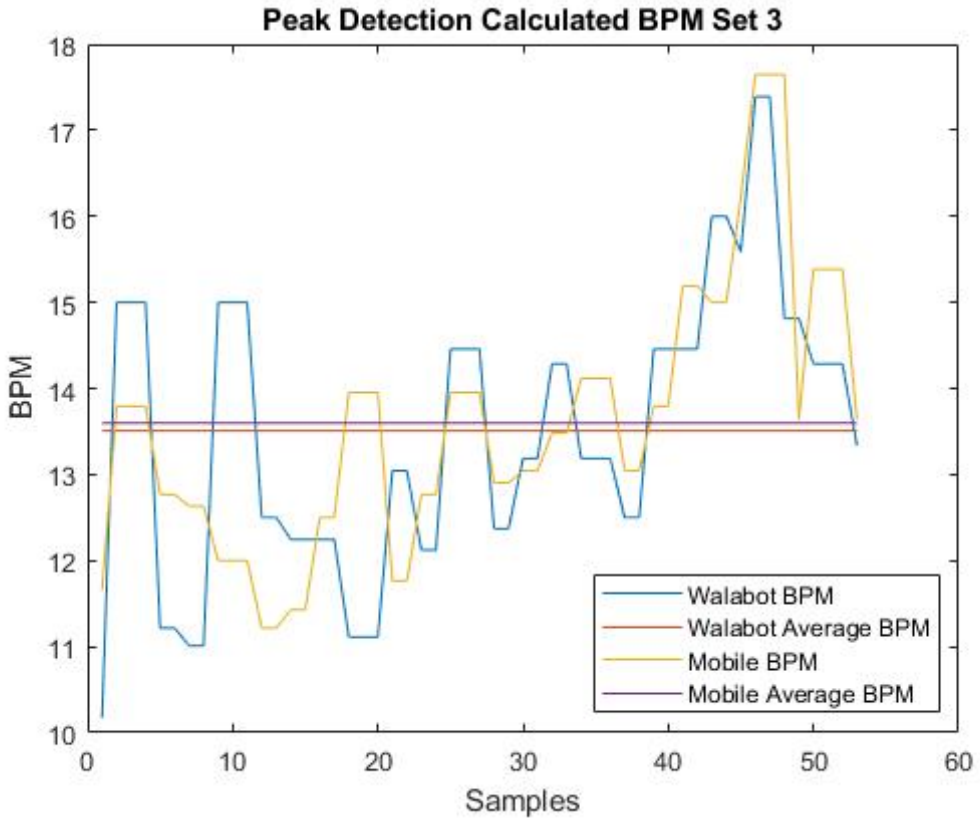

Figure 6.15: An example of BPM calculated from Walabot and Mobile data using the Peak Detection technique.

the user was asked to breathe normally. The user reported approximately 13, 15 and 13.5 BPM for sets 1, 2 and 3 respectively.

In addition to the accuracy calculations performed by the two signal processing techniques, one extra accuracy metric was added. This metric quantifies the Mobile to Walabot BPM Calculation Ratio in terms of percentage, using Equation 6.3. This calculation was added in order to compare the similarity of the two calculations. When this value is within 10% of 100%, the two calculations are considered statistically equivalent and this indicates high correlation of signals and high stability of the associated breathing rate derivation technique.

Table 6.2: Mobile reported BPM preliminary testing results.

Set	User Reported BPM	Mobile Reported BPM	Mobile Reported BPM Accuracy
1	13	11.15	85.77%
2	15	11.63	77.51%
3	13.5	11.21	83.00%

$$Ratio = \frac{Mobile\_BPM\_Calculation}{Walabot\_BPM\_Calculation} * 100 \tag{6.3}$$

Table 6.2 contains the average Mobile reported breathing rates and the respective accuracies. Prior to testing, the Mobile reported breathing rate was expected to be the most accurate. However, the accuracy in all cases is significantly lower than 90%. Further, none of the reported averages are within 10% of the expected value. Due to this testing, the Mobile reported breathing rate values were not used in further testing.

Table 6.3 shows the results from the calculations made by the FFT technique using window sizes of 5, 7 and 10 seconds, and the respective accuracies. All of calculations made with a window size of 5 seconds are within 10% of the expected value. Additionally, the calculations made on the Mobile data with a window size of 7 and 10 seconds are within 10% of the expected value. However, one calculation made on the Walabot data with a window size of 7 seconds and two of the calculations made on the Walabot data with a window size of 10 seconds are not within 10% of the expected value. In fact, the second set is only 55.24% accurate when using a window size of 10 seconds. This is an interesting observation since increasing the window size increases the resolution, which should improve the accuracy.

The effect on window size is also apparent in the ratio calculations. Specifically, the ratios are within 10% for the calculations made with a window size of 5 seconds, but the ratios are outside of the 10% bounds for calculations made with larger windows. Due to these results,

Table 6.3: FFT technique preliminary testing results.

Set	Window Size	User Reported BPM	Mobile BPM Calculation	Mobile BPM Accuracy	Walabot BPM Calculation	Walabot BPM Accuracy	Mobile to Walabot Ratio
1	5	13	12.37	95.16%	13.35	97.32%	92.66%
	7	13	13.20	98.48%	11.70	90.03%	112.82%
	10	13	12.06	92.75%	9.36	71.96%	128.85%
2	5	15	13.69	91.27%	13.99	93.28%	97.86%
	7	15	16.49	90.04%	11.41	76.04%	144.52%
	10	15	14.87	99.10%	8.29	55.24%	179.37%
3	5	13.5	12.53	92.84%	12.81	94.92%	97.81%
	7	13.5	13.87	97.27%	13.74	98.25%	100.95%
	10	13.5	12.85	95.18%	12.16	90.04%	105.67%

Table 6.4: Peak detection technique preliminary testing results.

Set	Window Size	User Reported BPM	Mobile BPM Calculation	Mobile BPM Accuracy	Walabot BPM Calculation	Walabot BPM Accuracy	Mobile to Walabot Ratio
1	5	13	12.97	99.74%	13.26	97.97%	97.81%
	7	13	12.99	99.91%	13.12	99.09%	99.01%
	10	13	13.07	99.45%	13.27	97.93%	98.49%
2	5	15	15.05	99.68%	15.05	98.21%	100%
	7	15	15.15	99.02%	14.89	99.25%	101.75%
	10	15	15.25	98.33%	14.66	97.75%	104.02%
3	5	13.5	13.60	99.27%	13.51	99.94%	106.66%
	7	13.5	13.59	99.36%	13.52	99.86%	100.52%
	10	13.5	13.60	99.30%	13.51	99.96%	106.66%

a window size of 5 seconds was used in further testing of the FFT technique.

Finally, Table 6.4 reveals the results from the calculations made by the Peak Detection technique using window sizes of 5, 7 and 10 seconds, and the respective accuracies. As seen, all of calculations made are within 10% of the expected value and the ratios are all within 10% as well. An interesting observation is that the window size does not have a significant impact on the accuracy of the calculation. In order to maintain consistency with the FFT technique, a window size of 5 seconds was used in further testing.

Chapter 7

Testing

As introduced in Chapter 4, a comparative evaluation was designed and performed on one user. The goal of the study was to compare the accuracy of the Walabot breathing rate application to a medical grade wearable breathing rate monitor, the Mobile.

The study was designed to answer the research question and to address the discussed research challenges. In Chapter 4, we introduced the five design choices that were determined by the research question and challenges. These choices and the specific implementations are discussed below. Additionally, this chapter elaborates on the preliminary test setup and process. Finally, the data is presented here, including a qualitative and quantitative analysis of the study results.

7.1 Test Design

The comparative evaluation was carefully designed in such a way that allows for insight into both the research question and the provided research challenges. Additionally, it was emphasized that the test design should reflect how the device would be theoretically used in a real living space in order to make the data useful for real world applications.

As introduced in Chapter 3, the research question is the following: can UWB radar be utilized to enable a fully functional breathing rate monitoring system for an active user in a confined

SBE? In this context, the concept of a fully functional breathing rate monitoring system was clarified as a device that calculates breathing rate within 10% to the true breathing rate at all times that a single user is present within a confined space.

The research question and daily living emphasis dictated the first four choices: (1) only one user can be present in the designated space, (2) the user must use different breathing rates to test the full range of possible breathing rates, (3) the device must be tested while the user is both still and moving to address the continuity aspect, and (4) the confined space should be approximately the size of an average living room or bedroom. To meet the first design choice, only one participant was involved in the data acquisition session. Additionally, the person conducting the test stood out of range of the Walabot, to ensure their presence did not have an affect on the data.

To meet the second design choice, the user was told to use the following breathing rates during different sets of data acquisition: normal, deep and fast. To ensure the deep and fast rates were within reason, the user aimed to have a breathing rate between 8 and 12 BPM during deep breathing and between 15 and 20 BPM during fast breathing.

In regards to the third design choice, the participant was instructed to remain still for a set time and to perform a predetermined movement for a set time during the data acquisition session. The chosen positions and movement were specified in a later design decision.

Regarding the fourth design choice, the participant and the device were placed in a specified area, within the size of a standard living room or bedroom. This stems from the assumption that the device would be placed in a common living area to be utilized frequently. With this in mind and given the constrains of the COVID-19 pandemic shelter-in-place order active at this time (Spring 2020), a den in a household was used. A sketch of the layout of the room can be seen in Figure 7.1 and a picture of the actual room is illustrated in Figure 7.2. The

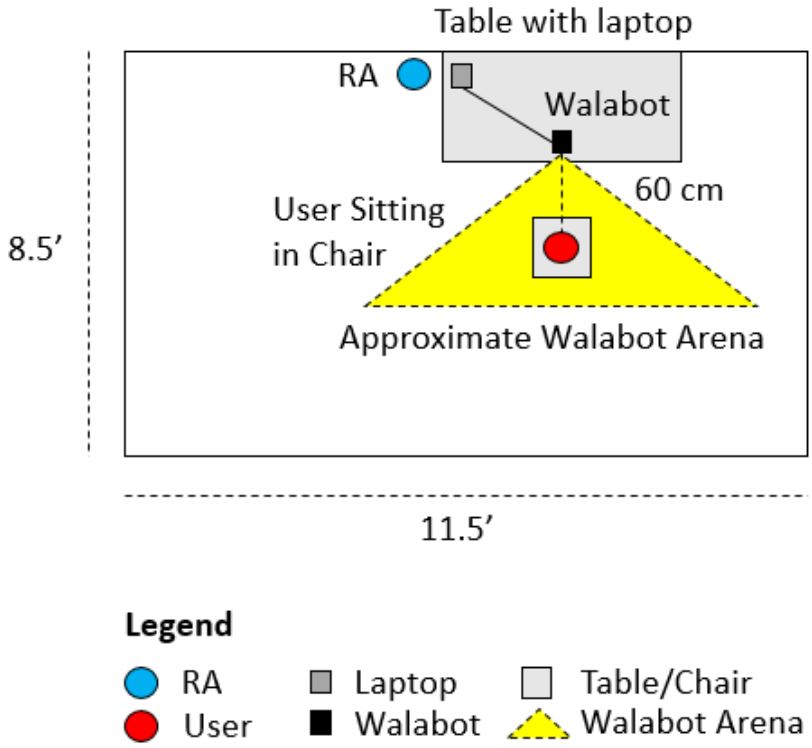

Figure 7.1: A sketch of the testing setup.

user was positioned 60 cm away from the Walabot along the Z axis and the exact positioning of the Walabot was varied within this layout throughout data acquisition, as explained later.

The six research challenges in this work are cost, user location, user orientation, user movement, system placement and signal processing. The third design choice addresses the user movement challenge by specifying that the user must be both still and moving during the study. The fourth design choice specifies the placement and Arena size of the Walabot, which addresses the user location and system placement challenges.

To address to the user orientation challenge, (5) the device must be placed in a variety of orientations with respect to the user's chest. Specifically, during testing, the device was moved to several positions in both the X and Y axes while the user remained in one position. Based on the work of Wang et. al, radar based respiratory systems become less effective as

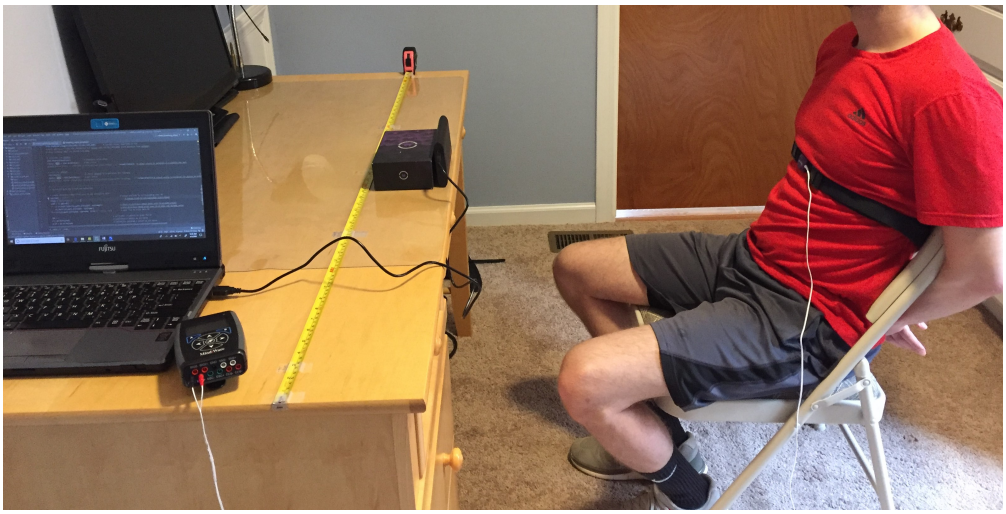

Figure 7.2: A picture of the testing setup.

the orientation between the device and the user is increased. Further, these devices generally stop working altogether when the angle is close to 90 degrees or larger [141]. To test the Walabot in positions that are expected to be relatively effective, the chosen angles were -45, -22.5, 22.5 and 45 degrees. Equation 7.1 was then used to calculate the corresponding locations of the Walabot along the vertical and horizontal axes.

$$Position = User\_Distance * \tan angle \tag{7.1}$$

Equation 7.1 was used four times, once for each angle. In each case, the $User\_Distance$ variable was 60 cm because the user was positioned 60 cm away from the Walabot along the Z axis, as discussed earlier. The calculated distances were -60, -24.85, 24.85 and 60 cm relative to the origin. Two sketches of this setup can be seen in Figures 7.3 and 7.4.

The next design choice specifies the type of positions and movement the user should perform during data acquisition. This choice is highly complex because the research question does not specify user positioning or movement, instead it encompasses general daily living activities.

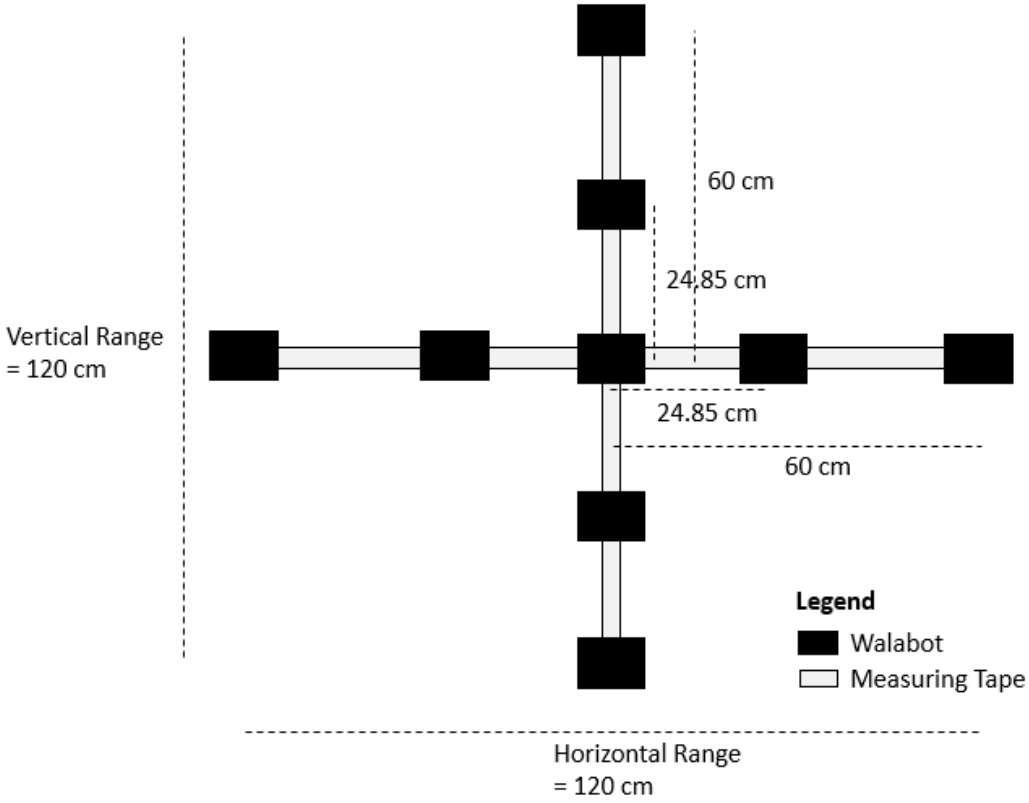

Figure 7.3: Front view of Walabot placements along the horizontal and vertical axes.

There are many Activities of Daily Living (ADLs) such as getting dressed, cooking, drinking, eating, walking and taking medicine [108].

The process of choosing ADLs to use for the test was difficult. One issue is that these activities may be completed inconsistently between users [108]. For example, the process of getting dressed uses various motions corresponding to the individuals preference and the type of clothing chosen. Additionally, many ADLs are difficult to reproduce without introducing objects in the setting. The motions used in cooking, for example, are hard to act out without any cooking equipment. For a comparative evaluation, it is important to pick a reproducible procedure and to not use any extra objects that could potentially affect the data collected. To complicate this further, typical ADLs require a change in user location and orientation. For this test, we wanted to maintain simple, consistent positions and movements.

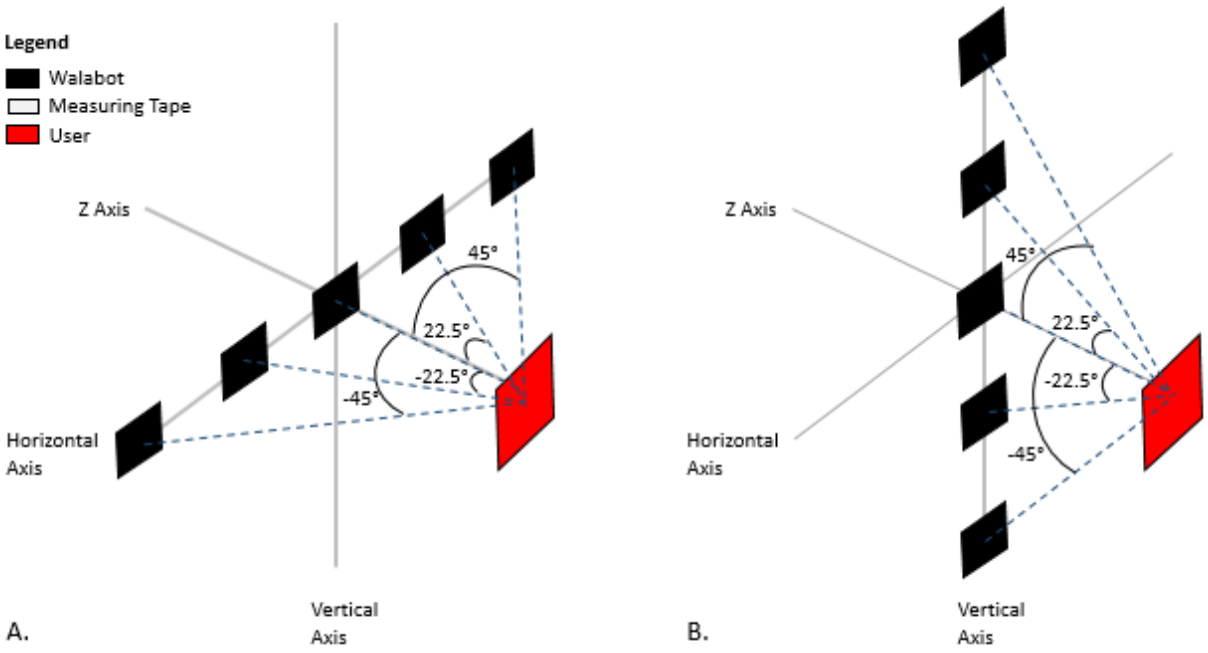

Figure 7.4: A perspective view of Walabot placements along the: **A)** Horizontal axis. **B)** Vertical axis.

To address these issues, the different positions and movements from common ADLs were broken into the simple elements of sitting and standing. Another simple element of ADLs in this context is simply the movement of the chest. To utilize these positions, (6) the user was asked to sit, stand and walk in place.

The final two research challenges not addressed thus far are cost and signal processing. These challenges do not directly influence the user study design. Instead, the challenges are affected by the device chosen. As stated, the Walabot is less expensive than other breathing rate monitors and can provide an affordable option for the common household. In the context of the signal processing challenge, we developed two signal processing techniques based on commonly implemented methods. The accuracy and limitations of these techniques will be determined by the test results.

With these study design choices in mind, four data acquisition procedures were designed to

fully test the Walabot in the context of the research question. The procedures were split into tests for breathing rate variation, horizontal placement variation, vertical placement variation and user movement variation. Within each procedure, data sets of one minute each were acquired and the user was asked to count their breaths taken during each set. Multiple sets were acquired within the same data file, or trial.

For the rate variation data acquisition session, the Walabot was positioned at the vertical, horizontal and Z origin. The user was then positioned sitting in the chair which was located at the vertical and horizontal origin and 60 cm along the Z axis. Data from both devices was then acquired four sets at a time, where the user was directed to breathe normally for the first two sets, then slower and finally quickly for the last two sets. This was repeated for three trials.

During the horizontal placement variation data acquisition session, the user remained in the same location and was instructed to breathe normally during every set. For each trial, the Walabot was positioned along the horizontal axis at one of the four premeasured locations discussed earlier and three sets of data were taken. The vertical placement variation data acquisition session followed a similar procedure, except the Walabot was positioned along the vertical axis.

Finally, the Walabot was positioned back at the vertical, horizontal and Z origin for the user movement variation procedure. During the first trial, the user was asked stand against a wall to ensure stability and limit the user from moving. Then, the user was instructed to stand freely in the second trial to test how small subconscious movements effect the data. Lastly, the user walked in place in order to determine the effect from large user movements in the last trial. Three sets of data were taken in each trial.

7.2 Quantitative Results

Data was collected on a 23 year old male using the breathing rate variation, horizontal placement variation, vertical placement variation and user movement procedures described in Section 7.1. The data was then processed using both the FFT and Peak Detection techniques discussed in Chapter 6.

7.2.1 Breathing Rate Variation

The results for the breathing rate variation trials are outlined in Table 7.1 and Table 7.2. The majority of the breathing rate calculations for both techniques were accurate within 10% of the user reported breathing rate. To illustrate this, the figures produced from set 4 of trial 1 are shown in Figures 7.5, 7.6, 7.7, and 7.8. The signals in this set had a high correlation of 0.8128, as well as very similar shapes and extrema numbers. Further, the breathing rate calculations using the FFT technique were approximately 93% accurate and the calculations using Peak Detection were approximately 98% accurate relative to the user reported 16 breaths taken in that minute. Additionally, the ratio of Mobile to Walabot BPM calculations were almost 100% for both techniques.

It should be noted that the user's rate of breathing started to slightly increase toward the end of this data set. This can be visually seen by the decrease in period between minimums in Figure 7.6. Both techniques also started to calculate higher breathing rates during this time (Spring 2020). This is encouraging because it shows that the techniques both produce results that adjust with the shape of the signal.

Although this procedure yielded primarily results with high accuracy, it also contains several results that reveal important issues. One pattern that emerges in these results is the decrease

Table 7.1: Breathing rate variation results using the FFT technique.

Trial	Set	User Reported BPM	Mobile BPM Calculation	Mobile BPM Accuracy	Walabot BPM Calculation	Walabot BPM Accuracy	Mobile to Walabot Ratio
1	1	14.5	13.18	90.88%	13.75	94.83%	95.85%
	2	13.75	12.60	91.64%	13.77	99.86%	91.50%
	3	11	12.64	87.12%	13.02	81.62%	97.08%
	4	16	14.89	93.06%	14.90	93.15%	99.93%
2	1	15.5	14.05	90.66%	14.51	93.58%	96.83%
	2	16	14.79	92.45%	14.87	92.92%	99.46%
	3	11	12.57	85.69%	12.35	87.75%	101.78%
	4	18.5	18.75	98.66%	16.02	86.57%	117.04%
3	1	14	13.00	92.83%	13.90	99.30%	93.53%
	2	12.5	12.51	99.89%	13.69	90.48%	91.38%
	3	9	12.77	58.12%	12.92	56.46%	101.17%
	4	16	15.57	97.31%	15.29	95.58%	101.83%

Table 7.2: Breathing rate variation results using the Peak Detection technique.

Trial	Set	User Reported BPM	Mobile BPM Calculation	Mobile BPM Accuracy	Walabot BPM Calculation	Walabot BPM Accuracy	Mobile to Walabot Ratio
1	1	14.5	14.77	98.15%	14.48	99.88%	102.00%
	2	13.75	13.66	99.36%	14.10	97.44%	96.88%
	3	11	12.20	89.06%	13.00	81.83%	93.85%
	4	16	15.73	98.29%	15.69	98.08%	100.25%
2	1	15.5	15.86	97.71%	15.78	98.23%	100.51%
	2	16	16.09	99.43%	15.89	99.29%	101.26%
	3	11	11.45	95.88%	11.00	99.98%	104.09%
	4	18.5	18.12	97.93%	17.17	92.82%	105.53%
3	1	14	14.56	96.02%	16.61	81.34%	87.66%
	2	12.5	12.68	98.54%	14.23	86.17%	89.11%
	3	9	9.94	89.53%	11.32	74.27%	87.81%
	4	16	16.30	98.12%	16.62	96.13%	98.07%

in the calculated Walabot breathing rate accuracy when the user reported a breathing rate below 12 BPM. As explained, the user was instructed to take slower breaths during the third data set of each trial. Consequently, the user reported 11, 11 and 9 BPM during these three trials. The resulting Walabot breathing rate calculations were almost all below 90%. The

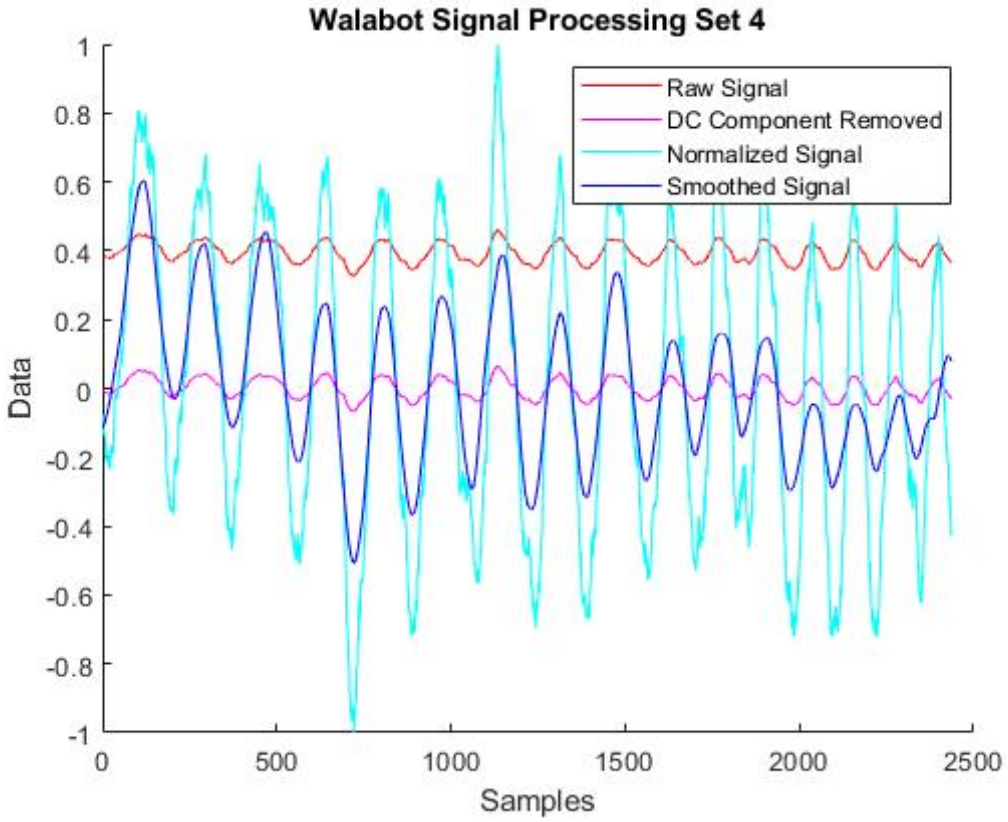

Figure 7.5: Walabot signal from trial 1, set 4 of rate variation procedure.

only exception was the breathing rate calculated using the Peak Detection technique in trial 2, which had an accuracy of 95% for the Walabot signal.

This decrease in accuracy is likely due to the chosen window size of 5 seconds. This window size is ideal for normal resting breathing rates, which are above 12 BPM, because at least one full breath is taken during this window. However, when the breathing rate is lower than 12 BPM, only a partial breath is taken during the window, which decreases the calculation's effectiveness. To test this theory, the window size was increased to 10 seconds and set 3 of trials 1 and 3 were calculated again, as shown in Table 7.3. This increased the accuracy of every calculation except one, verifying the theory. However, it did not improve the majority of the ratio calculations, which indicates the instability of this window size. Additionally,

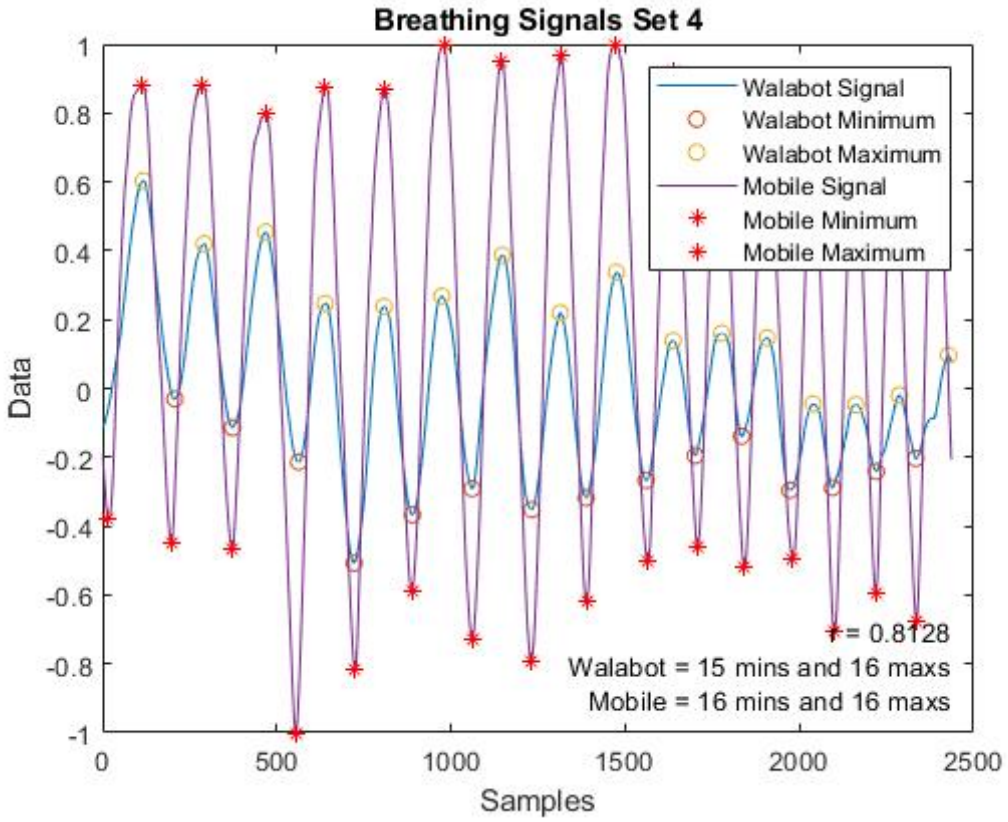

Figure 7.6: Breathing signals from trial 1, set 4 of rate variation procedure.

Table 7.3: Slow breathing with window size of 10 seconds results.

Trial	Technique	User Reported BPM	Mobile BPM Calculation	Mobile BPM Accuracy	Walabot BPM Calculation	Walabot BPM Accuracy	Mobile to Walabot Ratio
1	FFT	11	11.47	95.73%	10.02	91.13%	114.47%
	PD	11	11.89	92.17%	12.95	82.29%	91.81%
3	FFT	9	8.81	97.87%	7.88	87.53%	111.80%
	PD	9	9.57	93.64%	11.80	68.90%	81.10%

this window size decreases the accuracy of the FFT technique calculations for Walabot data with a reported BPM over 12, as determined in Chapter 6. Consequently, the window size was kept at 5 seconds for the remaining tests.

Another interesting observation from this data is the Walabot breathing rate calculations

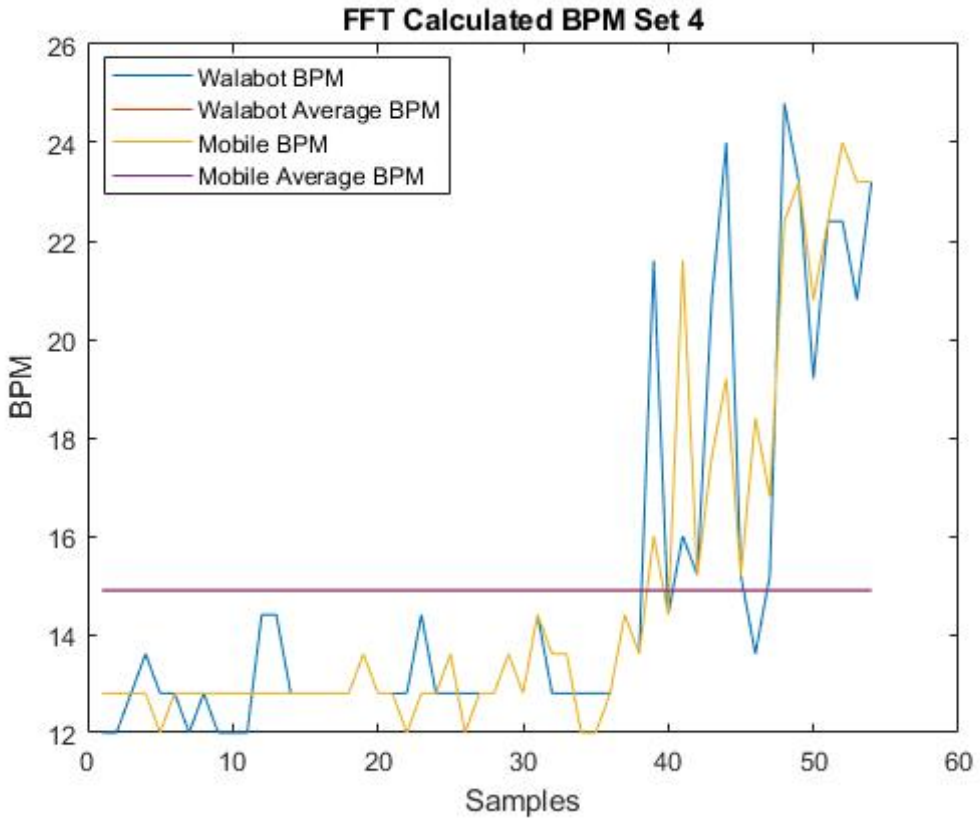

Figure 7.7: BPM calculated using the FFT technique from trial 1, set 4 of rate variation procedure.

using the Peak Detection method were lower than expected in trial 3. In the preliminary testing done in Chapter 6, the Peak Detection method resulted in calculations with accuracies all above 97%. However, in this testing, trial 3 revealed calculations with accuracies as low as 81% for normal rates. To investigate this trial, the shape of sets 1 and 2 from trial 3 were visually inspected. As seen in Figure 7.9, the raw signal from the Walabot in set 1 starts with a magnitude around 0.8 and drops to -0.8. A similar phenomenon occurs in set 2, but the magnitude increases this time, as seen in Figure 7.10. When these signals are smoothed, the magnitude change is so dominate that the parts of the breathing sine wave are treated as noise and almost completely removed. The resulting signal does not have a clear resemblance to a breathing waveform, so the Peak Detection technique does not work as

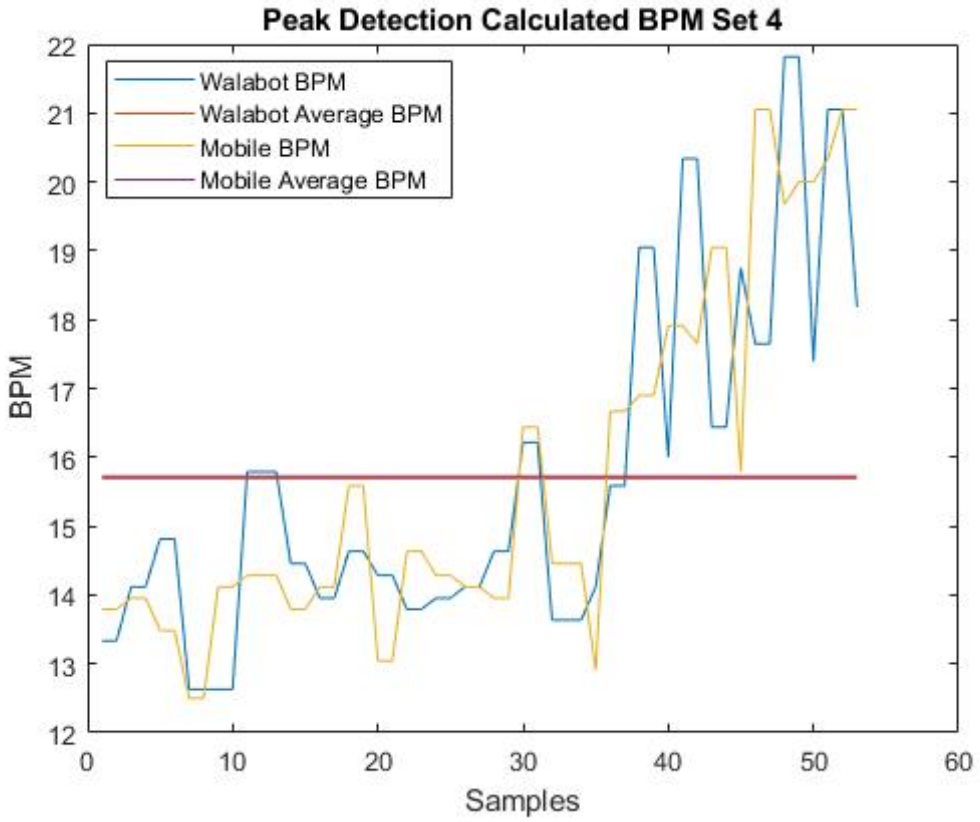

Figure 7.8: BPM calculated by Peak Detection from trial 1, set 4 of rate variation procedure.

accurately as expected. The parameters of the smoothing function were tested to ensure that the smoothing is done as well as possible. However, this phenomenon cannot be completely corrected so such data sets result in lower accuracy breathing rates for the Peak Detection technique. The FFT technique, on the other hand, is not effected by this phenomenon.

This type of signal was likely produced from a variation in the user's position or breathing technique. For example, if the user started sitting up straight and then relaxed their back into the chair during data acquisition, a magnitude change such as the one shown in Figure 7.10 would likely be recorded. The effect of user movement during data collection will be further investigated in Section 7.2.4.

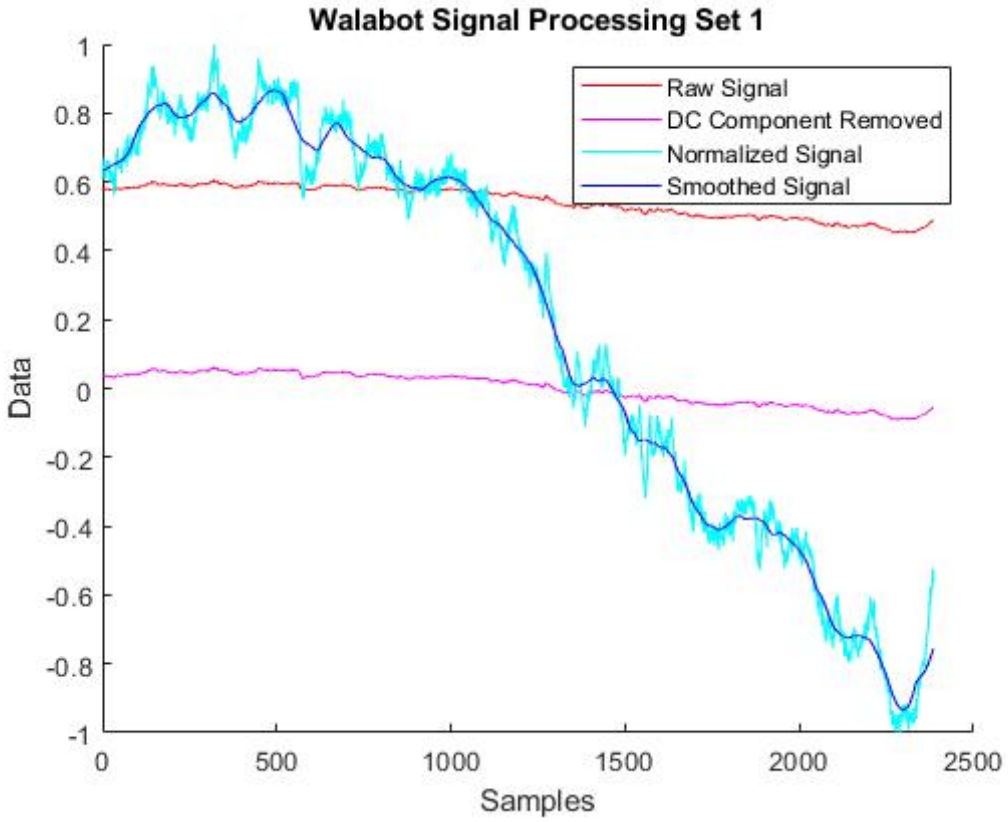

Figure 7.9: Breathing signals from trial 3, set 1 of rate variation procedure.

7.2.2 Horizontal Placement Variation

The results for the horizontal placement variation trials are shown in Tables 7.4 and 7.5. Significantly lower accuracy was expected for Walabot data taken at -45 or 45 degrees and slightly lower accuracy was expected for Walabot data taken at -22.5 or 22.5 degrees. However, the breathing rates computed via the FFT technique all reported relatively high accuracy. Specifically, the results from Walabot data taken at -22.5 and 22.5 degree were all above 88%. The accuracy of the Walabot data taken at -45 and 45 degrees was lower, but the lowest was still above 75%. Additionally, the ratio calculation for each set was within 11%. This is slightly outside of the 10% bound, but still indicates that this technique has relatively high stability.

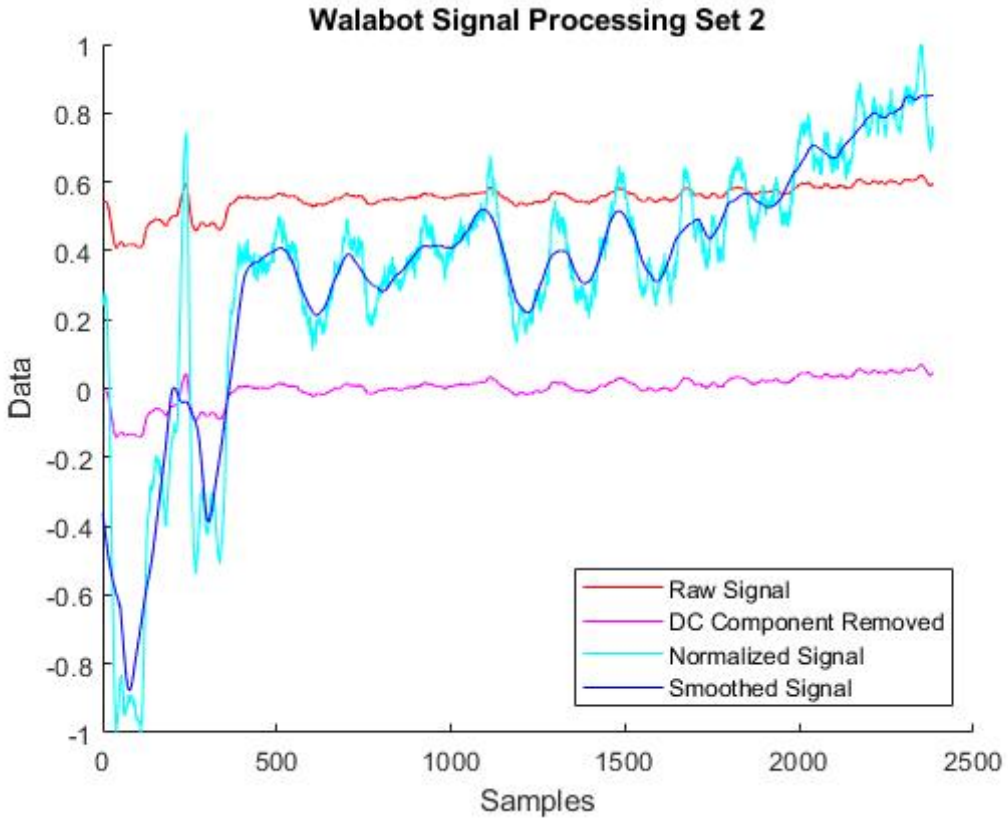

Figure 7.10: Breathing signals from trial 3, set 2 of rate variation procedure.

On the other hand, the calculations made by the Peak Detection technique were closer to what was expected. Specifically, the results from Walabot data taken at -22.5 and 22.5 degree were as low as 79%. The accuracy of the Walabot data taken at -45 and 45 degrees was much lower, with the lowest accuracy at 34% and the highest accuracy at 81%. Additionally, the ratio at the smaller angles were within 10%, but the ratio at the larger angles was as extreme as 37% away from 100%, suggesting increased instability at larger angles for this technique. These results suggest the use of the FFT technique for data taken when the user is not directly in front of the Walabot.

Table 7.4: Horizontal placement variation results using the FFT technique.

Angle	Set	User Reported BPM	Mobile BPM Calculation	Mobile BPM Accuracy	Walabot BPM Calculation	Walabot BPM Accuracy	Mobile to Walabot Ratio
-45	1	12.5	12.72	98.23%	13.71	90.32%	92.78%
	2	11.75	12.27	95.60%	13.38	86.15%	91.70%
	3	12	12.44	96.30%	13.85	84.57%	89.92%
-22.5	1	14	13.10	93.58%	13.62	97.25%	96.18%
	2	12.75	12.22	95.86%	12.64	99.11%	96.68%
	3	13.5	12.73	94.27%	13.76	98.05%	92.51%
22.5	1	15	13.75	91.67%	15.18	98.77%	90.58%
	2	14.75	12.59	85.37%	12.99	88.09%	96.92%
	3	12	12.36	97.04%	12.77	93.58%	96.79%
45	1	14.5	13.32	91.89%	14.04	96.80%	94.87%
	2	12.5	12.31	98.49%	13.76	89.90%	89.46%
	3	11	12.28	88.39%	13.69	75.52%	89.71%

Table 7.5: Horizontal placement variation results using the Peak Detection technique.

Angle	Set	User Reported BPM	Mobile BPM Calculation	Mobile BPM Accuracy	Walabot BPM Calculation	Walabot BPM Accuracy	Mobile to Walabot Ratio
-45	1	12.5	14.02	87.81%	14.85	81.22%	94.41%
	2	11.75	11.88	98.86%	14.23	78.95%	83.49%
	3	12	12.77	93.58%	16.68	61.01%	76.56%
-22.5	1	14	14.86	93.88%	14.93	93.33%	99.53%
	2	12.75	12.81	99.52%	13.44	94.57%	95.31%
	3	13.5	14.21	94.76%	15.49	85.27%	91.74%
22.5	1	15	16.30	91.35%	18.06	79.58%	90.25%
	2	14.75	13.19	89.39%	13.14	89.11%	100.38%
	3	12	12.18	98.47%	12.85	92.88%	94.79%
45	1	14.5	14.71	98.58%	18.31	73.74%	80.34%
	2	12.5	12.26	98.06%	18.54	51.70%	66.13%
	3	11	11.51	95.37%	18.23	34.28%	63.14%

7.2.3 Vertical Placement Variation

The results for the vertical placement variation trials are shown in Tables 7.6 and 7.7. As discussed in Subsection 7.2.2, significantly lower accuracy was expected for Walabot data

Table 7.6: Vertical placement variation results using the FFT technique.

Angle	Set	User Reported BPM	Mobile BPM Calculation	Mobile BPM Accuracy	Walabot BPM Calculation	Walabot BPM Accuracy	Mobile to Walabot Ratio
-45	1	14.5	13.48	92.96%	14.25	98.27%	94.60%
	2	14	14.59	95.80%	13.87	99.05%	105.19%
	3	13.5	13.06	96.72%	13.69	98.59%	95.40%
-22.5	1	14.5	13.86	95.56%	13.80	95.15%	100.43%
	2	13.5	13.08	96.87%	13.72	98.35%	95.34%
	3	14.25	13.51	94.78%	13.99	98.19%	96.57%
22.5	1	15.5	14.15	91.28%	13.90	89.65%	101.80%
	2	15	13.69	91.26%	13.35	88.99%	102.55%
	3	15	14.02	93.48%	14.05	93.69%	99.79%
45	1	13	12.91	99.32%	14.50	88.49%	89.03%
	2	14	13.04	93.14%	14.54	96.11%	89.68%
	3	11.5	12.69	89.63%	13.00	86.96%	97.62%

taken at -45 or 45 degrees and slightly lower accuracy was expected for Walabot data taken at -22.5 or 22 degrees. Similarly to the horizontal placement variation results, the breathing rates computed via the FFT technique all reported high accuracy. Specifically, the results from Walabot data taken at all locations were all above 86% and the ratio calculations were all within 11%. This further suggests that the FFT technique can be used when the user is not located directly in front of the Walabot.

The calculations made by the Peak Detection technique had lower accuracy for Walabot data taken at 45 and 45 degrees, as expected. This accuracy was as low as 76%. Although this is quite low, it is noticeably higher than the accuracy obtained during horizontal placement at the same angles using this technique. Additionally, the results computed by this technique from Walabot data taken at -22.5 and 22.5 degrees were all above 95%, which is quite high. The ratio calculations were also within 16%, which is significantly higher than the 37% range found in the horizontal test. This data suggests that the Walabot Arena has a vertical range larger than its horizontal range.

Table 7.7: Vertical placement variation results using the Peak Detection technique.

Angle	Set	User Reported BPM	Mobile BPM Calculation	Mobile BPM Accuracy	Walabot BPM Calculation	Walabot BPM Accuracy	Mobile to Walabot Ratio
-45	1	14.5	14.93	96.10%	14.75	98.26%	101.22%
	2	14	15.01	92.79%	15.97	85.89%	93.99%
	3	13.5	13.71	98.45%	13.60	99.26%	100.81%
-22.5	1	14.5	14.89	97.31%	15.15	95.53%	98.28%
	2	13.5	13.85	97.39%	13.53	99.80%	102.37%
	3	14.25	15.07	94.23%	15.53	91.03%	97.04%
22.5	1	15.5	15.46	99.76%	15.74	98.47%	98.22%
	2	15	14.39	95.94%	14.41	96.08%	99.86%
	3	15	15.32	97.85%	15.27	98.17%	100.33%
45	1	13	13.38	97.07%	15.36	81.84%	87.11%
	2	14	14.54	96.11%	17.22	76.97%	84.44%
	3	11.5	13.00	86.92%	13.67	81.14%	95.10%

7.2.4 User Movement Variation

The results for the user movement variation trials are shown in Tables 7.8 and 7.9. During the first trial, the user stood up and leaned their back against a wall for stability. In this position, the user should be able to relax and not move, just as they did in the sitting position. As expected, this yielded results within 10% accuracy for both the FFT and Peak Detection techniques and the ratio calculations.

In the second trial, the user stood again, but they did not lean against anything for support. Even when a user stands as still as they can, their body will naturally make small subconscious movements. These small movements caused the Walabot signal to look less like the expected sinusoidal shape, as shown in Figure 7.11. This also had a small affect on the Mobile signal, as seen in Figure 7.12. The shape of the waveforms directly effects the breathing rate calculation performed by the Peak Detection technique, causing these calculations to be slightly less accurate for both the Mobile and Walabot. As seen in Figure 7.14, only 35 calculations were counted toward the average breathing rate rather than the over 50 usually

Table 7.8: User movement variation results using the FFT technique.

Position	Set	User Reported BPM	Mobile BPM Calculation	Mobile BPM Accuracy	Walabot BPM Calculation	Walabot BPM Accuracy	Mobile to Walabot Ratio
Stand Against Wall	1	11.5	12.35	92.63%	12.59	90.53%	98.09%
	2	14.5	13.79	95.09%	14.18	97.80%	97.25%
	3	13.5	12.76	94.49%	13.47	99.75%	94.73%
Stand Freely	1	11.75	12.53	93.33%	14.06	80.35%	89.12%
	2	15	14.83	98.86%	14.03	93.53%	105.70%
	3	14	14.20	98.60%	13.86	98.97%	102.45%
Walk in Place	1	15	15.60	96.00%	14.35	95.69%	108.71%
	2	14	14.04	99.71%	13.62	97.26%	103.08%
	3	15	16.09	92.72%	13.80	92.00%	116.59%

Table 7.9: User movement variation results using the Peak Detection technique.

Position	Set	User Reported BPM	Mobile BPM Calculation	Mobile BPM Accuracy	Walabot BPM Calculation	Walabot BPM Accuracy	Mobile to Walabot Ratio
Stand Against Wall	1	11.5	12.32	92.83%	12.37	92.48%	99.60%
	2	14.5	15.42	93.66%	15.61	92.35%	98.78%
	3	13.5	13.67	98.74%	13.32	98.65%	102.63%
Stand Freely	1	11.75	12.25	96.04%	16.54	59.23%	74.06%
	2	15	16.54	89.74%	15.23	98.44%	108.60%
	3	14	16.29	83.64%	15.65	88.23%	104.09%
Walk in Place	1	15	16.55	89.64%	16.69	88.72%	99.16%
	2	14	16.41	82.76%	15.31	90.67%	107.18%
	3	15	17.81	81.26%	17.40	83.97%	102.36%

used. This indicates that in over 15 windows, the breathing rate was either not computed because there was not a minimum and maximum point present within the window or the calculation was deleted because it was outside the limits of 6 to 25 BPM.

The FFT technique, on the other hand, was still able to operate under these conditions, allowing the accuracy to still be within 10%, as seen in Figure 7.13. The only exception was the first set, where the user reported 11.75 BPM. As discussed in Section 7.2.1, this particular calculation could be increased by using a window size of ten seconds rather than

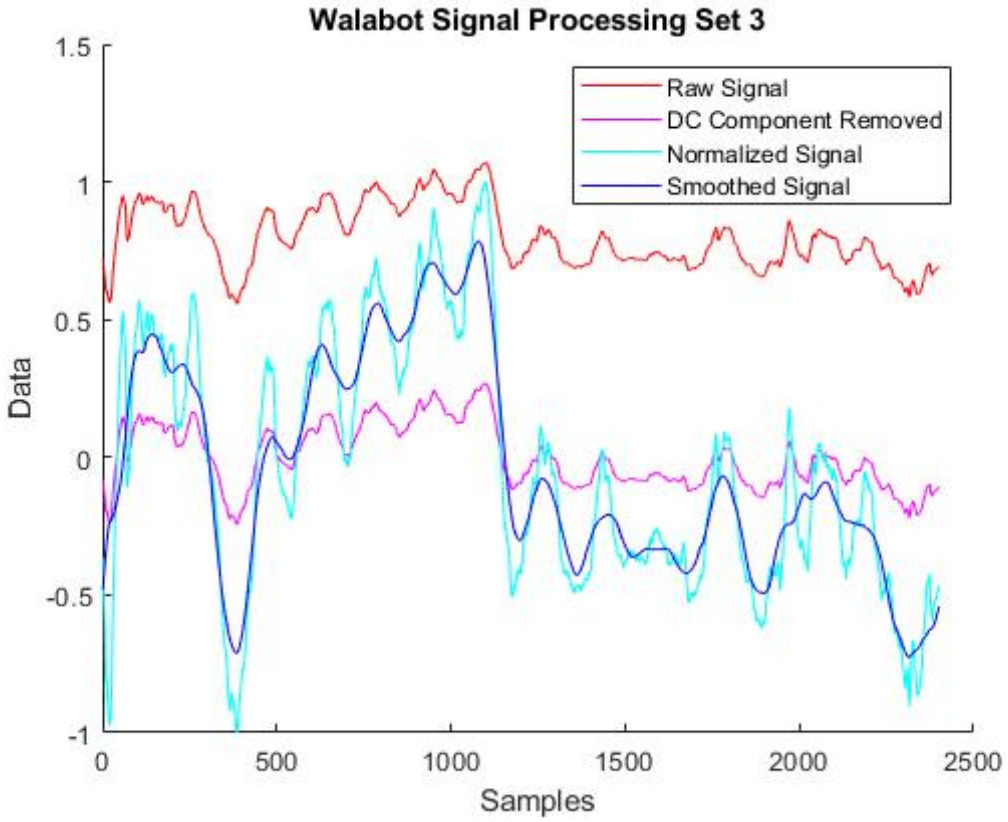

Figure 7.11: Walabot signal from standing trial, set 3 of user movement variation procedure.

5 seconds.

In the third trial, larger user movements were tested by asking the user to walk in place. These large movements caused the Walabot signal to contain extreme noise, as seen in Figure 7.11. The smoothing erases a significant portion of the noise, but the final signal still does not have a clear resemblance to expected breathing waveform. The movements also had an affect on the Mobile signal, as seen in Figure 7.12. Although the movements are larger, they have an affect of a similar magnitude on the Peak Detection technique calculations, as seen in Figure 7.18. In fact, the lowest accuracy for the standing and walking trials are both above 80%.

The FFT technique is not largely effected by the user movements, allowing all the accuracies

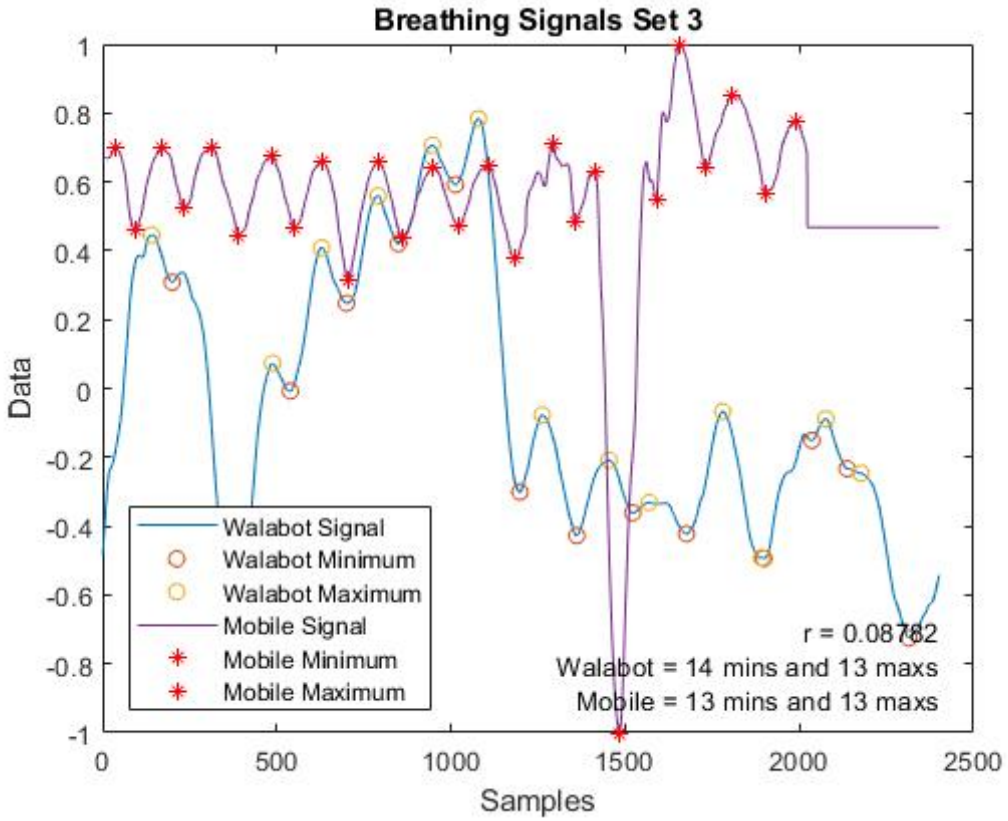

Figure 7.12: Breathing signals from standing trial, set 3 of user movement variation procedure.

to again be within 10%, as seen in Figure 7.17. These results suggest that the FFT technique should be used for moving users.

It should be noted that the ratio calculations were not largely effected by the user movement. This suggests that the user's movement caused similar effects on each signal, allowing their shapes and, therefore, their breathing rate calculations to be similar to each other.

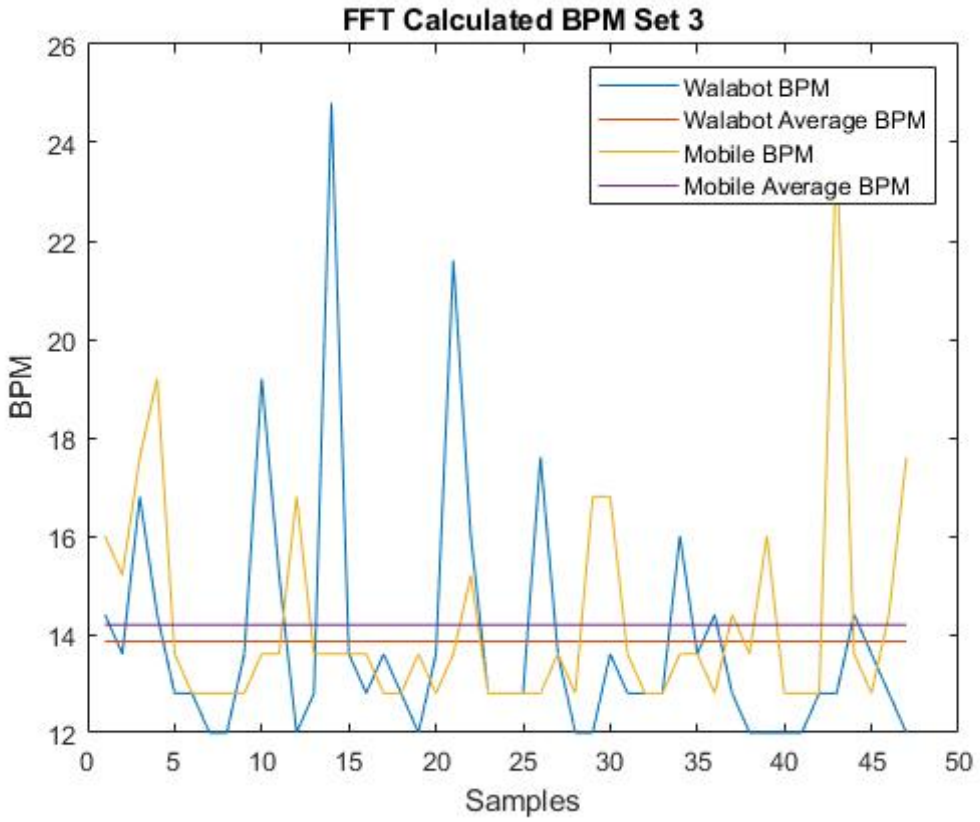

Figure 7.13: BPM calculated using the FFT technique from standing trial, set 3 of user movement variation procedure.

7.3 Qualitative Results

In addition to quantitative results, qualitative results were gathered by observing the user during testing and talking to the user about their experience. It should be noted that the same user was used for the preliminary testing documented in Chapter 6 and the comparative evaluation documented in Chapter 7.

During the preliminary testing stage, the user appeared to be slightly uncomfortable with the setup. Specifically, the user adjusted their sitting position and the respiration belt between data acquisition sessions. Additionally, the user appeared to be sitting rigidly, opposed to comfortably. As testing continued, the user became more comfortable and relaxed with both

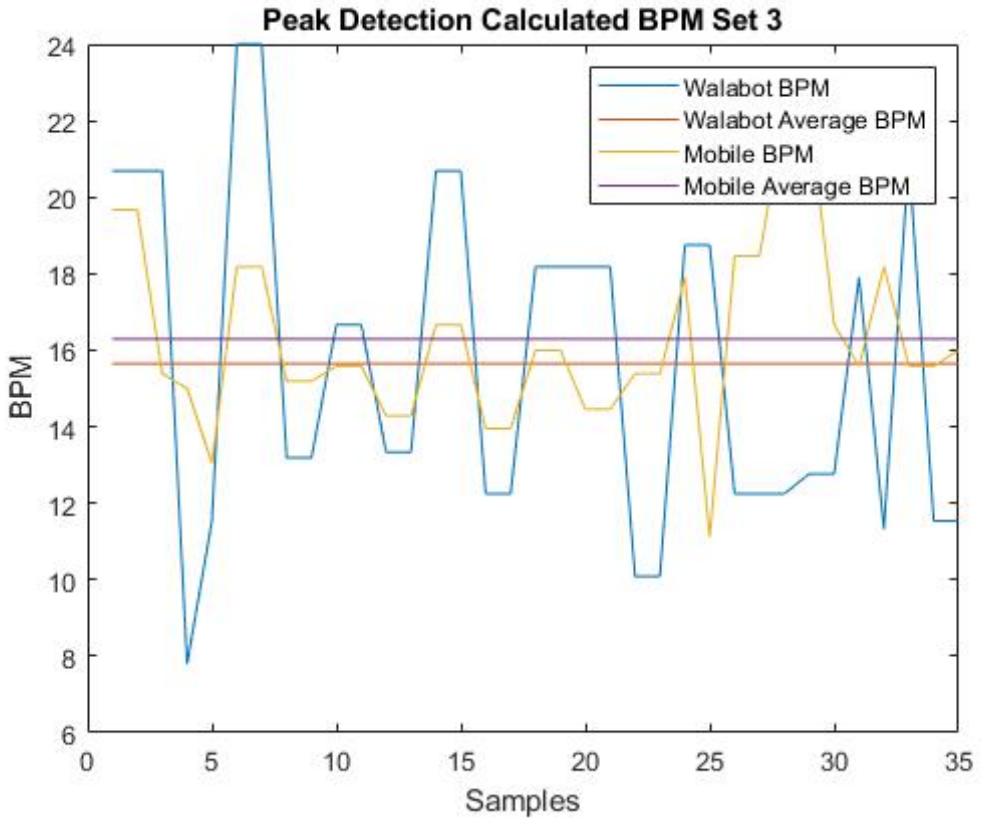

Figure 7.14: BPM calculated by Peak Detection from standing trial, set 3 of user movement variation procedure.

the sitting position and the devices. By the end of the preliminary testing stage, the user was acclimated to the environment and devices.

Prior to the start of the comparative evaluation, the user was asked to fill out the pre-study survey seen in Appendix A.1. This survey inquires about the user's past interactions with any wearable health devices and breathing rate sensors. This user indicated their participation in the preliminary testing stage of this research, but he did not have any other past experiences with such devices.

During comparative evaluation, we observed the user's increase in comfort with the devices. However, the user did have to adjust the respiration belt between trials still. The user

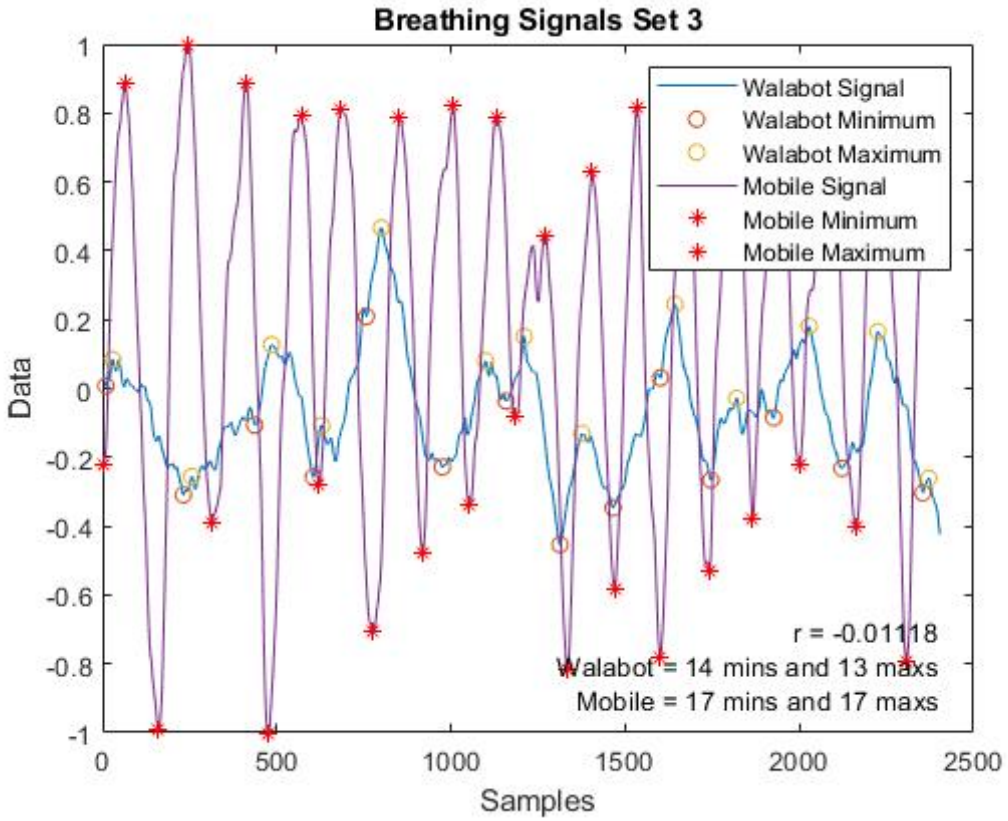

Figure 7.15: Walabot signal from walking trial, set 3 of user movement variation procedure.

reported that these adjustments were made because the belt had a tendency to fall down slightly.

We also observed the user for any movements during stationary tests. For the majority of the trials, the user appeared completely still from a visual perspective. However, we did observe a few small subconscious movements. For example, during one trial of the vertical variation procedure, we observed the user moving their right index finger. When this trial was over, the user was asked about this movement and the user reported a lack of realization that this was occurring, indicating this was a subconscious movement. Additionally, the user reported that a few minor involuntary movements occurred during various trials. Upon quantitative analysis, these movements did not appear to alter the results significantly, but

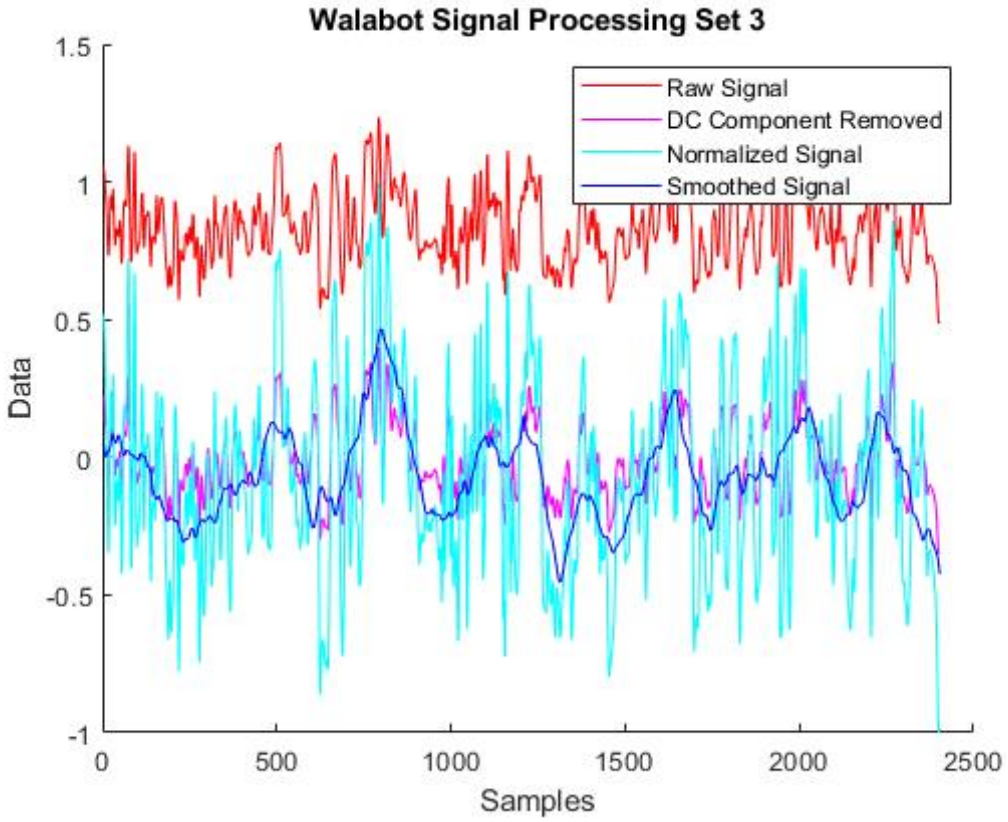

Figure 7.16: Breathing signals from walking trial, set 3 of user movement variation procedure.

they may have caused the phenomenon described in Section 7.2.1.

At the end of testing, the user was asked to fill out the survey seen in Appendix A.2 that inquires about their experience. The user rated the overall study experience as a 3 out of 5 because the study was "lengthy and required a lot of focus." When asked to elaborate, the user stated that counting his breaths during each set was difficult and required high concentration. With this in mind, future work should be done with a wearable device that has the capability of counting the user's breaths accurately so the user does not have to count.

The user rated their experience with the Mobile as a 4 out of 5. Specifically, the user indicated that the tension from the belt helped moderate his breathing, but it also required

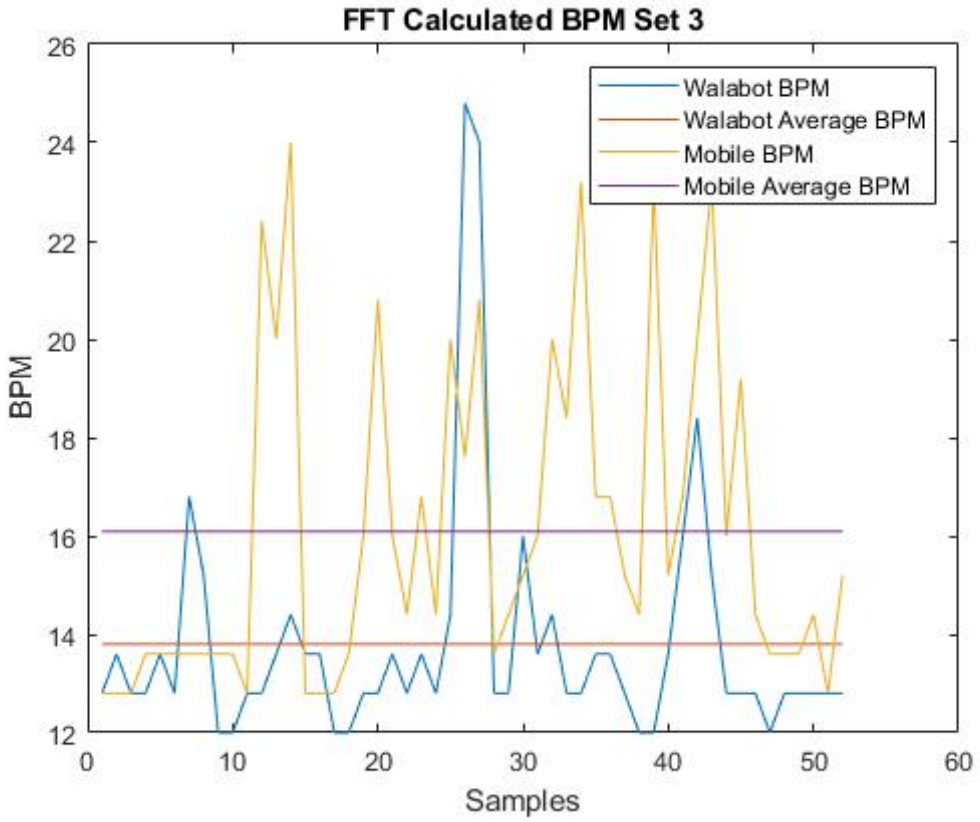

Figure 7.17: BPM calculated using the FFT technique from walking trial, set 3 of user movement variation procedure.

adjustments because it had a tendency to fall down. Finally, the user rated their experience with the Walabot as a 5 out of 5 because it was comfortable to use due to the lack of contact required.

7.4 Future Testing

The results from the comparative evaluation are promising and advocate for further testing of the Walabot as a breathing rate monitor. The next step is to run a complete user study in order to test the Walabot across a larger set of users. To pursue this step, a user study protocol was submitted to the Institutional Review Board (IRB) and approved on January

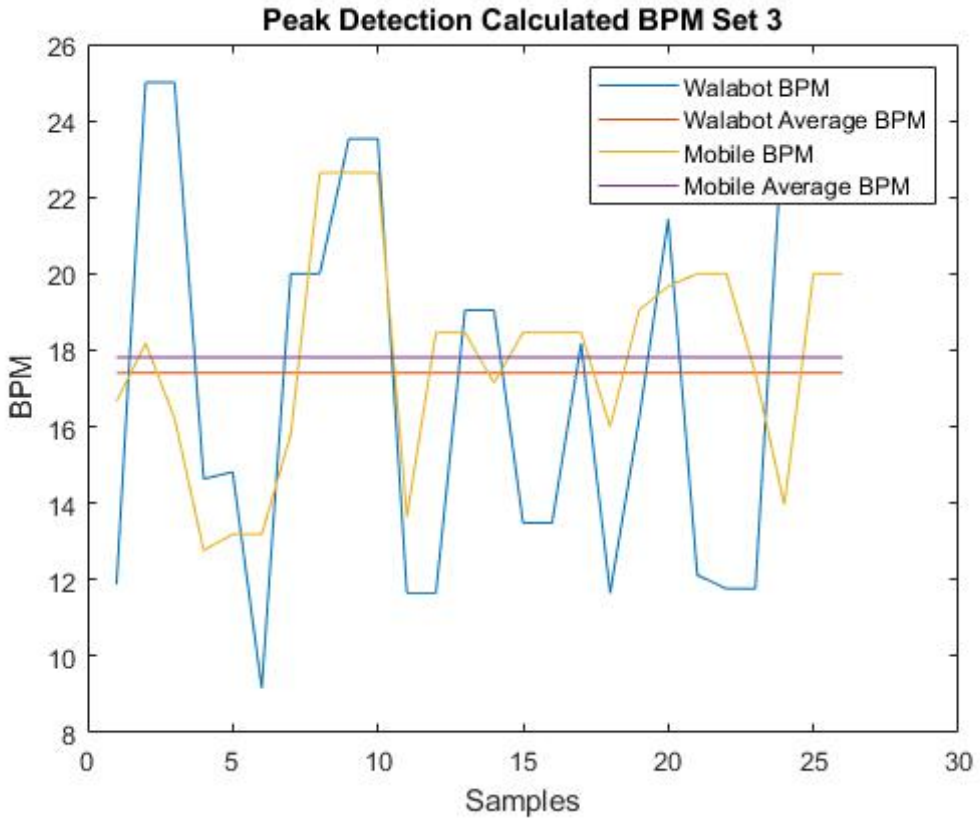

Figure 7.18: BPM calculated by Peak Detection from walking trial, set 3 of user movement variation procedure.

15th, 2020 (IRB no. 19-857). Slight modifications were made, including the specification of the use of the Mobile as the medical grade wearable device, and the protocol was re-approved on March 16th, 2020. The approval letter can be seen in Appendix A.3.

This protocol calls for a user study with up to 30 participants. As specified, volunteers should be recruited to participate via flyers and emails. After volunteering, a phone screening should be done to determine if the user is eligible to participate. Volunteers should be considered eligible to participate if they are aged 18 to 30 and do not have any physical disabilities or respiratory conditions (such as asthma) that would prevent them from safely completing the study.

Prior to the start of the study, the user should be asked to fill out the consent form, shown in Appendix A.4, and the pre-study survey. The procedure that is described in the consent form and further specified in the protocol should then be followed to collected the necessary data. Finally, the user should fill out the post-study survey. These surveys are identical to what the user that participated in the comparative evaluation filled out.

The recruitment process was planned to begin in late March, 2020. However, all IRB sanctioned studies were instructed to halt immediately as of March 14th, 2020, due to the outbreak of COVID-19. Notice of this is included in the approval letter in Appendix A.3. This user study protocol can be used in future work to continue the test of the Walabot as a breathing rate monitor.

Chapter 8

Discussion

The data from the comparative evaluation is an essential first step toward understanding the accuracy and limitations of the Walabot breathing rate measurement capabilities. Further, the design of the study allows the Walabot to be analyzed in the context of the research question and challenges presented in Chapter 3. To restate, we defined the following research question:

> Can UWB radar be utilized to enable a fully functional breathing rate monitoring system for an active user in a confined SBE?

For the purposes of this work, the concept of a fully functional breathing rate monitoring system was defined as a device that calculates breathing rate within 10% of the true breathing rate at all times that a single user is present within a confined space. The following six research challenges were derived from this question and background research on current systems: cost, user location, user orientation, user movement, system placement and signal processing. Further, it was determined that a system had to overcome all the research challenges in order to answer yes to the research question.

Prior to testing the Walabot, we addressed the first research challenge: cost. In fact, the low cost and availability of this device was one of the reasons it was selected. Currently, the least expensive version of the Walabot is $74.95 and no subscription purchase is required [139]. This one time cost was considered affordable for an average household for a

medically beneficial device.

Two other research challenges were addressed before testing: user location and system placement. The details of these challenges are outlined in Chapter 3. To summarize, many of the current systems are only functional when the user is positioned in particular locations relative to the device and when the device is placed appropriately within the room.

The Walabot provided an advantage over other systems for these challenges because the antennas are all located in one piece of hardware, rather than having a separate transmitter and receiver. With this design, a user can simply set up the device on one side of a room with the front of the device facing the chosen area and the back facing the wall. This set up was used during the comparative evaluation and essentially eliminated the system placement challenge.

Regarding the user location challenge, the Walabot was alleged to be functional whenever a user is within the Arena. As discussed in Chapter 5, the Arena is specified within the data acquisition software by the values of R, *phi* and *theta*. To reiterate, the R value determines the range in the Z axis. This allowed for the simplification of the location challenge because the R range could simply be set based on the user's locations during the study. Specifically, the R range in the Arena was set as 20 to 80 cm for this work because the user was always positioned 60 cm away from the device in the Z direction. In the context of future applications, the R minimum value is 1 cm and the maximum value is 1000 cm, which allows the Z axis to be set such that it reaches the total length of any average living or bedroom. This large and adjustable range in the Z axis dismisses the user location challenge.

The next challenge is signal processing. In this work, signal processing techniques were developed and implemented to align the data sets and perform two breathing rate derivation techniques: FFT and Peak Detection. The breathing rate calculations were then compared

against the user reported breathing rate to obtain an accuracy measurement.

Preliminary testing was described in Chapter 6 to determine the best window size for the sliding windows implemented in each breathing rate derivation technique. During these trials, the user reported breathing rates of 13, 15 and 13.5 BPM. With this data, a window size of 5 seconds was chosen for both techniques because all the results were within 10% of the reported values when using this window size.

During the breathing rate variation procedure of the comparative evaluation, an issue with the window size was uncovered. Essentially, using a window size of 5 seconds is ideal for breathing rates between 12 and 20 BPM, but this window size is too small for breathing rates lower than 12. This is caused by fact that the calculation techniques require a window size of at least one breath to accurately determine breathing rate, but only a partial breath is taken during a 5 second window when the breathing rate is lower than 12 BPM. When the window size was increased to 10 seconds, the accuracy of sets with a breathing rate lower than 12 did increase. However, increasing the window size decreases the accuracy of calculations during sets with breathing rates above 12 BPM. The original window size of 5 seconds was used for the rest of testing during the comparative evaluation. In future work, a window size adjustment capability could be added in order to maximize the accuracy of the calculations for any breathing rate. These signal processing techniques were further tested during every other trial of the comparative evaluation, as discussed below.

To test the user orientation challenge, the horizontal and vertical placement variation procedures were followed. Within each of these procedures, the Walabot was positioned such that it was angled -45, -22.5, 22.5 and 45 degrees away from the user's chest in the X or Y axis. The results showed relatively high accuracy of breathing rate computed by the FFT technique. Specifically, the results from data taken at all locations were all above 85% for both horizontal and vertical testing when the reported breathing rate was above 12 BPM.

The calculations performed by the Peak Detection technique, on the other hand, had quite low accuracy. These results suggest that the FFT technique can be utilized to obtain a more accurate breathing rate when the user is not located directly in front of the Walabot. However, these results were not all within 10% accuracy. Consequently, the Walabot, coupled with the developed signal processing techniques, does not fully address the user orientation research challenge.

It is important to note that the *theta* and *phi* values determine the cone shape of the Arena in the X and Y axes. For this work, the ranges for both *theta* and *phi* were set as -1 to 1° because this allowed for the highest fs. Further testing should be done with higher *theta* and *phi* values to determine if the user orientation challenge is minimized by increasing the Arena size.

To test the user movement challenge, the user movement variation procedure was followed in which the user was asked to stand against a wall, stand freely and walk in place. Results revealed that the Walabot signal becomes highly concentrated with noise during moving trials, which caused the Peak Detection technique accuracy to drop below 90%. Nonetheless, the FFT technique was able to accurately compute breathing rate regardless of the user's movement during the trials when the reported breathing rate was above 12 BPM. This suggests that the Walabot coupled with the FFT techniques does address the user movement research challenge. However, this challenge should be further tested by taking data while the user is moving faster and with a wider range of movements.

Results from the horizontal, vertical and user movement variation procedures revealed the high accuracy and reliability of the FFT technique when the reported breathing rate is above 12 BPM. To reiterate, the FFT technique yielded results with higher accuracy than the Peak Detection technique during these tests. The primary reason for this is that the FFT technique is not significantly affected by the noise in the shape signal, while the Peak

Detection technique is highly affected. For this reason, the FFT technique should be the primary focus in future testing.

However, the FFT technique is not robust at this point. We already discovered that this technique does not obtain high accuracy against sets where the reported breathing rate is lower than 12 BPM. As stated, an adjustable window size should be implemented to increase the accuracy of the FFT technique. Additionally, this technique requires further testing before this challenge can be defined as overcome. Specifically, the Walabot coupled with the FFT technique should be tested against a medical grade device that accurately determines breathing rate to obtain more reliable accuracy calculations. Additionally, a user study should be run to test this system against multiple users.

In summary, the comparative evaluation has shown that the Walabot, coupled with the FFT technique, has addressed some of the research challenges, but not every one. Specifically, this system has addressed the cost, user location and system placement research challenges, but further testing is required to determine if the system can fully address the user orientation, user movement and signal processing research challenges. Consequently, the research question cannot be firmly answered at this time. The results from this work suggest the possibility that the Walabot coupled with the FFT breathing rate derivation technique could be utilized to enable a fully functional breathing rate monitoring system for an active user in a confined SBE. However, further testing is required.

Chapter 9

Conclusion

Health monitoring is a large research area that utilizes physiological signals to determine health status. Most of this research is focused on developing accurate wearable and contactless breathing rate monitors. The area of contactless monitors in particular is growing because such devices have the potential to constantly monitor a user without any direct user contact. Further, the system can be set up in the user's home and the user can continue with their daily lives without wearing or interacting with the health monitoring systems. This is very important since the users may not be capable of correctly and constantly using wearable devices due to their state of health.

One method for collecting breathing rate data without contact utilizes UWB radar. Such systems determine the chest displacement during breathing by emitting a wide spectrum of low energy RF signals. The development of a robust and fully functional UWB radar based system has the potential to enable complete monitoring of breathing rate. However, current UWB radar based systems have issues which hinder their accuracy or reliability.

This led to the following research question: can UWB radar be utilized to enable a fully functional breathing rate monitoring system for an active user in a confined SBE? The concept of a fully functional breathing rate monitoring system was defined as a system that calculates breathing rate within 10% of the true breathing rate at all times that a single user is present within a confined space. Additionally, the following six research challenges were identified: cost, user location, user orientation, user movement, system placement and signal

processing.

In order to investigate this research question, we first identified a commodity UWB radar based device that had an untested breathing rate application, called the Walabot. We investigated this device and developed a data acquisition technique to collect breathing rate data. Then, we chose the MindWare Respiration Belt coupled with the Mobile Impedance Cardiograph to provide a medical grade wearable system comparison. Next, we implemented two breathing rate derivation signal processing techniques: the FFT and Peak Detection.

To test the Walabot in the context of the research challenges, we designed and performed a comparative evaluation in which data was collected by following four procedures: breathing rate variation, horizontal placement variation, vertical placement variation and user movement variation. Results from this study were promising. Specifically, it was determined that this system addresses the cost, user location and system placement research challenges. However, further testing is required to determine if the system can fully address the user orientation, user movement and signal processing research challenges.

Overall, this work provides significant steps toward answering the research question and testing the Walabot breathing rate application. Specifically, this work demonstrates the utility of the FFT breathing derivation technique with the Walabot. The results from this work also prove the concept of using the Walabot as a breathing rate monitor. Further, the Walabot coupled with the FFT breathing rate derivation technique has the potential to be utilized to enable a fully functional breathing rate monitoring system for an active user in a confined SBE.

Bibliography

[1] Free vectors. https://all-free-download.com/free-vector/download/lifestyle-background-relaxing-people-living-room-furniture-icons_6838389.html, 2015. [last accessed 14 April 2020].

[2] Avent Abacus. Piezoelectric pressure sensors. https://www.avnet.com/wps/portal/abacus/solutions/technologies/sensors/pressure-sensors/core-technologies/piezoelectric/, 2020. [last accessed 14 April 2020].

[3] Fadel Adib, Hongzi Mao, Zachary Kabelac, Dina Katabi, and Robert C. Miller. Smart homes that monitor breathing and heart rate. In *Proceedings of the 33rd Annual ACM Conference on Human Factors in Computing Systems*, CHI '15, pages 837–846, April 2015.

[4] F.Q. AL-Khalidi, R. Saatchi, D. Burke, H. Elphick, and S. Tan. Respiration rate monitoring methods: A review. *Pediatric Pulmonology*, 46(6):523–529, June 2011.

[5] Andrea Aliverti. Wearable technology: role in respiratory health and disease. *Breathe*, 13(2):e27–e36, June 2017.

[6] Mohammed Alloulah, Anton Isopoussu, and Fahim Kawsar. On indoor human sensing using commodity radar. In *Proceedings of the 2018 ACM International Joint Conference and 2018 International Symposium on Pervasive and Ubiquitous Computing and Wearable Computers*, pages 1331–1336, Oct 2018.

[7] Giuseppe Andreoni, Carlo Emilio Standoli, and Paolo Perego. Wearable monitoring

of elderly in an ecologic setting: the SMARTA project. In *Proceedings of the 2nd International Conference on Sensors and Applications*, November 2015.

[8] H. Aoki, Y. Takemura, K. Mimura, and M. Nakajima. Development of non-restrictive sensing system for sleeping person using fiber grating vision sensor. In *Proceedings of the International Symposium on Micromechatronics and Human Science*, pages 155–160, Nagoya, Japan, September 2001.

[9] Apple. Watch. https://www.apple.com/watch/, 2020. [last accessed 14 April 2020].

[10] Amaya Arcelus, Megan Howell Jones, Rafik Goubran, and Frank Knoefel. Integration of smart home technologies in a health monitoring system for the elderly. In *Proceedings of the 21st International Conference on Advanced Information Networking and Applications Workshops*, volume 2, pages 820–825, May 2007.

[11] Canadian Lung Association. Respiratory system. https://www.lung.ca/lung-health/lung-info/respiratory-system, January 2019. [last accessed 14 April 2020].

[12] Guha Balakrishnan, Fredo Durand, and John Guttag. Detecting pulse from head motions in video. In *Proceedings of the IEEE Conference on Computer Vision and Pattern Recognition (CVPR)*, pages 3430–3437, June 2013.

[13] Gial D. Baura. *Medical Device Technologies: A System Based Overview Using Engineering Standards*. Elsevier, New York, 2012.

[14] Bboyho. Getting started with walabot. https://learn.sparkfun.com/tutorials/getting-started-with-walabot. [last accessed 14 April 2020].

[15] Thijs Beckers. Review: Walabot creator - an extraordinary 3d-sensor. https://www.elektormagazine.com/news/

review-walabot-creator-an-extraordinary-3d-sensor, September 2018. [last accessed 14 April 2020].

[16] Clara Benevolo, Renata Paola Dameri, and Beatrice D'Auria. Smart mobility in smart city. In Teresina Torre, Alessio Maria Braccini, and Riccardo Spinelli, editors, *Empowering Organizations*, pages 13–28, Cham, 2016. Springer International Publishing.

[17] BIOPAC Systems, Inc. Wireless respiration transducer – bionomadix. https://www.biopac.com/product/respiration-transducer-bionomadix/, 2020. [last accessed 14 April 2020].

[18] BIOPAC Systems, Inc. Products. https://www.biopac.com/products/, 2020. [last accessed 14 April 2020].

[19] BIOPAC Systems, Inc. Respiration recording. https://www.biopac.com/knowledge-base/respiration-recording/, 2020. [last accessed 14 April 2020].

[20] Richard Bishop. Intelligent vehicle applications worldwide. *IEEE Intelligent Systems and their Applications*, 15:78–81, January 2000.

[21] Dwaipayan Biswas, Neide Simões-Capela, Chris Van Hoof, and Nick Van Helleputte. Heart rate estimation from wrist-worn photoplethysmography: A review. *IEEE Sensors Journal*, 19(16):6560–6570, August 2019.

[22] Sheldon R. Braun. Respiratory rate and pattern. In H. K. Walker, W. D. Hall, and J. W. Hurst, editors, *Clinical Methods: The History, Physical, and Laboratory Examinations*, chapter 43, pages 226–230. Butterworths, Boston, 3 edition, 1990.

[23] Katherine E. Britton and Jennifer D. Britton-Colonnese. Privacy and security issues surrounding the protection of data generated by continuous glucose monitors. *Journal of Diabetes Science and Technology*, 11(2):216–219, March 2017.

[24] C. Brüser, C. H. Antink, T. Wartzek, M. Walter, and S. Leonhardt. Ambient and unobtrusive cardiorespiratory monitoring techniques. *IEEE Reviews in Biomedical Engineering*, 8:30–43, March 2015.

[25] Sophie Charara and Husain Sumara. We read your wearable tech's privacy policy so you don't have to. https://www.wareable.com/wearable-tech/terms-and-conditions-privacy-policy-765, May 2018. [last accessed 14 April 2020].

[26] Peter H. Charlton, Timothy Bonnici, Lionel Tarassenko, David A. Clifton, Richard Beale, and Peter J. Watkinson. An assessment of algorithms to estimate respiratory rate from the electrocardiogram and photoplethysmogram. *Physiological Measurement*, 37(4):610–626, March 2016.

[27] Peter H. Charlton, Drew A. Birrenkott, Timothy Bonnici, Marco A. F. Pimentel, Alistair E. W. Johnson, Jordi Alastruey, Lionel Tarassenko, Peter J. Watkinson, Richard Beale, and David A. Clifton. Breathing rate estimation from the electrocardiogram and photoplethysmogram: A review. *IEEE Reviews in Biomedical Engineering*, 11: 2–20, October 2018.

[28] Cleveland Clinic. Heart beat. https://my.clevelandclinic.org/health/articles/17064-heart-beat, May 2019. [last accessed 14 April 2020].

[29] Cleveland Clinic. Vital signs. https://my.clevelandclinic.org/health/articles/10881-vital-signs, January 2019. [last accessed 14 April 2020].

[30] Phil Corbishley and Esther Rodriguez-Villegas. Breathing detection: Towards a miniaturized, wearable, battery-operated monitoring system. *IEEE Transactions on Biomedical Engineering*, 55(1):196–204, January 2008.

[31] Michelle A. Cretikos, Rinaldo Bellomo, Ken Hillman, Jack Chen, Simon Finfer, and Arthas Flabouris. Respiratory rate: the neglected vital sign. *The Medical Journal of Australia*, 188:657–659, 2008.

[32] Taisa Daiana da Costa, Maria de Fatima Fernandes Vara, Camila Santos Cristino, Tyene Zoraski Zanella, Guilherme Nunes Nogueira Neto, and Percy Nohama. Breathing monitoring and pattern recognition with wearable sensors. In *Wearable Devices — the Big Wave of Innovation*. IntechOpen, June 2019.

[33] Andy Damico. Respiration belt placement training. https://support.mindwaretech.com/2016/10/respiration-belt-placement-training/, Oct 2016. [last accessed 14 April 2020].

[34] Archi Dasgupta, Nicole Buckingham, Denis Gračanin, Mohamed Handosa, and Reza Tasooji. A mixed reality based social interactions testbed: A game theory approach. In Jessie Y. C. Cheng and Gino Fragomeni, editors, *Virtual, Augmented and Mixed Reality: Applications in Health, Cultural Heritage, and Industry (VAMR 2018)*, pages 40–56. Springer, June 2018.

[35] George Demiris and B. K. Hensel. Technologies for an aging society: A systematic review of "smart home" applications. *Yearbook of Medical Informatics*, 17:33–40, 2008.

[36] Amy D. Droitcour, Todd B. Seto, Byung-Kwon Park, Shuhei Yamada, Alex Vergara, Charles El Hourani, Tommy Shing, Andrea Yuen, Victor M. Lubecke, and Olga Boric-Lubecke. Non-contact respiratory rate measurement validation for hospitalized patients. *Annual International Conference of the IEEE Engineering in Medicine and Biology Society*, page 4812–4815, September 2009.

[37] University of Utah Eccles Health Sciences Library. Normal ECG characteristics and

measurement abnormalities. https://ecg.utah.edu/test/2, 2020. [last accessed 14 April 2020].

[38] Fatema El-Amrawy, B.Pharm, and Mohamed Ismail Nounou. Are currently available wearable devices for activity tracking and heart rate monitoring accurate, precise, and medically beneficial? *Healthc Inform Res.*, 21:315–320, October 2015.

[39] David Evans, Brent Hodgkinson, and Judith Berry. Vital signs in hospital patients: a systematic review. *International Journal of Nursing Studies*, 38(6):643–650, December 2001.

[40] John F. Fieselmann, Michael S. Hendryx, Charles M. Helms, and Douglas S. Wakefield. Respiratory rate predicts cardiopulmonary arrest for internal medicine inpatients. *Journal of General Internal Medicine*, 8(7):354–360, July 1993.

[41] Fitbit. Charge HR 101 guide. https://www.fitbit.com/c/chargehr/chargehr-101. [last accessed 14 April 2020].

[42] M. Folke, L. Cernerud, M. Ekström, and B. Hök. Critical review of non-invasive respiratory monitoring in medical care. *Medical and Biological Engineering and Computing*, 41(4):377–383, July 2003.

[43] U.S. Food and Drug Administration. Consumers (medical devices). https://www.fda.gov/medical-devices/resources-you-medical-devices/consumers-medical-devices#What_is_a_Medical_Device_, April 2019. [last accessed 9 March 2020].

[44] National Center for Chronic Disease Prevention, Division for Heart Disease Health Promotion, and Stroke Prevention. Heart disease facts. https://www.cdc.gov/heartdisease/facts.htm, December 2019. [last accessed 14 April 2020].

[45] International Organization for Standardization. About us. https://www.iso.org/about-us.html. [last accessed 14 April 2020].

[46] Nicole Teresa Furtak, Ewa Skrzetuska, and Izabella Krucinska. Development of screen-printed breathing rate sensors. *Fibres and Textiles in Eastern Europe*, 21(6):84–88, December 2013.

[47] Maurizio Garbarino, Matteo Lai, Dan Bender, Rosalind W. Picard, and Simone Tognetti. Empatica E3 — a wearable wireless multi-sensor device for real-time computerized biofeedback and data acquisition. In *Proceedings of the 4th International Conference on Wireless Mobile Communication and Healthcare - Transforming Healthcare Through Innovations in Mobile and Wireless Technologies (MOBIHEALTH)*, pages 39–42, Athens, Greece, November 2014.

[48] Marc Garbey, Nanfei Sun, Arcangelo Merla, and Ioannis Pavlidis. Contact-free measurement of cardiac pulse based on the analysis of thermal imagery. *IEEE Transactions on Biomedical Engineering*, 54(8):1418–1426, August 2007.

[49] A. Garde, L. Sörnmo, R. Jané, and B.F. Giraldo. Breathing pattern characterization in chronic heart failure patients using the respiratory flow signal. *Annals of biomedical engineering*, 38:3572–3580, 2010.

[50] M. Gasior and J. L. Gonzalez. Improving FFT frequency measurement resolution by parabolic and gaussian spectrum interpolation. *AIP Conference Proceedings*, 732(1): 276–285, 2004.

[51] Mario Gerla, Eun-Kyu Lee, Giovanni Pau, and Uichin Lee. Internet of vehicles: From intelligent grid to autonomous cars and vehicular clouds. In *Proceedings of the IEEE World Forum on Internet of Things*, Seoul, South Korea, March 2014.

[52] Rudolf Giffinger and Haindlmaier Gudrun. Smart cities ranking: An effective instrument for the positioning of cities? *City and Environment*, 4:7–25, January 2010.

[53] Elisabetta De Giovanni, Srinivasan Murali, Francisco Rincon, and David Atienza. Ultra-low power estimation of heart rate under physical activity using a wearable photoplethysmographic system. In *Proceedings of the 19th Euromicro Conference on Digital System Design*, pages 553–560, Limassol, Cyprus, September 2016.

[54] Denis Gračanin, Mohamed Handosa, and Hicham Elmongui. A service infrastructure for human-centered IoT-based smart built environments. In Norbert Streitz and Panos Markopoulos, editors, *Proceedings of the 5th International Conference on Distributed, Ambient and Pervasive Interactions, DAPI 2017, Held as Part of HCI International 2017*, volume 10291 of *Lecture Notes in Computer Science*, pages 262–274, Cham, 9–14 July 2017. Springer International Publishing.

[55] Denis Gračanin, R. Benjamin Knapp, Thomas L. Martin, and Sarah Parker. Smart virtual care centers in the context of performance and privacy. In *Proceedings of the 15th International Conference on Telecommunications (ConTEL)*, pages 1–8, 3–5 July 2019.

[56] Changzhan Gu. Short-range noncontact sensors for healthcare and other emerging applications: A review. *Sensors*, 16(8), July 2016.

[57] Anoma Gunasekara. Contactless estimation of breathing rate using uwb radar. Master's thesis, School of Electrical Engineering and Computer Science University of Ottawa, 2017. [last accessed 6 February 2020].

[58] Sasha Hallett and John V. Ashurst. *Physiology, Tidal Volume*. StatPearls Publishing, Treasure Island, FL, February 2019.

[59] Colin Harrison and Ian Abbott Donnelly. A theory of smart cities. In *Proceedings of the 55th Annual Meeting of the International Society for the Systems Sciences*, January 2011.

[60] Spire Health. Spire health tag. https://spirehealth.com/pages/spire-health-tag-main. [last accessed 14 April 2020].

[61] Donald Albert Heath, David H. Elliott, Ewald R. Weibel, Peter H. Burri, Robert A. Klocke, and Arthur A. Siebens. Human respiratory system. https://www.britannica.com/science/human-respiratory-system, February 2020. [last accessed 14 April 2020].

[62] Peter Hillyard, Anh Luong, Alemayehu Solomon Abrar, Neal Patwari, Krishna Sundar, Robert Farney, Jason Burch, Christina A. Porucznik, and Sarah Hatch Pollard. Comparing respiratory monitoring performance of commercial wireless devices. Technical report, arXiv.org, Jul 2018.

[63] Judith Ann Hirsch and Beverly Bishop. Respiratory sinus arrhythmia in humans: how breathing pattern modulates heart rate. *American Journal of Physiology-Heart and Circulatory Physiology*, 241(4):H620–H629, October 1981.

[64] Andrew R. Houghton and David Gray. *Making Sense of the ECG: A Hands-on Guide*. Hodder Arnold, London, UK, 3 edition, 2008.

[65] Empatica Inc. E4 wristband. https://www.empatica.com/research/e4/, 2020. [last accessed 14 April 2020].

[66] Mohd Shoaib Iqbal. Imaging using radar. Diploma thesis, Indraprastha Institute of Information Technology Delhi, November 2017.

[67] Kanitthika Kaewkannate and Soochan Kim. A comparison of wearable fitness devices. *BMC Public Health*, 16(1):433, May 2016.

[68] Hang-Bong Kang. Various approaches for driver and driving behavior monitoring: A review. In *Proceedings of the IEEE International Conference on Computer Vision Workshops*, pages 616–623, June 2013.

[69] Yasser Khan, Aminy E. Ostfeld, Claire M. Lochner, Adrien Pierre, and Ana C. Arias. Monitoring of vital signs with flexible and wearable medical devices. *Advanced Materials*, 28(22):4373–4395, June 2016.

[70] Ramsey Kilani. Testing the viability of walabot for breathing detection. https://www.hackster.io/Ruleof2/testing-the-viability-of-walabot-for-breathing-detection-b0a14f, April 2017. [last accessed 14 April 2020].

[71] Jin Kim, Hyeok soo Choi, Hui Wang, Nazim Agoulmine, M. Jamal Deerv, and James Won-Ki Hong. POSTECH's U-Health smart home for elderly monitoring and support. In *Proceedings of the IEEE International Symposium on "A World of Wireless, Mobile and Multimedia Networks"*, pages 1–6, Montrreal, QC, Canada, June 2010.

[72] Tomas Komensky, Michal Jurcisin, Kornel Ruman, Ondrej Kovac, Daniel Laqua, and Peter Husar. Ultra-wearable capacitive coupled and common electrode-free ecg monitoring system. In *Proceedings of the Annual International Conference of the IEEE Engineering in Medicine and Biology Society*, page 1594–1597, San Diego, CA, August 2012.

[73] T. Kondo, T. Uhlig, P. Pemberton, and P.D. Sly. Laser monitoring of chest wall displacement. *European Respiratory Journal*, 10(8):1865–1869, 1997.

[74] Shiu Kumar and Seong Ro Lee. Android based smart home system with control via bluetooth and internet connectivity. In *Proceedings of the 18th IEEE International Symposium on Consumer Electronics*, pages 1–2, JeJu Island, South Korea, June 2014.

[75] Boon-Giin Lee and Wan-Young Chung. A smartphone-based driver safety monitoring system using data fusion. *Sensors*, 12(12):17536–17552, December 2012.

[76] Jeong Su Lee, Jeong Heo, Won Kyu Lee, Yong Gyu Lim, Youn Ho Kim, and Kwang Suk Park. Flexible capacitive electrodes for minimizing motion artifacts in ambulatory electrocardiograms. *Sensors*, 14(8):14732–14743, August 2014.

[77] Sung Joo Lee, Jaeik Jo, Ho Gi Jung, Kang Ryoung Park, and Jaihie Kim. Real-time gaze estimator based on driver's head orientation for forward collision warning system. *IEEE Transactions on Intelligent Transportation Systems*, 12(1):254–267, March 2011.

[78] Peter Leijdekkers and Valérie Gay. A self-test to detect a heart attack using a mobile phone and wearable sensors. In *Proceedings of the 21st IEEE International Symposium on Computer-Based Medical Systems*, pages 93–98, Jyvaskyla, Finland, June 2008.

[79] Rui Li, Daniel T. H. Lai, and WeeSit Lee. A survey on biofeedback and actuation in wireless body area networks (WBANs). *IEEE Reviews in Biomedical Engineering*, 10: 162–173, August 2017.

[80] Wenda Li, Bo Tan, and Robert J. Piechocki. Non-contact breathing detection using passive radar. In *Proceedings of the IEEE International Conference on Communications*, pages 1–6, Kuala Lumpur, Malaysia, May 2016.

[81] J. C. Lin. Noninvasive microwave measurement of respiration. *Proceedings of the IEEE*, 63(10):1530–1530, October 1975.

[82] Guan-zheng Liu, Dan Wu, Zhan-yong Mei, Qing-song Zhu, and Lei Wang. Automatic detection of respiratory rate from electrocardiogram, respiration induced plethysmography and 3D acceleration signals. *Journal of Central South University*, 20(9):2423–2431, September 2013.

[83] Nan Liu, Zhiping Lin, Zhixiong Koh, Guang-Bin Huang, Wee Ser, and Marcus Eng Hock Ong. Patient outcome prediction with heart rate variability and vital signs. *Journal of Signal Processing Systems*, 64(2):265–278, August 2011.

[84] Sumit Majumder, Tapas Mondal, and M. Jamal Deen. Wearable sensors for remote health monitoring. *Sensors*, 17(1), January 2017.

[85] Sumit Majumder, Leon Chen, Ognian Marinov, Chih-Hung Chen, Tapas Mondal, and M. Jamal Deen. Noncontact wearable wireless ecg systems for long-term monitoring. *IEEE Reviews in Biomedical Engineering*, 11:306–321, May 2018.

[86] Se Dong Min, Jin Kwon Kim, Hang Sik Shin, Yong Hyeon Yun, Chung Keun Lee, and Myoungho Lee. Noncontact respiration rate measurement system using an ultrasonic proximity sensor. *IEEE Sensors Journal*, 10(11):1732–1739, November 2010.

[87] MindWare Technologies LTD. Mindware mobile impedance cardiograph product manual. http://downloads.mindwaretech.com/Hardware/MindWare%20Mobile%20Impedance%20Cardiograph%201.0.0-1%20Manual.pdf, 2013. [last accessed 14 April 2020].

[88] MindWare Technologies LTD. Mindware mobile. https://mindwaretech.com/mindware-mobile/, 2020. [last accessed 14 April 2020].

[89] MindWare Technologies LTD. Downloads. https://support.mindwaretech.com/downloads/, 2020. [last accessed 14 April 2020].

[90] Dragos Mocrii, Yuxiang Chen, and Petr Musilek. IoT-based smart homes: A review of system architecture, software, communications, privacy and security. *Internet of Things*, 1-2:81–98, September 2018.

[91] Hamed Monkaresi, Rafael A. Calvo, and Hong Yan. A machine learning approach to improve contactless heart rate monitoring using a webcam. *IEEE Journal of Biomedical and Health Informatics*, 18(4):1153–1160, July 2014.

[92] George B. Moody, Roger G. Mark, Marjorie A. Bump, Joseph S. Weinstein, Aaron D. Berman, Joseph E. Mietus, and Ary L. Goldberger. Clinical validation of the ECG-derived respiration (EDR) technique. *IEEE Computer Society Press*, January 1986.

[93] Eric Morgan. All about HRV part 4: Respiratory sinus arrhythmia. https://support.mindwaretech.com/2017/09/all-about-hrv-part-4-respiratory-sinus-arrhythmia/#mwtoc-setting-up-respiration, September 2017. [last accessed 14 April 2020].

[94] Kazuki Nakajima, Yoshiaki Matsumoto, and Toshiyo Tamura. Development of real-time image sequence analysis for evaluating posture change and respiratory rate of a subject in bed. *Physiological Measurement*, 22(3):N21–N28, July 2001.

[95] Viswam Nathan and Roozbeh Jafari. Particle filtering and sensor fusion for robust heart rate monitoring using wearable sensors. *IEEE Journal of Biomedical and Health Informatics*, 22(6):1834–1846, December 2018.

[96] Ebrahim Nemati, M. Jamal Deen, and Tapas Mondal. A wireless wearable ECG sensor for long-term applications. *IEEE Communications Magazine*, 50:36–43, January 2012.

[97] Prathyusha Nimmagadda and Hemalatha Inteti. Signal analysis based radar imaging using radar sensor. *Pramana Research Journal*, 9:1919–1924, 2019.

[98] Zhaolong Ning, Feng Xia, Noor Ullah, Xiangjie Kong, and Xiping Hu. Vehicular social networks: Enabling smart mobility. *IEEE Communications Magazine*, 55(5):16–55, May 2017.

[99] Dany Obeid, Sawsan Sadek, Gheorghe Zaharia, and Ghaïs El Zein. Multitunable microwave system for touchless heartbeat detection and heart rate variability extraction. *Microwave and Optical Technology Letters*, 52(1):192–198, January 2010.

[100] Office for Civil Rights. Summary of the HIPAA privacy rule. OCR privacy brief, U.S. Department of Health & Human Services, Washington, DC, May 2003.

[101] R. Paradiso. Wearable health care system for vital signs monitoring. In *Proceedings of the 4th International IEEE EMBS Special Topic Conference on Information Technology Applications in Biomedicine*, pages 283–286, Birmingham, UK, April 2003.

[102] Neal Patwari, Lara Brewer, Quinn Tate, Ossi Kaltiokallio, and Maurizio Bocca. Breathfinding: A wireless network that monitors and locates breathing in a home. *IEEE Journal of Selected Topics in Signal Processing*, 8:30–42, February 2014.

[103] Alan Pierce. Walabot DIY can see into walls. *Tech Directions*, January 2017.

[104] Ming-Zher Poh, Daniel J. McDuff, and Rosalind W. Picard. Non-contact, automated cardiac pulse measurements using video imaging and blind source separation. *Opt. Express*, 18(10):10762–10774, May 2010.

[105] Carmen C. Y. Poon, Benny P. L. Lo, Mehmet Rasit Yuce, Akram Alomainy, and Yang Hao. Body sensor networks: In the era of big data and beyond. *IEEE Reviews in Biomedical Engineering*, 8:4–16, April 2015.

[106] Harvard Health Publishing. What your heart rate is telling you. https://www.health.harvard.edu/heart-health/what-your-heart-rate-is-telling-you, October 2018. [last accessed 14 April 2020].

[107] Huan Qi, Z. Jane Wang, and Chunyan Miao. Non-contact driver cardiac physiological monitoring using video data. In *Proceedings of the 2015 IEEE China Summit and International Conference on Signal and Information Processing*, pages 418–422, Chengdu, China, July 2015.

[108] Parisa Rashidi, Diane J. Cook, Lawrence B. Holder, and Maureen Schmitter-Edgecombe. Discovering activities to recognize and track in a smart environment. *IEEE Transactions on Knowledge and Data Engineering*, 23(4):527–539, April 2011.

[109] Vincent Rialle, Florence Duchene, Norbert Noury, Lionel Bajolle, and Jacques Demongeot. Health "smart" home: Information technology for patients at home. *Telemedicine Journal and e-Health*, 8, July 2004.

[110] Natalia V. Rivera, Swaroop Venkatesh, Chris Anderson, and R. Michael Buehrer. Multi-target estimation of heart and respiration rates using ultra wideband sensors. In *Proceedings of the 14th European Signal Processing Conference*, Florence, Italy, September 2006.

[111] Budiman P.A. Rohman, Muhammad Bagus Andra, and Masahiko Nishimoto. Toward a compact infant monitoring system using UWB radar and environmental sensors. In *Proceedings of the IEEE 1st Global Conference on Life Sciences and Technologies*, pages 4–5, March 2019.

[112] Samsung. All wearables. https://www.samsung.com/us/mobile/wearables/all-wearables/, 2020. [last accessed 14 April 2020].

[113] Udit Satija, Barathram Ramkumar, and M. Sabarimalai Manikandan. A review of signal processing techniques for electrocardiogram signal quality assessment. *IEEE Reviews in Biomedical Engineering*, 11:36–52, February 2018.

[114] Jay Schmidt. How to export data from mindware files. https://support.mindwaretech.com/knowledge-base/kb0040/, April 2016. [last accessed 14 April 2020].

[115] John Semmlow. *Signals and Systems for Bioengineers*. Elsevier, New York, second edition, 2012.

[116] John Semmlow. The big picture: Bioengineering signals and systems. In *Circuits, Signals and Systems for Bioengineers*, Biomedical Engineering, chapter 1, pages 3–50. Academic Press, 3 edition, 2017.

[117] Kirk H. Shelley. Photoplethysmography: Beyond the calculation of arterial oxygen saturation and heart rate. *Anesthesia & Analgesia*, 105:S31–S36, December 2007.

[118] Robert H. Shmerling. How's your heart rate and why it matters? https://www.health.harvard.edu/heart-health/hows-your-heart-rate-and-why-it-matters, March 2020. [last accessed 14 April 2020].

[119] Arindam Sikdar, Santosh Kumar Behera, and Debi Prosad Dogra. Computer-vision-guided human pulse rate estimation: A review. *IEEE Reviews in Biomedical Engineering*, 9:91–105, April 2016.

[120] GiriBabu Sinnapolu and Shadi Alawneh. Integrating wearables with cloud-based communication for health monitoring and emergency assistance. *Internet of Things*, 1-2: 40–54, September 2018.

[121] Gina Sprint, Diana J. Cook, Rochelle Fritz, and Maureen Schmitter-Edgecombe. Using smart homes to detect and analyze health events. *Computer*, 49(11):29–37, November 2016.

[122] Sarah E. Stahl, An Hyun-Sung, Danae M. Dinkel, John M. Noble, and Jung-Min Lee. How accurate are the wrist-based heart rate monitors during walking and running activities? Are they accurate enough? *BMJ Open Sport and Exercise Medicine*, 2(1): e000106, 2016.

[123] C. P. Subbe, R. G. Davies, E. Williams, P. Rutherford, and L. Gemmell. Effect of introducing the modified early warning score on clinical outcomes, cardio-pulmonary arrests and intensive care utilisation in acute medical admissions. *Anaesthesia*, 58(8): 797–802, August 2003.

[124] Nabil Sultan. Reflective thoughts on the potential and challenges of wearable technology for healthcare provision and medical education. *International Journal of Information Management*, 35(5):521–526, October 2015.

[125] Nick Sutrich. See through your walls with this walabot deal. https://www.androidheadlines.com/2019/07/walabot-primeday-cheap-sale-price.html, July 2019. [last accessed 14 April 2020].

[126] Takuji Suzuki, Ken ichi Kameyama, and Toshiyo Tamura. Development of the irregular pulse detection method in daily life using wearable photoplethysmographic sensor. In *Proceedings of the Annual International Conference of the IEEE Engineering in Medicine and Biology Society*, Minneapolis, MN, September 2009.

[127] Tayebeh Taheri and Anita Sant'Anna. Non-invasive breathing rate detection using a very low power ultra-wide-band radar. In *Proceedings of the IEEE International Conference on Bioinformatics and Biomedicine*, pages 78–83, November 2014.

[128] Yoshiro Tajitsu. Piezoelectret sensor made from an electro-spun fluoropolymer and its use in a wristband for detecting heart-beat signals. *IEEE Transactions on Dielectrics and Electrical Insulation*, 22:1355–1359, June 2015.

[129] Reza Tasooji, Archi Dasgupta, Denis Gračanin, Matthew LaGro, and Krešimir Matković. A multi-purpose IoT framework for smart built environments. In M. Rabe, A. A. Juan, N. Mustafee, A. Skoogh, S. Jain, and B. Johansson, editors, *Proceedings of the 2018 Winter Simulation Conference*, pages 4240–4241, 9–12 December 2018.

[130] Reza Tasooji, Nicole Buckingham, Denis Gračanin, and R. Benjamin Knapp. An approach to analysis of physiological responses to stimulus: From electrodermal activity to combined physiological responses. In Aaron Marcus and Wentao Wang, editors, *Design, User Experience, and Usability: Design Philosophy and Theory (International Conference on Human-Computer Interaction HCII 2019)*, volume 11583 of *Lecture Notes in Computer Science*, pages 492–509, Cham, 26–31 July 2019. Springer International Publishing.

[131] Kevin C. Tseng, Bor-Shyh Lin, Lun-De Liao, Yu-Te Wang, and Yu-Lin Wang. Development of a wearable mobile electrocardiogram monitoring system by using novel dry foam electrodes. *IEEE Systems Journal*, 8(3):900–906, September 2014.

[132] S. Venkatesh, C. R. Anderson, N. V. Rivera, and R. M. Buehrer. Implementation and analysis of respiration-rate estimation using impulse-based UWB. In *Proceedings of the IEEE Military Communications Conference*, Atlantic City, NJ, October 2005.

[133] VITALI Wear. The everyday smart bra: Your intuitive wellness coach. https://www.kickstarter.com/projects/vitaliwear/the-everyday-smart-bra-your-intuitive-wellness-coa, June 2017. [last accessed 14 April 2019].

[134] E. Wahlstrom, O. Masoud, and N. Papanikolopoulos. Vision-based methods for driver monitoring. In *Proceedings of the IEEE International Conference on Intelligent Transportation Systems*, volume 2, pages 903–908, Shanghai, China, October 2003.

[135] Walabot. Walabot API beta. https://api.walabot.com/, . [last accessed 14 April 2020].

[136] Walabot. Imaging features. https://api.walabot.com/_features.html, . [last accessed 14 April 2020].

[137] Walabot. Walabot home. https://walabot.com/walabot-home, . [last accessed 14 April 2020].

[138] Walabot. Walabot DIY. https://walabot.com/diy, 2020. [last accessed 14 April 2020].

[139] Walabot. Walabot maker. https://walabot.com/makers, 2020. [last accessed 14 April 2020].

[140] Walabot. Walabot technical brief. https://walabot.com/docs/walabot-tech-brief-416?type=pdf, 2020. [last accessed 14 April 2020].

[141] Hao Wang, Daqing Zhang, Junyi Ma, Yasha Wang, Yuxiang Wang, Dan Wu, Tao Gu, and Bing Xie. Human respiration detection with commodity wifi devices: Do user location and body orientation matter? In *Proceedings of the 2016 ACM International Joint Conference on Pervasive and Ubiquitous Computing*, UbiComp '16, pages 25–36, September 2016.

[142] T. Wang, D. Zhang, L. Wang, Y. Zheng, T. Gu, B. Dorizzi, and X. Zhou. Contactless respiration monitoring using ultrasound signal with off-the-shelf audio devices. *IEEE Internet of Things Journal*, 6(2):2959–2973, April 2019.

[143] Yu Wu, Dai Jiang, Andy Bardill, Serena de Gelidi, Richard Bayforda, and Andreas Demosthenous. A high frame rate wearable EIT system using active electrode ASICs for lung respiration and heart rate monitoring. *IEEE Transactions on Circuits and Systems I: Regular Papers*, 65(11):3810–3820, August 2018.

[144] Jiawei Xu, Srinjoy Mitra, Chris Van Hoof, Refet Firat Yazicioglu, and Kofi A. A. Makinwa. Active electrodes for wearable EEG acquisition: Review and electronics design methodology. *IEEE Reviews in Biomedical Engineering*, 10:187–198, January 2017.

[145] Ming Yan and Hao Shi. Smart living using bluetooth-based android smartphone. *International Journal of Wireless and Mobile Network*, 5:65–72, January 2013.

[146] Xiaofeng Yang, Guanghao Sun, and Koichiro Ishibashi. Non-contact acquisition of respiration and heart rates using doppler radar with time domain peak-detection algorithm. In *Proceedings of the 2017 39th Annual International Conference of the IEEE Engineering in Medicine and Biology Society (EMBC)*, pages 2847–2850, 2017.

[147] Hui-Shyong Yeo and Aaron Quigley. Radar sensing in human-computer interaction. *Interactions*, 25:70–73, 2018.

[148] Andrea Zanella, Nicola Bui, Angelo Castellani, Lorenzo Vangelista, and Michele Zorzi. Internet of things for smart cities. *IEEE Internet of Things Journal*, 1:22–32, February 2014.

[149] Qi Zhang, Guo qing Xu, Ming Wang, Yimin Zhou, and Wei Feng. Webcam based non-contact real-time monitoring for the physiological parameters of drivers. In *Proceedings of the 4th Annual IEEE International Conference on Cyber Technology in Automation, Control and Intelligent*, pages 648–652, Hong Kong, China, June 2014.

[150] Y.T Zhang. Editorial health engineering: Convergence transforming reactive medicine to proactive healthcare. *IEEE Reviews in Biomedical Engineering*, 11:1, July 2018.

[151] Mingmin Zhao, Tianhong Li, Mohammad Abu Alsheikh, Yonglong Tian, Hang Zhao, Antonio Torralba, and Dina Katabi. Through-wall human pose estimation using radio signals. In *Proceedings of the 2018 IEEE/CVF Conference on Computer Vision and Pattern Recognition*, pages 7356–7365, June 2018.

Appendices

Appendix A

Testing Documents

A.1 Pre-study Survey

Participant ID:

1. Age:
2. Gender:
    - Female
    - Male
    - Other, please specify:
    - Do not wish to specify
3. Do you have any physical disabilities?
    - No
    - Yes, please specify:
4. Do you have any respiratory conditions?
    - No
    - Yes, please specify:

5. Do you have any experience with wearable health devices (ex. fitness trackers, etc)?

    - No
    - Yes, please specify:

6. Do you have any experience with breathing pattern sensors?

    - No
    - Yes, please specify:

A.2 Post-study Survey

Participant ID:

Overall

1. Rate your overall experience: 1 2 3 4 5
2. What did you not enjoy about the study?
3. What did you enjoy about the study?

Chest band breathing rate sensor

1. Rate your experience with the device: 1 2 3 4 5
2. In your opinion, what are the negative aspects of this device?
3. In your opinion, what are the positive aspects of this device?

Contactless breathing rate sensor

1. Rate your experience with the device: 1 2 3 4 5
2. In your opinion, what are the negative aspects of this device?
3. In your opinion, what are the positive aspects of this device?

A.3 IRB Approval Letter

Pages 1 and 2 of the IRB approval letter are shown in Figures A.1 and A.2, respectively.

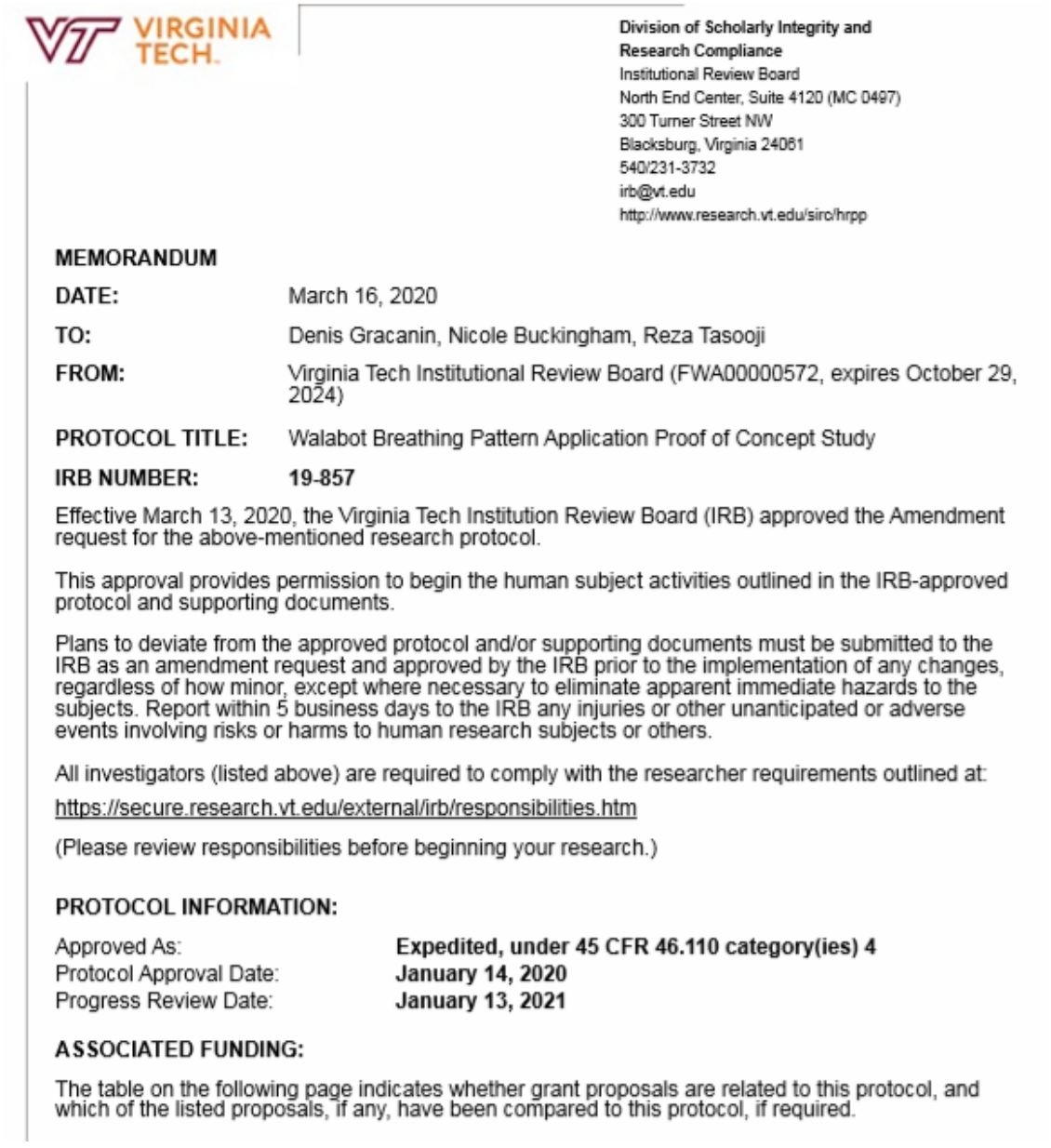

VIRGINIA TECH

Division of Scholarly Integrity and Research Compliance
Institutional Review Board
North End Center, Suite 4120 (MC 0497)
300 Turner Street NW
Blacksburg, Virginia 24061
540/231-3732
irb@vt.edu
http://www.research.vt.edu/sirc/hrpp

MEMORANDUM

DATE: March 16, 2020

TO: Denis Gracanin, Nicole Buckingham, Reza Tasooji

FROM: Virginia Tech Institutional Review Board (FWA00000572, expires October 29, 2024)

PROTOCOL TITLE: Walabot Breathing Pattern Application Proof of Concept Study

IRB NUMBER: **19-857**

Effective March 13, 2020, the Virginia Tech Institution Review Board (IRB) approved the Amendment request for the above-mentioned research protocol.

This approval provides permission to begin the human subject activities outlined in the IRB-approved protocol and supporting documents.

Plans to deviate from the approved protocol and/or supporting documents must be submitted to the IRB as an amendment request and approved by the IRB prior to the implementation of any changes, regardless of how minor, except where necessary to eliminate apparent immediate hazards to the subjects. Report within 5 business days to the IRB any injuries or other unanticipated or adverse events involving risks or harms to human research subjects or others.

All investigators (listed above) are required to comply with the researcher requirements outlined at:

https://secure.research.vt.edu/external/irb/responsibilities.htm

(Please review responsibilities before beginning your research.)

PROTOCOL INFORMATION:

Approved As:	**Expedited, under 45 CFR 46.110 category(ies) 4**
Protocol Approval Date:	**January 14, 2020**
Progress Review Date:	**January 13, 2021**

ASSOCIATED FUNDING:

The table on the following page indicates whether grant proposals are related to this protocol, and which of the listed proposals, if any, have been compared to this protocol, if required.

Figure A.1: Page 1 of the IRB approval letter.

SPECIAL INSTRUCTIONS:

*** The Virginia Tech IRB/HRPP has requested that research involving person-to-person contact or gatherings of human research participants be paused as soon as possible. The duration of the pause is unknown, but to reduce disruption to the extent possible, we will be reassessing daily. Although we continue to issue approval notices, Virginia Tech guidance should be followed. Please visit https://www.research.vt.edu/covid-19-updates-impacts.html for updates.

This amendment, submitted March 4, 2020, updates research protocol to change the wearable device. Consent forms were updated to change the wearable device.

Date*	OSP Number	Sponsor	Grant Comparison Conducted?

* Date this proposal number was compared, assessed as not requiring comparison, or comparison information was revised.

If this protocol is to cover any other grant proposals, please contact the HRPP office (irb@vt.edu) immediately.

Figure A.2: Page 2 of the IRB approval letter.

A.4 Consent Form

Title of research study: Walabot Breathing Pattern Application Proof of Concept Study, VT IRB Protocol Number: 19-857

Principal Investigator: Denis Gračanin, (540) 231-2060, gracanin@vt.edu

Other study contact(s): Nicole Buckingham, (989) 750-8692, nb31@vt.edu

Key Information: The following is a short summary of this study to help you decide whether or not to be a part of this study. More detailed information is listed later on in this form.

We invite you to take part in a research study because you are a between the ages of 18-30 and do not have any physical disabilities or respiratory conditions (such as asthma) that prevent you from safely completing the study.

What should I know about being in a research study?

- Someone will explain this research study to you
- Whether or not you take part is up to you
- You can choose not to take part
- You can agree to take part and later change your mind
- Your decision will not be held against you
- You can ask all the questions you want before you decide

What should I know about this research study?

The purpose of this study is to evaluate the effectiveness and limitations of a contactless breathing sensor (Walabot). To evaluate the sensor, it must be compared to a contact breathing pattern sensor. During the study, we will ask you to complete minimal breathing exercises and adjust your physical positioning relative to the contactless breathing pattern sensor while wearing a heart rate monitor wristband (Empatica, model E4) and a chest band breathing pattern sensor (MindWare Mobile Impedance Cardiograph with Respiration Transducer Belt). Additionally, you will be asked to fill out pre and post study questionnaires about your experience. (More detailed information about the study procedures can be found under "What happens if I say yes, I want to be in this research?").

There are no foreseeable risks, but you may experience mild physical discomfort or stress during the procedure. (More detailed information about the risks of this study can be found under "Is there any way being in this study could be bad for me? (Detailed Risks)"). We cannot promise any benefits to you or others from your taking part in this research. However, you may experience short-term reduction in stress due to the breathing rates requested during the study. Possible benefits to others include extended knowledge of and applications for the contactless breathing pattern sensor (Walabot). If you are a student, the decision whether to participate or not participate will have no effect on your grades or relationship with Virginia Tech.

Detailed Information: The following is more detailed information about this study in addition to the information listed above.

Who can I talk to?

If you have questions, concerns, or complaints, or think the research has hurt you, talk

to the research team at VTRespiratoryStudy@gmail.com or you can contact the Principal Investigator Denis Gracanin at (540) 231-2060.

This research has been reviewed and approved by the Virginia Tech Institutional Review Board (IRB). You may communicate with them at 540-231-3732 or irb@vt.edu if:

- You have questions about your rights as a research subject
- Your questions, concerns, or complaints are not being answered by the research team
- You cannot reach the research team
- You want to talk to someone besides the research team to provide feedback about this research

How many people will be studied?

We plan to include about 30 people in this research study.

What happens if I say yes, I want to be in this research?

If you decide to volunteer for this study, you will be asked to participate in a one-hour session. During the study, you will interact with a research assistant (RA) that is in charge of running the study. You will wear a heart rate monitor wristband and a chest band breathing pattern sensor. You will be asked to sit or stand in various positions relative to a contactless breathing pattern sensor. You will also be asked to complete minimal breathing exercises (deep breathing) and minimal physical tasks (jogging in place). At the end of the study, you will fill out a survey inquiring about your experience with the devices.

Detailed procedure:

1. Pre-study survey: You will complete a pre-study survey inquiring about demographic questions.

2. Setup: The RA will help you put on the wristband device and the chest band breathing pattern sensor. The RA will position the contactless breathing pattern sensor in the predetermined location.

3. Sitting:

   (a) Baseline: You will sit in the baseline chair. Baseline data will be collected for 3 minutes.

   (b) Positioning: You will be asked to sit in various chairs that are in predetermined locations that vary horizontally from the baseline position. Data will be collected from each position for 1 minute.

   (c) Rate variation: You will sit in the baseline chair. You will be asked to take deep breathes for 1 minute.

4. Standing:

   (a) Baseline: You will stand on a marked baseline spot. Baseline data will be collected for 3 minutes.

   (b) Positioning: You will remain standing. The RA will reposition the contactless breathing pattern sensor several times, in predetermined locations that vary vertically from the baseline position. Data will be collected from each position for 1 minute.

   (c) Rate variation: You will remain standing. The contactless breathing pattern sensor will be repositioned at the baseline position. You will be asked to take deep breathes for 1 minute. Then, you will be asked to jog in place for 3 minutes.

5. Post-study survey: You will be asked to take a short survey, inquiring about your interactions with the devices.

Device Information:

- Heart rate monitor wristband (Empatica, model E4): This device will fit around your wrist, similar to a watch. There are two electrodes on the band of the watch. A small amount of conductive gel will be added to the electrodes prior to device placement, to help seal the connection. The device will be cleaned with antibacterial wipes before and after each study visit.
- Chest band breathing pattern sensor (MindWare Mobile Impedance Cardiograph with Respiration Transducer Belt): This device will fit around your chest. You can adjust the sensor until it feels comfortable. The device will be cleaned with antibacterial wipes before and after each study visit.
- Contactless breathing pattern sensor (Walabot): This device is contactless. It will be placed in front of you during the study.

What happens if I say yes, but I change my mind later?

You can leave the research at any time, for any reason, and it will not be held against you. If you decide to leave the research, contact the investigator so that the investigator can remove you from the schedule and delete any information already gathered. You do not need to provide an explanation for withdrawal and you will not be asked for any additional data collection or information.

Is there any way being in this study could be bad for me? (Detailed Risks)

You are required to wear the wristband device and the chest band breathing pattern sensor. These devices are non-intrusive and do not present any foreseeable risks, but they may cause mild physical discomfort. You will be asked to jog in place for 3 minutes. This may also cause minor physical discomfort.

The following are the types of breathing in which you will be asked to breath: normal breathing and deep breathes twice for 1 minute. You may experience minor stress or discomfort due to these breathing requests.

What happens to the information collected for the research?

We will make every effort to limit the use and disclosure of your personal information, including research study and medical records, only to people who have a need to review this information. We cannot promise complete confidentiality. Organizations that may inspect and copy your information include the IRB, Human Research Protection Program, and other authorized representatives of Virginia Tech. The results of this research study may be presented in summary form at conferences, in presentations, reports to the sponsor, academic papers, and as part of a thesis/dissertation.

Can I be removed from the research without my OK?

The investigators or RA in charge of running the study can remove you from the research study without your approval. During the procedure, the RA will continuously monitor you for any signs of discomfort or stress. In the case of any signs, the study will be paused or terminated to ensure your safety.

What else do I need to know?

This research is being funded by the Institute for Creativity, Arts, and Technology (ICAT). If you agree to take part in this research study, you will receive $10 for your time and effort upon your completion of the study. We will not offer to share your individual test results with you.

Signature Block for Capable Adult

Your signature documents your permission to take part in this research. We will provide you with a signed copy of this form for your records.

Signature of subject:

Printed name of subject:

Date:

Signature of person obtaining consent:

Printed name of person obtaining consent:

Date: